NASA
Technical
Paper
2446
C3
July 1985

Effect of Leading-Edge Load Constraints on the Design and Performance of Supersonic Wings

Christine M. Darden

NASA

NASA Technical Paper 2446

1985

Effect of Leading-Edge Load Constraints on the Design and Performance of Supersonic Wings

Christine M. Darden

Langley Research Center
Hampton, Virginia

NASA
National Aeronautics
and Space Administration

Scientific and Technical Information Branch

Contents

Summary

A theoretical and experimental investigation was conducted to assess the effect of leading-edge load constraints on supersonic wing design and performance. For a planform characterized by a highly swept leading edge on the inboard region, a linear-theory optimization procedure for attached flow was used to design camber surfaces to minimize drag due to lift at the design lift coefficient of 0.08 and a design Mach number of 2.4. In an effort to delay flow separation and the formation of leading-edge vortices, two constrained optimization approaches were used to limit loadings on the leading edge. In the first approach, wing camber was constrained to have the normal Mach number less than 1 everywhere along the leading edge at the design lift coefficient; and in the second approach, wing camber was constrained to have a pressure-coefficient difference of 0 across the leading edge. Experimental force and moment tests were made on four wing models: two constrained camber wings, a flat reference wing, and an optimum camber design with no leading-edge constraints. All wings had identical planforms and thicknesses and were tested over a range of angle of attack from -5° to 8° in the Langley Unitary Plan Wind Tunnel. Results indicate that vortex strength and flow-separation regions were mildest for the wing designed to have a zero lifting pressure coefficient at the leading edge.

Introduction

The current interest in new and advanced military aircraft has increased the need for wing design methods that are applicable at the higher lift coefficients at supersonic speeds. Leading-edge separation problems, which already exist at low lift conditions on the highly swept, sharp-leading-edge planforms used for supersonic designs, are aggravated further at the higher lift conditions. In the absence of wing design methods that include nonlinear viscous effects, attempts have been made to find methods of using linear-theory design procedures for the higher lift operating conditions. This paper will discuss a study of one such approach.

Flow separation over the upper surface of the wing, especially at the leading edge, generates leading-edge vortices and results in a degradation of performance of a wing designed for attached flow. In addition to the highly swept planforms and sharp leading edges on most supersonic wing designs, another factor believed to contribute to early separation is the high loadings at the leading edge. Both this cause of flow separation and an experimental study of the effects of its elimination are addressed in this paper.

For many years, attached-flow optimization methods (refs. 1 to 6) based on linear theory have been used to design wings employing twist and camber for supersonic transport concepts. The original optimization method (ref. 1), which was based on three pressure loadings and the Lagrangian method of undetermined multipliers, provided camber surfaces that produced well-behaved pressure loadings over the surface. Unfortunately, however, there was no means of constraining the pitching moment and, in addition, the root camber was often so severe that a fuselage could not be easily integrated with the wing.

Later improvements to this method increased the number of allowable loadings and therefore allowed additional constraints to be included within the lifting-surface optimization code (ref. 2). This design code, with some additional modifications, has now been incorporated into the Supersonic Design and Analysis System (SDAS). (See refs. 3 to 6.) Self-trimming designs and an increased ability to control root camber resulted from the additional loadings available in the optimization code; however, undesirably high leading-edge loadings also resulted. This increased difference between the upper- and lower-surface pressures at the leading edge of the new designs led to earlier flow separation as lift increased, especially when sharp-leading-edge airfoils were used.

The planform used in this study is characterized by a complex leading edge of generally high sweep and has been shown experimentally (refs. 7 and 8) to be favorable to the delay of leading-edge separation. The camber design and optimization method used is that of references 3 to 6 in which drag due to lift is minimized at a given total lift. Within the optimization process, constraints may be placed on pressure, camber ordinates, pressure gradients, and pitching moment. Since it is believed that the extreme leading-edge pressure differences cause the early formation of vortices, the approach used in this study was to place limits on the loadings at the leading edge. This study was made to assess the effect of limiting the magnitude of the leading-edge loading on the formation of leading-edge vortices and on overall aerodynamic performance.

A single planform shape was used in the development of four camber surfaces: a flat surface, an unconstrained optimum, and two constrained optimums. For each of the two constrained optimums, a different method for selecting the leading-edge pressure constraint was used. The leading-edge constraints, the resultant camber, and the experimentally measured performance of these designs are discussed and compared in the present paper. Some

limited results of this investigation are included in reference 9.

Symbols

Force and moment data are referred to the body axis system except for lift and drag which are referred to the stability axis system. The moment reference center for the model is located 1.431 ft from the model nose. The symbols in parentheses are used in the data tables in appendix A.

b		wing span, 2 ft
	(CA)	axial-force coefficient, $\frac{\text{Axial force}}{qS}$
	(CAC)	axial-force coefficient due to model balance-housing chamber pressure
C_D	(CD)	drag coefficient, $\frac{\text{Drag}}{qS}$
$C_{D,o}$		zero lift drag of flat wing
$\Delta C_D/C_L^2$		drag-due-to-lift factor, $(C_D - C_{D,o})/C_L^2$
	(CDC)	drag coefficient due to model balance-housing chamber pressure
C_L	(CL)	lift coefficient, $\frac{\text{Lift}}{qS}$
C_l		rolling-moment coefficient, $\frac{\text{Rolling moment}}{qSb}$
C_{l_β}		roll stability parameter, per degree
	(CM)	pitching-moment coefficient, $\frac{\text{Pitching moment}}{qS\bar{c}}$
$C_{m,o}$		pitching-moment coefficient at zero lift
C_n	(CN)	yawing-moment coefficient, $\frac{\text{Yawing moment}}{qSb}$
C_{n_β}		directional-stability parameter, per degree
C_p		pressure coefficient
ΔC_p		lifting pressure coefficient, $C_{p,l} - C_{p,u}$
C_Y		side-force coefficient, $\frac{\text{Side force}}{qS}$
C_{Y_β}		side-force parameter, per degree
c		chord length
$\bar{c}$		wing reference chord, 1.6861 ft
L/D	(L/D)	lift-drag ratio, C_L/C_D
M	(MACH)	Mach number
M_N		component of Mach number normal to leading edge
q	(DYN PRS)	dynamic pressure, psf
	(R/FT)	Reynolds number per foot
S		reference area, 2.5375 ft^2
x		longitudinal distance from nose of model (see fig. 1)
x'		$= x - x_{\text{LE}}$
y		coordinate in spanwise direction (see fig. 1)
z_c		camber coordinate with respect to reference plane
α	(ALPHA)	angle of attack, deg
β		$= \sqrt{M^2 - 1}$
Λ		sweep angle, deg
ψ		angle of yaw, deg
Subscripts:		
LE		leading edge
l		lower surface
min		minimum value
u		upper surface
Abbreviations:		
L.E.		leading edge
SDAS		Supersonic Design and Analysis System

Description of Models

The investigation included tests of four wing models: two cambered models designed by using different constraints on the leading-edge loadings, one cambered model that had no leading-edge constraints, and an uncambered flat-plate section that was used

Table A

Spanwise stations	Leading edge	Trailing edge
$0 \le y \le 0.3$	$x = 12y^2$	$x = 1.388097y^2 + 2.58618$
$0.3 \le y \le 0.6$	$x = 0.6377349 + 2.523619(y - 0.2692869)^{1/2}$	$x = 0.83286(y - 0.3) + 2.71111$
$0.6 \le y \le 0.95$	$x = 2.19418(y - 0.6) + 2.08901$	$x = 0.83286(y - 0.3) + 2.71111$
$0.95 \le y \le 1.0$	$(x - 3.106973)^2 + (y - 0.3971721)^2 = 0.3634$	$x = 0.83286(y - 0.3) + 2.71111$

for reference. All four wings had identical planforms and 3-percent-thick parabolic-arc airfoils with sharp leading and trailing edges. The three cambered wings were designed to have a value of C_L of 0.08 at zero angle of attack at the design Mach number of 2.4.

The planform selected for the series of wings is shown in figure 1 and described in table A. Note that the leading-edge sweep angles varied with spanwise position so as to give velocity components normal to the leading edge that varied from low subsonic for much of the inboard region to nearly sonic at the tip for the design Mach number of 2.4. A minimum body was included to house the strain-gauge balance for the force tests.

The first leading-edge constraint model was designed to have $M_N < 1$ everywhere along the leading edge. Leading-edge pressures for this model were developed by using elementary sweep theory with the leading-edge root C_p constrained to 0, as shown in figure 2. Suction pressures over the entire upper surface were constrained to stay within a pressure distribution that varied linearly from the leading edge (where the pressure was established by elementary sweep theory) to the trailing edge (where the limiting pressure was set at 70 percent of vacuum). The model designed by using these constraints shall be referred to as either "constrained ($M_N < 1$)" or "moderately constrained."

The second leading-edge constraint model was designed to have the upper- and lower-surface pressures equal at the leading edge. This constraint was imposed by choosing only those loadings that were 0 at the leading edge, which in turn required that the resultant leading edge be aligned everywhere with the local upwash. Additionally, the upper-surface pressures were constrained to values greater than 70-percent vacuum. This second constrained model shall be referred to as either "constrained ($\Delta C_{p,\mathrm{LE}} = 0$)" or "severely constrained." The third cambered design shall be referred to as the "unconstrained" design; however, in the unconstrained optimization, the 70-percent-vacuum limit on the upper-surface pressure was applied.

The geometry for the four models is given in tables I to IV (using the format of ref. 10). The reference moment centers were -0.29, -0.68, and -0.539 in. below the horizontal reference plane for the unconstrained, the moderately constrained, and the severely constrained models, respectively. For the three cambered models, camber surfaces at three different span stations are shown in figure 3. These three models were sheared to the zero horizontal reference plane at 70-percent chord.

Midspan pressure distributions as predicted by the design program for the three cambered models are shown in figure 4. The difference between lower C_p and upper C_p (that is, ΔC_p) was larger for the unconstrained model than for the moderately constrained model; and as required, ΔC_p is 0 at the leading edge of the severely constrained model. Figure 5 shows each of the four test models installed in the Langley Unitary Plan Wind Tunnel (UPWT).

Test Program

Wind-tunnel tests were conducted in the low Mach number leg of the Langley Unitary Plan Wind Tunnel. The cross-section dimensions of the test section are 4 ft by 4 ft, and the allowable Mach number range is from 1.469 to 2.869. Further information on this tunnel is available in reference 11.

Tests were conducted at a Reynolds number of 2×10^6 per foot. Boundary-layer transition was fixed on the models by means of a 0.063-in-wide strip of No. 50 carborundum grit located 0.4 in. aft of the model leading edge. Tests were conducted over a range of Mach numbers from 1.8 to 2.8 and a range of angle of attack from $-5°$ to $8°$.

Vapor-screen and oil-flow photographs were taken at the design Mach number for several angles of attack. For vapor-screen photographs, model preparation consisted of painting one coat of flat black paint over a coat of zinc chromate primer to reduce the glare of the lights. White dots (reference marks)

were painted on the model upper-surface centerline at locations where vapor-screen data were desired. A high-intensity tungsten light source mounted outside the tunnel on the sidewall was used to produce a thin light sheet across the tunnel test section. The light sheet was oriented normal to the flow and was positioned so that the model could be moved longitudinally to align the light sheet with all the white dots. Photographs were taken by a camera mounted to the ceiling inside the tunnel and located approximately 3 ft downstream from the model.

For the oil-flow photographs, the model surfaces were painted flat black, as done for the vapor-screen photographs. The model surface was then brushed with a mixture of 90W oil and yellow fluorescent dye. The model was illuminated by ultraviolet lamps, and photographs were taken through the window of the test section by using two cameras with Polaroid[1] adaptors mounted outside the tunnel on the sidewall door. During the tunnel start-up period, the model was kept in a wings-horizontal position to prevent the oil from running. To obtain photographs, the model was rolled 90° (wings vertical) and the angle of attack was set by yawing the model. After the model was positioned, a time period of approximately 3 to 4 min was required for the oil-flow pattern to stabilize. Normally, only three or four different angles of attack could be documented before the oil had to be replaced.

Nominal test conditions with a stagnation temperature of 125°F are summarized in the following chart:

M	Stagnation pressure, psf
1.8	1154
2.0	1253
2.16	1349
2.4	1520
2.6	1686
2.8	1873

Forces and moments were measured by means of a six-component strain-gauge balance contained within the model. The balance was attached through a supporting sting to the permanent strut support system in the wind tunnel. Base cavity pressures were measured by means of two tubes routed along the sting and connected to two pressure tranducers located outside the tunnel. These pressures were measured throughout the test program in order to correct the data to a condition of free-stream static pressure acting over the total model base. The data were corrected for deflections of the balance-sting combination due to aerodynamic loads and for test-section flow angularity.

[1] Polaroid: Registered trademark of Polaroid Corporation.

Presentation of Data

A tabular and graphical presentation of the wind-tunnel data is located in appendixes A and B, respectively, of this report.

Results and Discussion

The intent of this study was to assess the effect of leading-edge load constraints on the performance of the resultant designs. The approach was to design for a relatively low lift coefficient C_L of 0.08 at the design Mach number of 2.4, and then to evaluate the performance over a larger range in lift. The performance of the constrained wings in comparison with that of the two reference wings was determined by examining drag levels at several lift coefficients as a function of Mach number, pitching moment, and lift-drag ratio. These experimental results indicate that the constrained wings suffer penalties in drag and L/D at the lower lift coefficients, but the benefits of the constraints appear in drag levels and in L/D as lift is increased. This trend is more evident in the severely constrained wing than in the wing having the more moderate constraint.

In addition to the experimental data, some theoretically predicted results have been included to assess the effectiveness of using the SDAS design code (refs. 3 to 6) in predicting the actual levels of performance. The geometry input format was identical to that of reference 10, and the zero lift drag was obtained from the skin friction and far-field wave-drag portions of the SDAS. Lift, drag due to lift, and moments were obtained by using thin-wing lifting theory that did not include leading-edge thrust or vortex effects.

Theoretical drag-due-to-lift factors as predicted by the SDAS are shown in figure 6. These results follow the expected trend. The flat, unoptimized wing would be expected to have the highest drag due to lift, as predicted here. Likewise, the unconstrained optimization would also be expected to have the lowest drag due to lift. The application of constraints in the optimization process would be expected to produce values of the drag-due-to-lift factor somewhere between that for the flat wing and the unconstrained optimum values. The level of predicted drag due to lift on the constrained wing with $M_N < 1$ and the higher level on the constrained wing with $\Delta C_{p,\mathrm{LE}} = 0$ were the determining factors in calling

these wings moderately constrained and severely constrained, respectively. Note that the SDAS predicted the drag due to lift to be nearly as high for the more severely constrained wing as for the flat wing.

Experimental values of drag due to lift for each of the reference wings for each Mach number in the investigation are shown in figure 7 at the design lift coefficient of 0.08. Note at the design Mach number of 2.4 that the flat wing has approximately the level of drag due to lift that was predicted by the SDAS. However, this level is the lowest of the four wings. The unconstrained optimized wing produced the same level of drag due to lift as the flat wing at this lift coefficient, thus indicating no benefit for the cambered wing. The two constrained wings followed the expected trend; that is, the moderately constrained wing ($M_N < 1$) had a more moderate penalty in drag due to lift than the severely constrained wing ($\Delta C_{p,\mathrm{LE}} = 0$), although both had levels higher than predicted. The relative levels of drag due to lift of the four wings are seen to be different at the other Mach numbers.

Experimental and theoretical pitching-moment levels at zero lift are shown in figure 8. Generally, more positive levels of $C_{m,o}$ in a stable configuration indicate that less control deflection is required, and thus less trim drag results when the aircraft is trimmed at high lift conditions. These results indicate that the flat wing exhibits the most unfavorable $C_{m,o}$ and the unconstrained wing exhibits the most favorable. The constraints on the remaining designs reduced $C_{m,o}$ to more unfavorable values—again with the more severe constraint having the greater penalty. The theoretical predictions for $C_{m,o}$ at the design Mach number agreed well with the experimental results for all models. There was less agreement between theory and experiment at the other Mach numbers, especially for the severely constrained wing ($\Delta C_{p,\mathrm{LE}} = 0$).

Minimum drag as a function of Mach number is shown in figure 9 for each of the models. These results, along with the drag levels at zero lift (fig. 10), are an indication of camber severity. The drag levels shown indicate that the camber drag for the moderately constrained model is about equal to that of the unconstrained models. A more severe penalty in camber drag is indicated for the constrained model with $\Delta C_{p,\mathrm{LE}} = 0$, again indicating why it is called severely constrained. Theoretical predictions for zero lift drag were higher than the measured values, although the relative levels for the different wings were correctly predicted. Both the theoretical and experimental data show a slight decrease in the drag at zero lift with increasing Mach number.

Drag values at the design lift coefficient for each of the wings are shown in figure 11. Theoretical predictions by the SDAS are also shown in figure 11, and in the center plot the experimental values for the four wings are overlayed. The theoretical predictions for the drag at design lift are lower than the experimental values for the three cambered wings but are higher for the flat wing. The leading edges of the models actually displayed a small radius and, as noted, thrust effects were not accounted for in the SDAS. This lower experimental drag for the flat wing probably indicates some leading-edge thrust effects. The predicted levels of drag differ from experimental values by, at most, 10 drag counts, with the agreement at Mach 2.4 being even better. The overlay of the experimental points shows that at the design Mach number, the drag levels for the flat and unconstrained models were nearly equal. The penalty for using a constraint in the optimization remains evident at this lift coefficient. Again, relative drag levels at the other Mach numbers vary, but the penalty for the severe constraint remains evident.

To get an indication of the effect of the constraints on drag at higher lift coefficients, the drag level at $C_L = 0.18$ for each of the models is shown as a function of Mach number in figure 12. The benefits in reducing drag levels displayed by the two constrained models is now evident. There has been a complete reversal in relative drag levels displayed by the four wings, with the two constrained models now having the lowest drag. The more severely constrained model displays a slightly lower level of drag than that of the moderately constrained model.

The effect of the two constraints on the performance of these models as a function of lift coefficient is shown in figure 13 in terms of lift-drag ratio for each Mach number. Indicated on each plot in figure 13 is the wing giving the best performance for a given C_L region. At all Mach numbers, the two constrained wings performed better at the higher values of C_L than either the unconstrained or flat wing; and in all cases the severely constrained wing showed better performance at the highest values of C_L included in this study. In figure 13(a), for example, the best performance at $M = 1.8$ was achieved by the severely constrained wing, which attained a value of L/D of about 8.95 at $C_L \approx 0.145$. At this Mach number, the severely constrained wing maintained its better performance over the other wings as C_L increased. The exception to this was the moderately constrained wing that gave a slightly better performance at values of C_L between 0.062 and 0.128. Below $C_L = 0.062$, the flat wing showed the best performance. At Mach 2.0 (fig. 13(b)), the moderately constrained wing gave the best performance

from $C_L = 0.032$ to as high as $C_L = 0.234$, which included most of the range shown in figure 13. For Mach numbers of 2.16, 2.4, and 2.6 (figs. 13(c), (d), and (e), respectively), each of the wings had a region of best performance, with the moderately and severely constrained always being best at the higher values of C_L. At Mach 2.8 (fig. 13(f)), the unconstrained wing had no area in which it outperformed the other wings, whereas the constrained wings continued to give good performance at the higher lift coefficients. These performance plots show that the benefit of the leading-edge constraints does appear at the higher lift conditions.

The ranges of best performance for each of the wings at each Mach number are summarized in figure 14. The benefits of the leading-edge constraints at the higher lift coefficients are evident throughout the Mach number range shown. Also evident from this figure is the fact that the wing with the more severe constraint performs better over a larger range in lift at the higher lift conditions. Another observation that should be noted concerns the unconstrained design. This wing, as expected, has the best performance at and around the design condition, but its region of best performance decreases to 0 at Mach 2 and 2.8. Thus, it seems that an added benefit of the constrained wings is their ability to maintain their regions of better performance over a larger range of Mach numbers.

Flow-Visualization Results

Flow-visualization photographs indicate that a smoother flow pattern is maintained to higher lift conditions on the two constrained wings than on the two reference wings. Some insight into flow phenomena that occur on each of the four wing designs can be seen in the photographs presented in figures 15 to 18. Photographs of oil flows at $\alpha = 0°$ and 5° and a vapor-screen photograph at $\alpha = 5°$ are shown for each model.

The flow pattern of figure 15(a) indicates the very smooth, attached potential flow for the uncambered flat wing at $\alpha = 0°$. At $\alpha = 5°$, which represents a value of C_L of 0.135, the photograph in figure 15(b) shows evidence of vortices trailing back over the wing from the region near the nose on the leading edge. Some slight separation is also indicated near the outboard regions of the trailing edge. The vapor-screen photograph of figure 15(c) shows evidence of the vortex from the nose region and a region of separation near the leading edge (ref. 12).

Photographs for the unconstrained wing are shown in figure 16. In the photograph of the oil flow at $\alpha = 0°$ (fig. 16(a)), evidence can be seen of vortex flow behind that portion of the leading edge with greatest sweep. The vapor screen at this condition, which is not shown, does indicate some slight degree of separation behind the nose region. The lift coefficient of the unconstrained model at an angle of attack of 5° is approximately 0.198. The oil flow at this angle of attack shows a very complicated flow pattern. There is evidence of vortex flow just outboard of the root chord as well as at several regions along the leading edge and at the tip of the trailing edge that show indications of flow separation. Also, there is strong spanwise flow all along the trailing edge. The accompanying vapor-screen photograph indicates a well-formed vortex inboard and a separation region near the leading edge.

The flow at $\alpha = 0°$ with $C_L = 0.064$ for the moderately constrained wing ($M_N < 1$) appears to be smooth and attached (fig. 17(a)). Although the flow has a slight spanwise tendency near the root of the trailing edge, there appears to be no separation or vortex flow. At $\alpha = 5°$ with $C_L = 0.192$ (fig. 17(b)), the flow again becomes quite complicated. There is evidence of two vortices trailing behind the leading edge and extreme spanwise flow near the trailing edge. Regions of separation are seen in at least two places along the leading edge and at the trailing edge. Evidence of the vortex flow can be seen in the accompanying vapor-screen photograph (fig. 17(c)), which also indicates some separation near the leading edge.

Flow-visualization photographs for the most severely constrained wing ($\Delta C_{p,\mathrm{LE}} = 0$) are shown in figure 18. At the design C_L with $\alpha = 0°$, the flow near the front and outboard portions of the wing appears very smooth and attached. Although there is some spanwise flow near the root of the trailing edge that meets a slightly inward flow near the shoulder region of the wing, there is no evidence of any vortices or separation. When the wing is placed at $\alpha = 5°$, its accompanying lift coefficient is 0.198. The flow patterns for $\alpha = 5°$ are shown in figure 18(b). The flow continues to look smooth and attached on the forward parts of the wing. There appears to be a region of vortex flow near the base of the root chord, and slight areas of separation are evident along the tip regions of the trailing edge. Some slight areas of separation near the leading edge are verified by the accompanying vapor-screen photographs. A weaker vortex is partially hidden by the wing camber.

In summary, at an angle of attack of 0°, the flat wing displays the smoothest flow pattern, but this pattern apparently degenerates rapidly with angle of attack as does performance. These oil-flow photographs clearly show that the severely constrained wing displays the desired characteristic of being able to suppress the formation of vortices and separa-

tion to a higher angle of attack, thus explaining why it achieved the best performance at the higher lift coefficients.

Conclusions

In an attempt to design wings for higher lift at supersonic speeds and yet delay the separation and vortex flows that often occur on highly swept, sharp-leading-edge wings, two wings were designed by using linear-theory methods in which constraints were placed on the allowable leading-edge pressures. Based on experimental results, the following conclusions are presented:

1. When employing linear-theory design methods, the use of constraints that limit pressure loadings on the leading edge result in designs that have enhanced performance at the higher lift conditions, when compared with designs with no such constraints. This enhancement may, however, suffer because of increased trim drag.

2. Of the two constrained wings, the one having the more severe constraint, although suffering a greater penalty in performance at the lower lift coefficients, performs better over a larger range in lift at the higher lift coefficients.

3. The constraints on the leading edge were successful in delaying flow separation and the formation of vortices since the regions of separated flow were mildest on the severely and moderately constrained wings when compared with flow patterns on the flat and unconstrained wings at the same angle of attack.

4. Theoretical drag predictions from the Supersonic Design and Analysis System (SDAS) design code were slightly low for the cambered wings but were all within 10 counts of the experimental values.

NASA Langley Research Center
Hampton, VA 23665
April 1, 1985

References

1. Carlson, Harry W.; and Middleton, Wilbur D.: *A Numerical Method for the Design of Camber Surfaces of Supersonic Wings With Arbitrary Planforms.* NASA TN D-2341, 1964.
2. Sorrells, Russell B.; and Miller, David S.: *Numerical Method for Design of Minimum-Drag Supersonic Wing Camber With Constraints on Pitching Moment and Surface Deformation.* NASA TN D-7097, 1972.
3. Middleton, W. D.; and Lundry, J. L.: *A System for Aerodynamic Design and Analysis of Supersonic Aircraft. Part 1—General Description and Theoretical Development.* NASA CR-3351, 1980.
4. Middleton, W. D.; Lundry, J. L.; and Coleman, R. G.: *A System for Aerodynamic Design and Analysis of Supersonic Aircraft. Part 2—User's Manual.* NASA CR-3352, 1980.
5. Middleton, W. D.; Lundry, J. L.; and Coleman, R. G.: *A System for Aerodynamic Design and Analysis of Supersonic Aircraft. Part 3—Computer Program Description.* NASA CR-3353, 1980.
6. Middleton, W. D.; and Lundry, J. L.: *A System for Aerodynamic Design and Analysis of Supersonic Aircraft. Part 4—Test Cases.* NASA CR-3354, 1980.
7. Robins, A. Warner; Carlson, Harry W.; and Mack, Robert J.: *Supersonic Wings With Significant Leading-Edge Thrust at Cruise.* NASA TP-1632, 1980.
8. Robins, A. Warner; Lamb, Milton; and Miller, David S.: *Aerodynamic Characteristics at Mach Numbers of 1.5, 1.8, and 2.0 of a Blended Wing-Body Configuration With and Without Integral Canards.* NASA TP-1427, 1979.
9. Darden, Christine M.: The Influence of Leading-Edge Load Alleviation on Supersonic Wing Design. AIAA-84-0138, Jan. 1984.
10. Craidon, Charlotte B.: *Description of a Digital Computer Program for Airplane Configuration Plots.* NASA TM X-2074, 1970.
11. Jackson, Charlie M., Jr.; Corlett, William A.; and Monta, William J.: *Description and Calibration of the Langley Unitary Plan Wind Tunnel.* NASA TP-1905, 1981.
12. Miller, David S.; and Wood, Richard M.: An Investigation of Wing Leading-Edge Vortices at Supersonic Speeds. AIAA-83-1816, July 1983.

TABLE I. NUMERICAL DESCRIPTION OF FLAT WING

```
  1   1                  20  20                                                   GEOM 3
2.5375 1.6856 1.4392
  0.000   0.500   0.750   1.250   2.500   5.000   7.500  10.000  20.000  30.000   GEOM 5
 40.000  50.000  60.000  70.000  75.000  80.000  85.000  90.000  95.000100.000    GEOM 5
  0.000   0.000   0.000   2.584                                                   GEOM 6
  0.008   0.025   0.000   2.577                                                   GEOM 6
  0.030   0.050   0.000   2.558                                                   GEOM 6
  0.067   0.075   0.000   2.524                                                   GEOM 6
  0.120   0.100   0.000   2.478                                                   GEOM 6
  0.187   0.125   0.000   2.418                                                   GEOM 6
  0.270   0.150   0.000   2.345                                                   GEOM 6
  0.375   0.175   0.000   2.253                                                   GEOM 6
  0.480   0.200   0.000   2.160                                                   GEOM 6
  0.749   0.250   0.000   1.921                                                   GEOM 6
  1.079   0.300   0.000   1.630                                                   GEOM 6
  1.354   0.350  00.000   1.397                                                   GEOM 6
  1.549   0.400  00.000   1.243                                                   GEOM 6
  1.848   0.500  00.000   1.027                                                   GEOM 6
  2.087   0.600  00.000   0.871                                                   GEOM 6
  2.307   0.700  00.000   0.735                                                   GEOM 6
  2.526   0.800  00.000   0.599                                                   GEOM 6
  2.745   0.900  00.000   0.463                                                   GEOM 6
  2.855   0.950  00.000   0.395                                                   GEOM 6
  2.964   1.000  00.000   0.327                                                   GEOM 6
 0.0000  0.0000  0.0000  0.0000  0.0000  0.0000  0.0000  0.0000  0.0000  0.0000   GEOM 7
 0.0000  0.0000  0.0000  0.0000  0.0000  0.0000  0.0000  0.0000  0.0000  0.0000   GEOM 7
 0.0000  0.0000  0.0000  0.0000  0.0000  0.0000  0.0000  0.0000  0.0000  0.0000   GEOM 7
 0.0000  0.0000  0.0000  0.0000  0.0000  0.0000  0.0000  0.0000  0.0000  0.0000   GEOM 7
 0.0000  0.0000  0.0000  0.0000  0.0000  0.0000  0.0000  0.0000  0.0000  0.0000   GEOM 7
 0.0000  0.0000  0.0000  0.0000  0.0000  0.0000  0.0000  0.0000  0.0000  0.0000   GEOM 7
 0.0000  0.0000  0.0000  0.0000  0.0000  0.0000  0.0000  0.0000  0.0000  0.0000   GEOM 7
 0.0000  0.0000  0.0000  0.0000  0.0000  0.0000  0.0000  0.0000  0.0000  0.0000   GEOM 7
 0.0000  0.0000  0.0000  0.0000  0.0000  0.0000  0.0000  0.0000  0.0000  0.0000   GEOM 7
 0.0000  0.0000  0.0000  0.0000  0.0000  0.0000  0.0000  0.0000  0.0000  0.0000   GEOM 7
 0.0000  0.0000  0.0000  0.0000  0.0000  0.0000  0.0000  0.0000  0.0000  0.0000   GEOM 7
 0.0000  0.0000  0.0000  0.0000  0.0000  0.0000  0.0000  0.0000  0.0000  0.0000   GEOM 7
 0.0000  0.0000  0.0000  0.0000  0.0000  0.0000  0.0000  0.0000  0.0000  0.0000   GEOM 7
 0.0000  0.0000  0.0000  0.0000  0.0000  0.0000  0.0000  0.0000  0.0000  0.0000   GEOM 7
 0.0000  0.0000  0.0000  0.0000  0.0000  0.0000  0.0000  0.0000  0.0000  0.0000   GEOM 7
 0.0000  0.0000  0.0000  0.0000  0.0000  0.0000  0.0000  0.0000  0.0000  0.0000   GEOM 7
 0.0000  0.0000  0.0000  0.0000  0.0000  0.0000  0.0000  0.0000  0.0000  0.0000   GEOM 7
 0.0000  0.0000  0.0000  0.0000  0.0000  0.0000  0.0000  0.0000  0.0000  0.0000   GEOM 7
 0.0000  0.0000  0.0000  0.0000  0.0000  0.0000  0.0000  0.0000  0.0000  0.0000   GEOM 7
 0.0000  0.0000  0.0000  0.0000  0.0000  0.0000  0.0000  0.0000  0.0000  0.0000   GEOM 7
 0.0000  0.0000  0.0000  0.0000  0.0000  0.0000  0.0000  0.0000  0.0000  0.0000   GEOM 7
 0.0000  0.0000  0.0000  0.0000  0.0000  0.0000  0.0000  0.0000  0.0000  0.0000   GEOM 7
 0.0000  0.0000  0.0000  0.0000  0.0000  0.0000  0.0000  0.0000  0.0000  0.0000   GEOM 7
 0.0000  0.0000  0.0000  0.0000  0.0000  0.0000  0.0000  0.0000  0.0000  0.0000   GEOM 7
 0.0000  0.0000  0.0000  0.0000  0.0000  0.0000  0.0000  0.0000  0.0000  0.0000   GEOM 7
 0.0000  0.0000  0.0000  0.0000  0.0000  0.0000  0.0000  0.0000  0.0000  0.0000   GEOM 7
 0.0000  0.0000  0.0000  0.0000  0.0000  0.0000  0.0000  0.0000  0.0000  0.0000   GEOM 7
 0.0000  0.0000  0.0000  0.0000  0.0000  0.0000  0.0000  0.0000  0.0000  0.0000   GEOM 7
 0.0000  0.0000  0.0000  0.0000  0.0000  0.0000  0.0000  0.0000  0.0000  0.0000   GEOM 7
 0.0000  0.0000  0.0000  0.0000  0.0000  0.0000  0.0000  0.0000  0.0000  0.0000   GEOM 7
 0.0000  0.0000  0.0000  0.0000  0.0000  0.0000  0.0000  0.0000  0.0000  0.0000   GEOM 7
 0.0000  0.0000  0.0000  0.0000  0.0000  0.0000  0.0000  0.0000  0.0000  0.0000   GEOM 7
```

TABLE I. Concluded

0.0000	0.0000	0.0000	0.0000	0.0000	0.0000	0.0000	0.0000	0.0000	0.0000	GEOM 7
0.0000	0.0000	0.0000	0.0000	0.0000	0.0000	0.0000	0.0000	0.0000	0.0000	GEOM 7
0.0000	0.0000	0.0000	0.0000	0.0000	0.0000	0.0000	0.0000	0.0000	0.0000	GEOM 7
0.0000	0.0000	0.0000	0.0000	0.0000	0.0000	0.0000	0.0000	0.0000	0.0000	GEOM 7
0.0000	0.0000	0.0000	0.0000	0.0000	0.0000	0.0000	0.0000	0.0000	0.0000	GEOM 7
0.0000	0.0000	0.0000	0.0000	0.0000	0.0000	0.0000	0.0000	0.0000	0.0000	GEOM 7
0.0000	0.0000	0.0000	0.0000	0.0000	0.0000	0.0000	0.0000	0.0000	0.0000	GEOM 7
0.0000	0.0000	0.0000	0.0000	0.0000	0.0000	0.0000	0.0000	0.0000	0.0000	GEOM 7
0.0000	0.0000	0.0000	0.0000	0.0000	0.0000	0.0000	0.0000	0.0000	0.0000	GEOM 7
0.0000	0.0000	0.0000	0.0000	0.0000	0.0000	0.0000	0.0000	0.0000	0.0000	GEOM 7
0.0000	0.0000	0.0000	0.0000	0.0000	0.0000	0.0000	0.0000	0.0000	0.0000	GEOM 7
0.0	.02985	.04466	.07406	.14625	.28500	.41625	.54000	.96000	1.2600	GEOM8
1.4400	1.5000	1.4400	1.2600	1.1250	.96000	.76500	.54000	.28500	0.00	GEOM8
0.0	.02985	.04466	.07406	.14625	.28500	.41625	.54000	.96000	1.2600	GEOM8
1.4400	1.5000	1.4400	1.2600	1.1250	.96000	.76500	.54000	.28500	0.00	GEOM8
0.0	.02985	.04466	.07406	.14625	.28500	.41625	.54000	.96 00	1.2600	GEOM8
1.4400	1.5000	1.4400	1.2600	1.1250	.96000	.76500	.54000	.28500	0.00	GEOM8
0.0	.02985	.04466	.07406	.14625	.28500	.41625	.54000	.96000	1.2600	GEOM8
1.4400	1.5000	1.4400	1.2600	1.1250	.96000	.76500	.54000	.28500	0.00	GEOM8
0.0	.02985	.04466	.07406	.14625	.28500	.41625	.54000	.96000	1.2600	GEOM8
1.4400	1.5000	1.4400	1.2600	1.1250	.96000	.76500	.54000	.28500	0.00	GEOM8
0.0	.02985	.04466	.07406	.14625	.28500	.41625	.54000	.96000	1.2600	GEOM8
1.4400	1.5000	1.4400	1.2600	1.1250	.96000	.76500	.54000	.28500	0.00	GEOM8
0.0	.02985	.04466	.07406	.14625	.28500	.41625	.54000	.96000	1.2600	GEOM8
1.4400	1.5000	1.4400	1.2600	1.1250	.96000	.76500	.54000	.28500	0.00	GEOM8
0.0	.02985	.04466	.07406	.14625	.28500	.41625	.54000	.96000	1.2600	GEOM8
1.4400	1.5000	1.4400	1.2600	1.1250	.96000	.76500	.54000	.28500	0.00	GEOM8
0.0	.02985	.04466	.07406	.14625	.28500	.41625	.54000	.96000	1.2600	GEOM8
1.4400	1.5000	1.4400	1.2600	1.1250	.96000	.76500	.54000	.28500	0.00	GEOM8
0.0	.02985	.04466	.07406	.14625	.28500	.41625	.54000	.96000	1.2600	GEOM8
1.4400	1.5000	1.4400	1.2600	1.1250	.96000	.76500	.54000	.28500	0.00	GEOM8
0.0	.02985	.04466	.07406	.14625	.28500	.41625	.54000	.96000	1.2600	GEOM8
1.4400	1.5000	1.4400	1.2600	1.1250	.96000	.76500	.54000	.28500	0.00	GEOM8
0.0	.02985	.04466	.07406	.14625	.28500	.41625	.54000	.96000	1.2600	GEOM8
1.4400	1.5000	1.4400	1.2600	1.1250	.96000	.76500	.54000	.28500	0.00	GEOM8
0.0	.02985	.04466	.07406	.14625	.28500	.41625	.54000	.96000	1.2600	GEOM8
1.4400	1.5000	1.4400	1.2600	1.1250	.96000	.76500	.54000	.28500	0.00	GEOM8
0.0	.02985	.04466	.07406	.14625	.28500	.41625	.54000	.96000	1.2600	GEOM8
1.4400	1.5000	1.4400	1.2600	1.1250	.96000	.76500	.54000	.28500	0.00	GEOM8
0.0	.02985	.04466	.07406	.14625	.28500	.41625	.54000	.96000	1.2600	GEOM8
1.4400	1.5000	1.4400	1.2600	1.1250	.96000	.76500	.54000	.28500	0.00	GEOM8
0.0	.02985	.04466	.07406	.14625	.28500	.41625	.54000	.96000	1.2600	GEOM8
1.4400	1.5000	1.4400	1.2600	1.1250	.96000	.76500	.54000	.28500	0.00	GEOM8
0.0	.02985	.04466	.07406	.14625	.28500	.41625	.54000	.96000	1.2600	GEOM8
1.4400	1.5000	1.4400	1.2600	1.1250	.96000	.76500	.54000	.28500	0.00	GEOM8
0.0	.02985	.04466	.07406	.14625	.28500	.41625	.54000	.96000	1.2600	GEOM8
1.4400	1.5000	1.4400	1.2600	1.1250	.96000	.76500	.54000	.28500	0.00	GEOM8
0.0	.02985	.04466	.07406	.14625	.28500	.41625	.54000	.96000	1.2600	GEOM8
1.4400	1.5000	1.4400	1.2600	1.1250	.96000	.76500	.54000	.28500	0.00	GEOM8
0.0	.02985	.04466	.07406	.14625	.28500	.41625	.54000	.96000	1.2600	GEOM8
1.4400	1.5000	1.4400	1.2600	1.1250	.96000	.76500	.54000	.28500	0.00	GEOM8

TABLE II. NUMERICAL DESCRIPTION OF UNCONSTRAINED CAMBERED WING WITH $C_L = 0.08$

```
  1  1                    20 20                                                    GEOM 3
2.5375 1.6856 1.4392
  0.000  0.500  0.750  1.250  2.500  5.000  7.500 10.000 20.000 30.000  GEOM 5
 40.000 50.000 60.000 70.000 75.000 80.000 85.000 90.000 95.000100.000  GEOM 5
  0.000  0.000  0.000  2.594                                                      GEOM 6
  0.008  0.025  0.000  2.577                                                      GEOM 6
  0.030  0.050  0.000  2.558                                                      GEOM 6
  0.067  0.075  0.000  2.524                                                      GEOM 6
  0.120  0.100  0.000  2.478                                                      GEOM 6
  0.187  0.125  0.000  2.418                                                      GEOM 6
  0.270  0.150  0.000  2.345                                                      GEOM 6
 0.375  0.175  0.000  2.253                                                      GEOM 6-8
  0.480  0.200  0.000  2.160                                                      GEOM 6
  0.749  0.250  0.000  1.921                                                      GEOM 6
  1.079  0.300  0.000  1.630                                                      GEOM 6
  1.354  0.350 00.000  1.397                                                      GEOM 6
  1.549  0.400 00.000  1.243                                                      GEOM 6
  1.848  0.500 00.000  1.027                                                      GEOM 6
  2.087  0.600 00.000  0.871                                                      GEOM 6
  2.307  0.700 00.000  0.735                                                      GEOM 6
  2.526  0.8 0 00.000  0.599                                                      GEOM 6
  2.745  0.900 00.000  0.463                                                      GEOM 6
  2.855  0.950 00.000  0.395                                                      GEOM 6
  2.964  1.000 00.000  0.327                                                      GEOM 6
 0.1182 0.1173 0.1168 0.1159 0.1135 0.1083 0.1025 0.0965 0.0721 0.0494  GEOM 7
 0.0307 0.0163 0.0063-0.0000-0.0023-0.0040-0.0057-0.0075-0.0098-0.0130  GEOM 7
 0.1347 0.1337 0.1332 0.1323 0.1299 0.1245 0.1186 0.1127 0.0875 0.0633  GEOM 7
 0.0421 0.0246 0.0108-0.0000-0.0046-0.0091-0.0136-0.0184-0.0237-0.0301  GEOM 7
 0.1380 0.1371 0.1367 0.1358 0.1336 0.1286 0.1231 0.1173 0.0924 0.0679  GEOM 7
 0.0459 0.0275 0.0124-0.0000-0.0054-0.0107-0.0156-0.0213-0.0274-0.0344  GEOM 7
 0.1378 0.1371 0.1367 0.1360 0.1342 0.1299 0.1248 0.1193 0.0952 0.0708  GEOM 7
 0.0484 0.0291 0.0132-0.0000-0.0059-0.0115-0.0169-0.0226-0.0288-0.0357  GEOM 7
 0.1345 0.1340 0.1338 0.1334 0.1323 0.1290 0.1247 0.1195 0.0968 0.0727  GEOM 7
 0.0501 0.0304 0.0139 0.0000-0.0061-0.0117-0.0173-0.0228-0.0285-0.0350  GEOM 7
 0.1290 0.1289 0.1289 0.1288 0.1286 0.1259 0.1224 0.1183 0.0970 0.0737  GEOM 7
 0.0513 0.0313 0.0141 0.0000-0.0062-0.0117-0.0171-0.0222-0.0274-0.0331  GEOM 7
 0.1250 0.1252 0.1253 0.1254 0.1260 0.1252 0.1223 0.1187 0.0986 0.0756  GEOM 7
 0.0529 0.0323 0.0146 0.0000-0.0062-0.0118-0.0169-0.0217-0.0263-0.0312  GEOM 7
 .11745 .11790 .11815 .11855 .11970 .12040 .11865 .11570 .09790 .07600  GEOM7-15
 .05365 .03290 .01485 .00000-.00620-.01175-.01166-.02105-.02515-.02930  GEOM7-16
 0.1099 0.1106 0.1110 0.1117 0.1134 0.1156 0.1150 0.1127 0.0972 0.0764  GEOM 7
 0.0544 0.0335 0.0151-0.0000-0.0062-0.0117-0.0163-0.0204-0.0240-0.0274  GEOM 7
 0.0871 0.0882 0.0888 0.0899 0.0926 0.0977 0.1000 0.0997 0.0902 0.0728  GEOM 7
 0.0527 0.0329 0.0151-0.0000-0.0063-0.0119-0.0166-0.0207-0.0240-0.0268  GEOM 7
 0.0357 0.0371 0.0377 0.0391 0.0424 0.0487 0.0531 0.0557 0.0560 0.0485  GEOM 7
 0.0374 0.0249 0.0122-0.0000-0.0056-0.0110-0.0159-0.0204-0.0245-0.0282  GEOM 7
 0.0095 0.0105 0.0110 0.0120 0.0144 0.0189 0.0224 0.0246 0.0280 0.0264  GEOM 7
 0.0218 0.0153 0.0079-0.0000-0.0040-0.0079-0.0119-0.0156-0.0194-0.0229  GEOM 7
 0.0059 0.0066 0.0069 0.0076 0.0092 0.0123 0.0142 0.0157 0.0184 0.0176  GEOM 7
 0.0148 0.0104 0.0054-0.0000-0.0028-0.0057-0.0085-0.0113-0.0141-0.0169  GEOM 7
 0.0026 0.0029 0.0030 0.0033 0.0041 0.0053 0.0065 0.0073 0.0090 0.0088  GEOM 7
 0.0075 0.0055 0.0029-0.0000-0.0015-0.0031-0.0047-0.0063-0.0079-0.0096  GEOM 7
 0.0018 0.0019 0.0020 0.0021 0.0024 0.0029 0.0035 0.0039 0.0048 0.0046  GEOM 7
```

TABLE II. Concluded

```
 0.0040 0.0028 0.0015-0.0000-0.0007-0.0016-0.0024-0.0032-0.0040-0.0049  GEOM 7
 0.0007 0.0008 0.0008 0.0009 0.0010 0.0013 0.0016 0.0018 0.0023 0.0023  GEOM 7
 0.0019 0.0014 0.0008-0.0000-0.0003-0.0007-0.0011-0.0014-0.0018-0.0023  GEOM 7
-0.0012-0.0012-0.0011-0.0011-0.0010-0.0009-0.0007-0.0005 0.0001 0.0003  GEOM 7
 0.0004 0.0003 0.0002-0.0000-0.0001-0.0002-0.0003-0.0004-0.0005-0.0006  GEOM 7
-0.0020-0.0020-0.0019-0.0019-0.0019-0.0018-0.0016-0.0015-0.0010-0.0007  GEOM 7
-0.0004-0.0003-0.0001 0.0000 0.0001 0.0002 0.0002 0.0003 0.0003 0.0003  GEOM 7
-0.0019-0.0019-0.0019-0.0018-0.0018-0.0017-0.0016-0.0015-0.0011-0.0008  GEOM 7
-0.0005-0.0002-0.0001-0.0000-0.0000-0.0001-0.0001-0.0003-0.0004-0.0006  GEOM 7
-0.0063-0.0063-0.0063-0.0063-0.0063-0.0062-0.0062-0.0061-0.0059-0.0048  GEOM 7
-0.0038-0.0026-0.0013 0.0000 0.0007 0.0013 0.0020 0.0026 0.0033 0.0039  GEOM 7
0.0     .02985 .04466 .07406 .14625 .28500 .41625 .54000 .96000 1.2600   GEOM8-11
1.4400 1.5000 1.4400 1.2600 1.1250 .96000 .76500 .54000 .28500 0.00      GEOM8-12
0.0     .02985 .04466 .07406 .14625 .28500 .41625 .54000 .96000 1.2600   GEOM8-13
1.4400 1.5000 1.4400 1.2600 1.1250 .96000 .76500 .54000 .28500 0.00      GEOM8-14
0.0     .02985 .04466 .07406 .14625 .28500 .41625 .54000 .96 00 1.2600   GEOM8-15
1.4400 1.5000 1.4400 1.2600 1.1250 .96000 .76500 .54000 .28500 0.00      GEOM8-16
0.0     .02985 .04466 .07406 .14625 .28500 .41625 .54000 .96000 1.2600   GEOM8-17
1.4400 1.5000 1.4400 1.2600 1.1250 .96000 .76500 .54000 .28500 0.00      GEOM8-18
0.0     .02985 .04466 .07406 .14625 .28500 .41625 .54000 .96000 1.2600   GEOM8-19
1.4400 1.5000 1.4400 1.2600 1.1250 .96000 .76500 .54000 .28500 0.00      GEOM8-20
0.0     .02985 .04466 .07406 .14625 .28500 .41625 .54000 .96000 1.2600   GEOM8-21
1.4400 1.5000 1.4400 1.2600 1.1250 .96000 .76500 .54000 .28500 0.00      GEOM8-22
0.0     .02985 .04466 .07406 .14625 .28500 .41625 .54000 .96000 1.2600   GEOM8-23
1.4400 1.5000 1.4400 1.2600 1.1250 .96000 .76500 .54000 .28500 0.00      GEOM8-24
0.0     .02985 .04466 .07406 .14625 .28500 .41625 .54000 .96000 1.2600   GEOM8-25
1.4400 1.5000 1.4400 1.2600 1.1250 .96000 .76500 .54000 .28500 0.00      GEOM8-26
0.0     .02985 .04466 .07406 .14625 .28500 .41625 .54000 .96000 1.2600   GEOM8-27
1.4400 1.5000 1.4400 1.2600 1.1250 .96000 .76500 .54000 .28500 0.00      GEOM8-28
0.0     .02985 .04466 .07406 .14625 .28500 .41625 .54000 .96000 1.2600   GEOM8-29
1.4400 1.5000 1.4400 1.2600 1.1250 .96000 .76500 .54000 .28500 0.00      GEOM8-30
0.0     .02985 .04466 .07406 .14625 .28500 .41625 .54000 .96000 1.2600   GEOM8-31
1.4400 1.5000 1.4400 1.2600 1.1250 .96000 .76500 .54000 .28500 0.00      GEOM8-32
0.0     .02985 .04466 .07406 .14625 .28500 .41625 .54000 .96000 1.2600   GEOM8-33
1.4400 1.5000 1.4400 1.2600 1.1250 .96000 .76500 .54000 .28500 0.00      GEOM8-34
0.0     .02985 .04466 .07406 .14625 .28500 .41625 .54000 .96000 1.2600   GEOM8-35
1.4400 1.5000 1.4400 1.2600 1.1250 .96000 .76500 .54000 .28500 0.00      GEOM8-36
0.0     .02985 .04466 .07406 .14625 .28500 .41625 .54000 .96000 1.2600   GEOM8-37
1.4400 1.5000 1.4400 1.2600 1.1250 .96000 .76500 .54000 .28500 0.00      GEOM8-38
0.0     .02985 .04466 .07406 .14625 .28500 .41625 .54000 .96000 1.2600   GEOM8-39
1.4400 1.5000 1.4400 1.2600 1.1250 .96000 .76500 .54000 .28500 0.00      GEOM8-40
0.0     .02985 .04466 .07406 .14625 .28500 .41625 .54000 .96000 1.2600   GEOM8-41
1.4400 1.5000 1.4400 1.2600 1.1250 .96000 .76500 .54000 .28500 0.00      GEOM8-42
0.0     .02985 .04466 .07406 .14625 .28500 .41625 .54000 .96000 1.2600   GEOM8-43
1.4400 1.5000 1.4400 1.2600 1.1250 .96000 .76500 .54000 .28500 0.00      GEOM8-44
0.0     .02985 .04466 .07406 .14625 .28500 .41625 .54000 .96000 1.2600   GEOM8-45
1.4400 1.5000 1.4400 1.2600 1.1250 .96000 .76500 .54000 .28500 0.00      GEOM8-46
0.0     .02985 .04466 .07406 .14625 .28500 .41625 .54000 .96000 1.2600   GEOM8-47
1.4400 1.5000 1.4400 1.2600 1.1250 .96000 .76500 .54000 .28500 0.00      GEOM8-48
0.0     .02985 .04466 .07406 .14625 .28500 .41625 .54000 .96000 1.2600   GEOM8-49
1.4400 1.5000 1.4400 1.2600 1.1250 .96000 .76500 .54000 .28500 0.00      GEOM8-50
```

TABLE III. NUMERICAL DESCRIPTION OF MODERATELY CONSTRAINED WING ($M_N < 1$) WITH $C_L = 0.08$

```
  1  1                      20 20                                                    GEOM 3
2.5375 1.6856 1.4392
  0.000  0.500  0.750  1.250  2.500  5.000  7.500 10.000 20.000 30.000  GEOM 5
 40.000 50.000 60.000 70.000 75.000 80.000 85.000 90.000 95.000100.000  GEOM 5
  0.000  0.000  0.000  2.584                                             GEOM 6
  0.008  0.025  0.000  2.577                                             GEOM 6
  0.030  0.050  0.000  2.558                                             GEOM 6
  0.067  0.075  0.000  2.524                                             GEOM 6
  0.120  0.100  0.000  2.476                                             GEOM 6
  0.187  0.125  0.000  2.418                                             GEOM 6
  0.270  0.150  0.000  2.345                                             GEOM 6
  0.375  0.175  0.000  2.253                                             GEOM 6
  0.480  0.200  0.000  2.150                                             GEOM 6
  0.749  0.250  0.000  1.921                                             GEOM 6
  1.079  0.300  0.000  1.630                                             GEOM 6
  1.354  0.350 00.000  1.397                                             GEOM 6
  1.549  0.400 00.000  1.243                                             GEOM 6
  1.848  0.500 00.000  1.027                                             GEOM 6
  2.087  0.600 00.000  0.871                                             GEOM 6
  2.307  0.700 00.000  0.735                                             GEOM 6
  2.526  0.800 00.000  0.599                                             GEOM 6
  2.745  0.900 00.000  0.463                                             GEOM 6
  2.855  0.950 00.000  0.395                                             GEOM 6
  2.964  1.000 00.000  0.327                                             GEOM 6
 0.2063 0.2057 0.2054 0.2047 0.2031 0.1994 0.1952 0.1905 0.1673 0.1385  GEOM 7
 0.1060 0.0712 0.0354-0.0000-0.0172-0.0342-0.0506-0.0666-0.0822-0.0976  GEOM 7
 0.1666 0.1660 0.1657 0.1650 0.1634 0.1599 0.1559 0.1515 0.1309 0.1065  GEOM 7
 0.0796 0.0520 0.0250-0.0000-0.0116-0.0224-0.0323-0.0415-0.0498-0.0576  GEOM 7
 0.1499 0.1493 0.1490 0.1484 0.1469 0.1438 0.1401 0.1361 0.1170 0.0945  GEOM 7
 0.0701 0.0454 0.0216-0.0000-0.0096-0.0186-0.0265-0.0336-0.0399-0.0454  GEOM 7
 0.1360 0.1356 0.1353 0.1348 0.1336 0.1310 0.1278 0.1242 0.1068 0.0862  GEOM 7
 0.0638 0.0412 0.0196-0.0000-0.0087-0.0167-0.0237-0.0299-0.0353-0.0400  GEOM 7
 0.1230 0.1227 0.1226 0.1224 0.1217 0.1196 0.1169 0.1137 0.0983 0.0795  GEOM 7
 0.0591 0.0383 0.0183-0.0000-0.0081-0.0156-0.0222-0.0281-0.0333-0.0378  GEOM 7
 0.1110 0.1110 0.1110 0.1110 0.1108 0.1091 0.1070 0.1045 0.0909 0.0741  GEOM 7
 0.0554 0.0362 0.0173-0.0000-0.0079-0.0151-0.0217-0.0277-0.0330-0.0379  GEOM 7
 0.0999 0.1000 0.1000 0.1002 0.1005 0.1001 0.0984 0.0964 0.0846 0.0694  GEOM 7
 0.0523 0.0343 0.0166 0.0000-0.0077-0.0148-0.0215-0.0275-0.0332-0.0384  GEOM 7
 .08810 .08840 .08850 .08880 .08950 .09000 .08905 .08750 .07780 .06445  GEOM7
 .04905 .03250 .01585 .00000-.00750-.01460-.02135-.02765-.03365-.03940  GEOM7
 0.0763 0.0768 0.0770 0.0774 0.0785 0.0799 0.0797 0.0786 0.0710 0.0595  GEOM 7
 0.0458 0.0307 0.0151-0.0000-0.0073-0.0144-0.0212-0.0278-0.0341-0.0404  GEOM 7
 0.0488 0.0495 0.0499 0.0506 0.0523 0.0556 0.0572 0.0574 0.0542 0.0467  GEOM 7
 0.0366 0.0251 0.0127-0.0000-0.0065-0.0129-0.0194-0.0259-0.0325-0.0393  GEOM 7
 0.0032 0.0041 0.0045 0.0054 0.0076 0.0118 0.0148 0.0168 0.0198 0.0193  GEOM 7
 0.0167 0.0124 0.0068-0.0000-0.0039-0.0080-0.0125-0.0173-0.0224-0.0280  GEOM 7
-0.0121-0.0114-0.0111-0.0104-0.0087-0.0057-0.0032-0.0016 0.0029 0.0050  GEOM 7
 0.0055 0.0048 0.0029-0.0000-0.0019-0.0040-0.0065-0.0092-0.0122-0.0157  GEOM 7
-0.0076-0.0071-0.0069-0.0064-0.0053-0.0031-0.0018-0.0007 0.0022 0.0036  GEOM 7
 0.0040 0.0034 0.0021-0.0000-0.0012-0.0028-0.0045-0.0064-0.0086-0.0110  GEOM 7
-0.0049-0.0047-0.0046-0.0044-0.0038-0.0029-0.0020-0.0014 0.0004 0.0013  GEOM 7
 0.0016 0.0015 0.0009-0.0000-0.0006-0.0013-0.0022-0.0031-0.0043-0.0056  GEOM 7
-0.0008-0.0007-0.0007-0.0006-0.0004 0.0001 0.0005 0.0008 0.0015 0.0018  GEOM 7
```

TABLE III. Concluded

0.0017	0.0014	0.0008	0.0000	-0.0005	-0.0010	-0.0016	-0.0023	-0.0031	-0.0041	GEOM 7
0.0008	0.0008	0.0008	0.0009	0.0010	0.0012	0.0014	0.0015	0.0018	0.0019	GEOM 7
0.0016	0.0012	0.0007	-0.0000	-0.0004	-0.0008	-0.0013	-0.0018	-0.0024	-0.0031	GEOM 7
0.0010	0.0010	0.0010	0.0010	0.0011	0.0012	0.0013	0.0014	0.0017	0.0015	GEOM 7
0.0013	0.0010	0.0005	-0.0000	-0.0003	-0.0006	-0.0010	-0.0014	-0.0019	-0.0024	GEOM 7
0.0011	0.0011	0.0011	0.0011	0.0011	0.0012	0.0013	0.0013	0.0014	0.0014	GEOM 7
0.0011	0.0008	0.0005	-0.0000	-0.0003	-0.0005	-0.0008	-0.0012	-0.0016	-0.0020	GEOM 7
0.0013	0.0013	0.0013	0.0013	0.0013	0.0013	0.0014	0.0014	0.0014	0.0014	GEOM 7
0.0012	0.0009	0.0005	-0.0000	-0.0004	-0.0008	-0.0012	-0.0018	-0.0024	-0.0030	GEOM 7
-0.0031	-0.0030	-0.0030	-0.0030	-0.0030	-0.0030	-0.0029	-0.0029	-0.0027	-0.0021	GEOM 7
-0.0016	-0.0010	-0.0005	0.0000	0.0002	0.0004	0.0005	0.0006	0.0007	0.0008	GEOM 7
0.0	.02985	.04466	.07406	.14625	.28500	.41625	.54000	.96000	1.2600	GEOM8
1.4400	1.5000	1.4400	1.2600	1.1250	.96000	.76500	.54000	.28500	0.00	GEOM8
0.0	.02985	.04466	.07406	.14625	.28500	.41625	.54000	.96000	1.2600	GEOM8
1.4400	1.5000	1.4400	1.2600	1.1250	.96000	.76500	.54000	.28500	0.00	GEOM8
0.0	.02985	.04466	.07406	.14625	.28500	.41625	.54000	.96000	1.2600	GEOM8
1.4400	1.5000	1.4400	1.2600	1.1250	.96000	.76500	.54000	.28500	0.00	GEOM8
0.0	.02985	.04466	.07406	.14625	.28500	.41625	.54000	.96000	1.2600	GEOM8
1.4400	1.5000	1.4400	1.2600	1.1250	.96000	.76500	.54000	.28500	0.00	GEOM8
0.0	.02985	.04466	.07406	.14625	.28500	.41625	.54000	.96000	1.2600	GEOM8
1.4400	1.5000	1.4400	1.2600	1.1250	.96000	.76500	.54000	.28500	0.00	GEOM8
0.0	.02985	.04466	.07406	.14625	.28500	.41625	.54000	.96000	1.2600	GEOM8
1.4400	1.5000	1.4400	1.2600	1.1250	.96000	.76500	.54000	.28500	0.00	GEOM8
0.0	.02985	.04466	.07406	.14625	.28500	.41625	.54000	.96000	1.2600	GEOM8
1.4400	1.5000	1.4400	1.2600	1.1250	.96000	.76500	.54000	.28500	0.00	GEOM8
0.0	.02985	.04466	.07406	.14625	.28500	.41625	.54000	.96000	1.2600	GEOM8
1.4400	1.5000	1.4400	1.2600	1.1250	.96000	.76500	.54000	.28500	0.00	GEOM8
0.0	.02985	.04466	.07406	.14625	.28500	.41625	.54000	.96000	1.2600	GEOM8
1.4400	1.5000	1.4400	1.2600	1.1250	.96000	.76500	.54000	.28500	0.00	GEOM8
0.0	.02985	.04466	.07406	.14625	.28500	.41625	.54000	.96000	1.2600	GEOM8
1.4400	1.5000	1.4400	1.2600	1.1250	.96000	.76500	.54000	.28500	0.00	GEOM8
0.0	.02985	.04466	.07406	.14625	.28500	.41625	.54000	.96000	1.2600	GEOM8
1.4400	1.5000	1.4400	1.2600	1.1250	.96000	.76500	.54000	.28500	0.00	GEOM8
0.0	.02985	.04466	.07406	.14625	.28500	.41625	.54000	.96000	1.2600	GEOM8-35
1.4400	1.5000	1.4400	1.2600	1.1250	.96000	.76500	.54000	.28500	0.00	GEOM8-36
0.0	.02985	.04466	.07406	.14625	.28500	.41625	.54000	.96000	1.2600	GEOM8-37
1.4400	1.5000	1.4400	1.2600	1.1250	.96000	.76500	.54000	.28500	0.00	GEOM8-38
0.0	.02985	.04466	.07406	.14625	.28500	.41625	.54000	.96000	1.2600	GEOM8-39
1.4400	1.5000	1.4400	1.2600	1.1250	.96000	.76500	.54000	.28500	0.00	GEOM8-40
0.0	.02985	.04466	.07406	.14625	.28500	.41625	.54000	.96000	1.2600	GEOM8-41
1.4400	1.5000	1.4400	1.2600	1.1250	.96000	.76500	.54000	.28500	0.00	GEOM8-42
0.0	.02985	.04466	.07406	.14625	.28500	.41625	.54000	.96000	1.2600	GEOM8-43
1.4400	1.5000	1.4400	1.2600	1.1250	.96000	.76500	.54000	.28500	0.00	GEOM8-44
0.0	.02985	.04466	.07406	.14625	.28500	.41625	.54000	.96000	1.2600	GEOM8-45
1.4400	1.5000	1.4400	1.2600	1.1250	.96000	.76500	.54000	.28500	0.00	GEOM8-46
0.0	.02985	.04466	.07406	.14625	.28500	.41625	.54000	.96000	1.2600	GEOM8-47
1.4400	1.5000	1.4400	1.2600	1.1250	.96000	.76500	.54000	.28500	0.00	GEOM8-48
0.0	.02985	.04466	.07406	.14625	.28500	.41625	.54000	.96000	1.2600	GEOM8-49
1.4400	1.5000	1.4400	1.2600	1.1250	.96000	.76500	.54000	.28500	0.00	GEOM8-50

TABLE IV. NUMERICAL DESCRIPTION OF SEVERELY CONSTRAINED WING ($\Delta C_{p,\mathrm{LE}} = 0$) WITH $C_L = 0.08$

```
  1  1                    20 20                                                    GEOM 3
2.5375 1.6856 1.4392
  0.000  0.500  0.750  1.250  2.500  5.000  7.500 10.000 20.000 30.000  GEOM 5
 40.000 50.000 60.000 70.000 75.000 80.000 85.000 90.000 95.000100.000  GEOM 5
  0.000  0.000  0.000  2.584                                             GEOM 6
  0.008  0.025  0.000  2.577                                             GEOM 6
  0.030  0.050  0.000  2.558                                             GEOM 6
  0.067  0.075  0.000  2.524                                             GEOM 6
  0.120  0.100  0.000  2.478                                             GEOM 6
  0.187  0.125  0.000  2.418                                             GEOM 6
  0.270  0.150  0.000  2.345                                             GEOM 6
  0.375  0.175  0.000  2.253                                             GEOM 6
  0.480  0.200  0.000  2.160                                             GEOM 6
  0.749  0.250  0.000  1.921                                             GEOM 6
  1.079  0.300  0.000  1.630                                             GEOM 6
  1.354  0.350 00.000  1.397                                             GEOM 6
  1.549  0.400 00.000  1.243                                             GEOM 6
  1.848  0.500 00.000  1.027                                             GEOM 6
  2.087  0.600 00.000  0.871                                             GEOM 6
  2.307  0.700 00.000  0.735                                             GEOM 6
  2.526  0.800 00.000  0.599                                             GEOM 6
  2.745  0.900 00.000  0.463                                             GEOM 6
  2.855  0.950 00.000  0.395                                             GEOM 6
  2.964  1.000 00.000  0.327                                             GEOM 6
 0.1395 0.1394 0.1394 0.1394 0.1392 0.1387 0.1378 0.1366 0.1272 0.1109  GEOM 7
 0.0882 0.0606 0.0302-0.0000-0.0139-0.0263-0.0365-0.0441-0.0480-0.0476  GEOM 7
 0.1378 0.1378 0.1378 0.1377 0.1376 0.1371 0.1363 0.1350 0.1259 0.1099  GEOM 7
 0.0876 0.0602 0.0301-0.0000-0.0139-0.0263-0.0366-0.0442-0.0484-0.0482  GEOM 7
 0.1342 0.1342 0.1341 0.1341 0.1340 0.1336 0.1328 0.1317 0.1232 0.1078  GEOM 7
 0.0861 0.0594 0.0298-0.0000-0.0139-0.0264-0.0371-0.0451-0.0499-0.0506  GEOM 7
 0.1291 0.1291 0.1291 0.1290 0.1289 0.1286 0.1279 0.1269 0.1191 0.1047  GEOM 7
 0.0841 0.0584 0.0295-0.0000-0.0140-0.0267-0.0379-0.0466-0.0524-0.0545  GEOM 7
 0.1217 0.1217 0.1217 0.1217 0.1216 0.1213 0.1209 0.1200 0.1132 0.1002  GEOM 7
 0.0811 0.0568 0.0290-0.0000-0.0140-0.0271-0.0387-0.0483-0.0555-0.0594  GEOM 7
 0.1114 0.1114 0.1114 0.1114 0.1114 0.1113 0.1110 0.1104 0.1051 0.0939  GEOM 7
 0.0767 0.0543 0.0281-0.0000-0.0138-0.0271-0.0393-0.0499-0.0585-0.0642  GEOM 7
 0.1031 0.1031 0.1031 0.1031 0.1032 0.1032 0.1032 0.1028 0.0987 0.0891  GEOM 7
 0.0736 0.0527 0.0276 0.0000-0.0139-0.0276-0.0404-0.0522-0.0622-0.0701  GEOM 7
0.08855 .08855 .08855 .08860 .08875 .08900 .08930 .08925 .08705 .07975  GEOM7
 .06685 .04855 .02580 .00000-.01343-.02685-.03985-.05210-.06325-.07270  GEOM7
 0.0740 0.074  0.0740 0.0741 0.0743 0.0748 0.0754 0.0757 0.0754 0.0704  GEOM 7
 0.0601 0.0444 0.0240-0.0000-0.0129-0.0261-0.0393-0.0520-0.0643-0.0753  GEOM 7
 0.0323 0.0325 0.0326 0.0327 0.0332 0.0343 0.0356 0.0369 0.0411 0.0420  GEOM 7
 0.0384 0.0302 0.0171-0.0000-0.0100-0.0206-0.0319-0.0435-0.0555-0.0673  GEOM 7
-0.0288-0.0285-0.0284-0.0281-0.0273-0.0256-0.0236-0.0214-0.0127-0.0050  GEOM 7
 0.0006 0.0035 0.0034-0.0000-0.0030-0.0067-0.0114-0.0169-0.0230-0.0300  GEOM 7
-0.0383-0.0380-0.0379-0.0376-0.0370-0.0354-0.0337-0.0320-0.0247-0.0174  GEOM 7
-0.0109-0.0056-0.0019 0.0000 0.0001-0.0002-0.0011-0.0025-0.0046-0.0072  GEOM 7
-0.0275-0.0273-0.0272-0.0270-0.0265-0.0254-0.0242-0.0230-0.0178-0.0128  GEOM 7
-0.0082-0.0044-0.0016 0.0000 0.0004 0.0003-0.0001-0.0008-0.0019-0.0033  GEOM 7
-0.0133-0.0132-0.0132-0.0131-0.0128-0.0123-0.0116-0.0110-0.0086-0.0060  GEOM 7
-0.0039-0.0021-0.0008 0.0000 0.0001 0.0001-0.0001-0.0004-0.0009-0.0016  GEOM 7
-0.0056-0.0055-0.0055-0.0055-0.0053-0.0050-0.0047-0.0044-0.0031-0.0020  GEOM 7
```

TABLE IV. Concluded

```
-0.0010-0.0004-0.0000 0.0000-0.0002-0.0004-0.0007-0.0011-0.0017-0.0023  GEOM 7
-0.0022-0.0022-0.0022-0. 021-0.0020-0.0019-0.0017-0.0015-0.0009-0.0004  GEOM 7
 0.0000 0.0002 0.0003-0.0000-0.0002-0.0005-0.0009-0.0013-0.0018-0.0023  GEOM 7
-0.0012-0.0012-0.0012-0.0011-0.0011-0.0010-0.0009-0.0008-0.0005-0.0001  GEOM 7
 0.0001 0.0002 0.0002-0.0000-0.0001-0.0003-0.0005-0.0008-0.0011-0.0014  GEOM 7
-0.0008-0.0008-0.0008-0.0008-0.0008-0.0007-0.0006-0.0006-0.0004-0.0002  GEOM 7
-0.0001 0.0001 0.0001-0.0000-0.0001-0.0002-0.0002-0.0004-0.0005-0.0006  GEOM 7
-0.0007-0.0007-0.0007-0.0007-0.0007-0.0006-0.0006-0.0006-0.0004-0.0002  GEOM 7
-0.0001-0.0000 0.0000 0.0000-0.0000-0.0001-0.0001-0.0002-0.0003-0.0005  GEOM 7
-0.0013-0.0013-0.0013-0.0013-0.0012-0.0012-0.0012-0.0012-0.0011-0.0010  GEOM 7
-0.0009-0.0007-0.0004 0.0000 0.0002 0.0004 0.0005 0.0008 0.0010 0.0012  GEOM 7
0.0     .02985  .04466  .07406  .14625  .28500  .41625  .54000  .96000 1.2600   GEOM8-11
1.4400 1.5000 1.4400 1.2600 1.1250 .96000 .76500 .54000 .28500 0.00     GEOM8-12
0.0     .02985  .04466  .07406  .14625  .28500  .41625  .54000  .96000 1.2600   GEOM8-13
1.4400 1.5000 1.4400 1.2600 1.1250 .96000 .76500 .54000 .28500 0.00     GEOM8-14
0.0     .02985  .04466  .07406  .14625  .28500  .41625  .54000  .96000 1.2600   GEOM8-15
1.4400 1.5000 1.4400 1.2600 1.1250 .96000 .76500 .54000 .28500 0.00     GEOM8-16
0.0     .02985  .04466  .07406  .14625  .28500  .41625  .54000  .96000 1.2600   GEOM8-17
1.4400 1.5000 1.4400 1.2600 1.1250 .96000 .76500 .54000 .28500 0.00     GEOM8-18
0.0     .02985  .04466  .07406  .14625  .28500  .41625  .54000  .96000 1.2600   GEOM8-19
1.4400 1.5000 1.4400 1.2600 1.1250 .96000 .76500 .54000 .28500 0.00     GEOM8-20
0.0     .02985  .04466  .07406  .14625  .28500  .41625  .54000  .96000 1.2600   GEOM8-21
1.4400 1.5000 1.4400 1.2600 1.1250 .96000 .76500 .54000 .28500 0.00     GEOM8-22
0.0     .02985  .04466  .07406  .14625  .28500  .41625  .54000  .96000 1.2600   GEOM8-23
1.4400 1.5000 1.4400 1.2600 1.1250 .96000 .76500 .54000 .28500 0.00     GEOM8-24
0.0     .02985  .04466  .07406  .14625  .28500  .41625  .54000  .96000 1.2600   GEOM8-25
1.4400 1.5000 1.4400 1.2600 1.1250 .96000 .76500 .54000 .28500 0.00     GEOM8-26
0.0     .02985  .04466  .07406  .14625  .28500  .41625  .54000  .96000 1.2600   GEOM8-27
1.4400 1.5000 1.4400 1.2600 1.1250 .96000 .76500 .54000 .28500 0.00     GEOM8-28
0.0     .02985  .04466  .07406  .14625  .28500  .41625  .54000  .96000 1.2600   GEOM8-29
1.4400 1.5000 1.4400 1.2600 1.1250 .96000 .76500 .54000 .28500 0.00     GEOM8-30
0.0     .02985  .04466  .07406  .14625  .28500  .41625  .54000  .96000 1.2600   GEOM8-31
1.4400 1.5000 1.4400 1.2600 1.1250 .96000 .76500 .54000 .28500 0.00     GEOM8-32
0.0     .02985  .04466  .07406  .14625  .28500  .41625  .54000  .96000 1.2600   GEOM8-33
1.4400 1.5000 1.4400 1.2600 1.1250 .96000 .76500 .54000 .28500 0.00     GEOM8-34
0.0     .02985  .04466  .07406  .14625  .28500  .41625  .54000  .96000 1.2600   GEOM8-35
1.4400 1.5000 1.4400 1.2600 1.1250 .96000 .76500 .54000 .28500 0.00     GEOM8-36
0.0     .02985  .04466  .07406  .14625  .28500  .41625  .54000  .96000 1.2600   GEOM8-37
1.4400 1.5000 1.4400 1.2600 1.1250 .96000 .76500 .54000 .28500 0.00     GEOM8-38
0.0     .02985  .04466  .07406  .14625  .28500  .41625  .54000  .96000 1.2600   GEOM8-39
1.4400 1.5000 1.4400 1.2600 1.1250 .96000 .76500 .54000 .28500 0.00     GEOM8-40
0.0     .02985  .04466  .07406  .14625  .28500  .41625  .54000  .96000 1.2600   GEOM8-41
1.4400 1.5000 1.4400 1.2600 1.1250 .96000 .76500 .54000 .28500 0.00     GEOM8-42
0.0     .02985  .04466  .07406  .14625  .28500  .41625  .54000  .96000 1.2600   GEOM8-43
1.4400 1.5000 1.4400 1.2600 1.1250 .96000 .76500 .54000 .28500 0.00     GEOM8-44
0.0     .02985  .04466  .07406  .14625  .28500  .41625  .54000  .96000 1.2600   GEOM8-45
1.4400 1.5000 1.4400 1.2600 1.1250 .96000 .76500 .54000 .28500 0.00     GEOM8-46
0.0     .02985  .04466  .07406  .14625  .28500  .41625  .54000  .96000 1.2600   GEOM8-47
1.4400 1.5000 1.4400 1.2600 1.1250 .96000 .76500 .54000 .28500 0.00     GEOM8-48
0.0     .02985  .04466  .07406  .14625  .28500  .41625  .54000  .96000 1.2600   GEOM8-49
1.4400 1.5000 1.4400 1.2600 1.1250 .96000 .76500 .54000 .28500 0.00     GEOM8-50
```

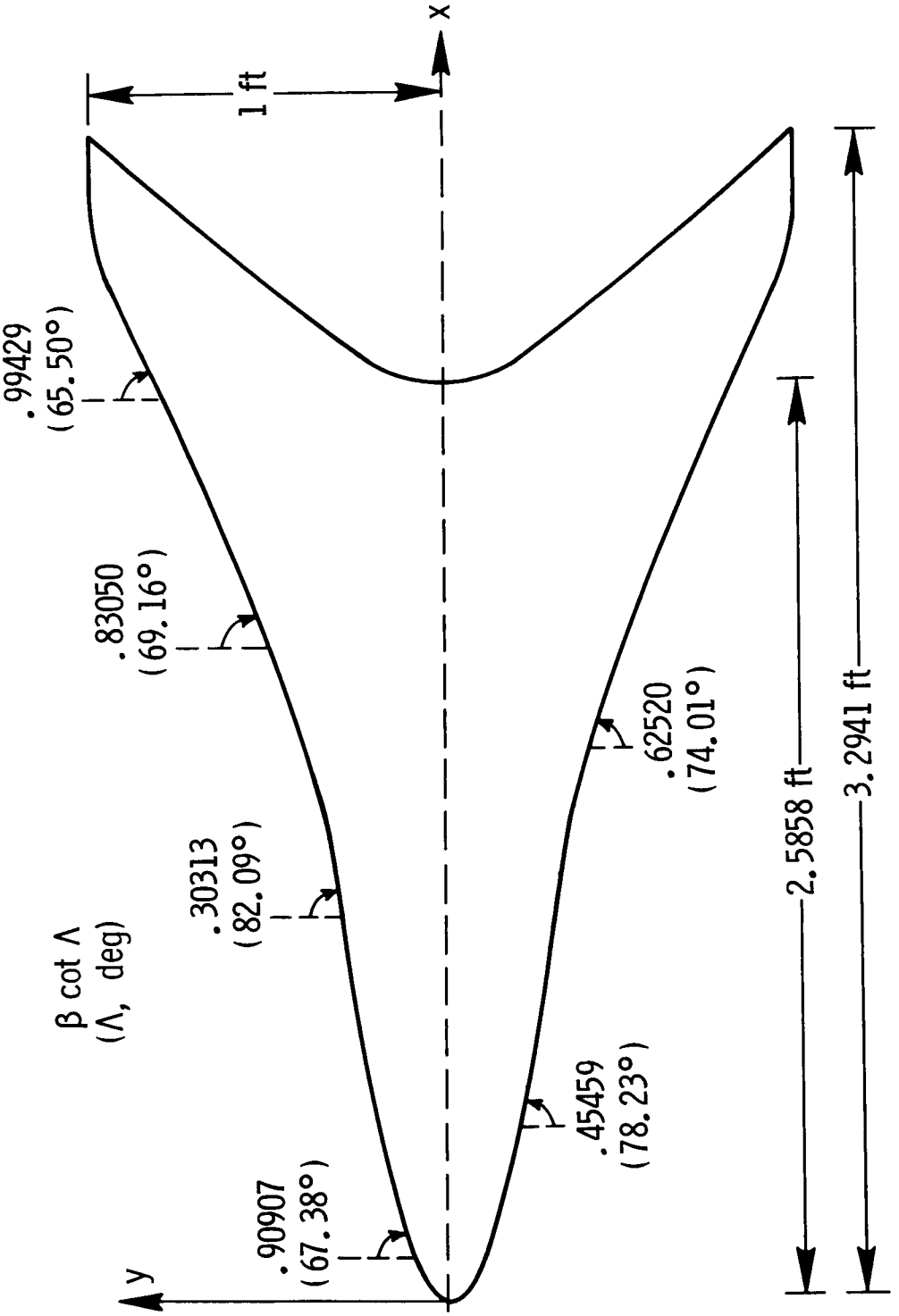

Figure 1. Wing planform. Wing area, 2.5375 ft^2.

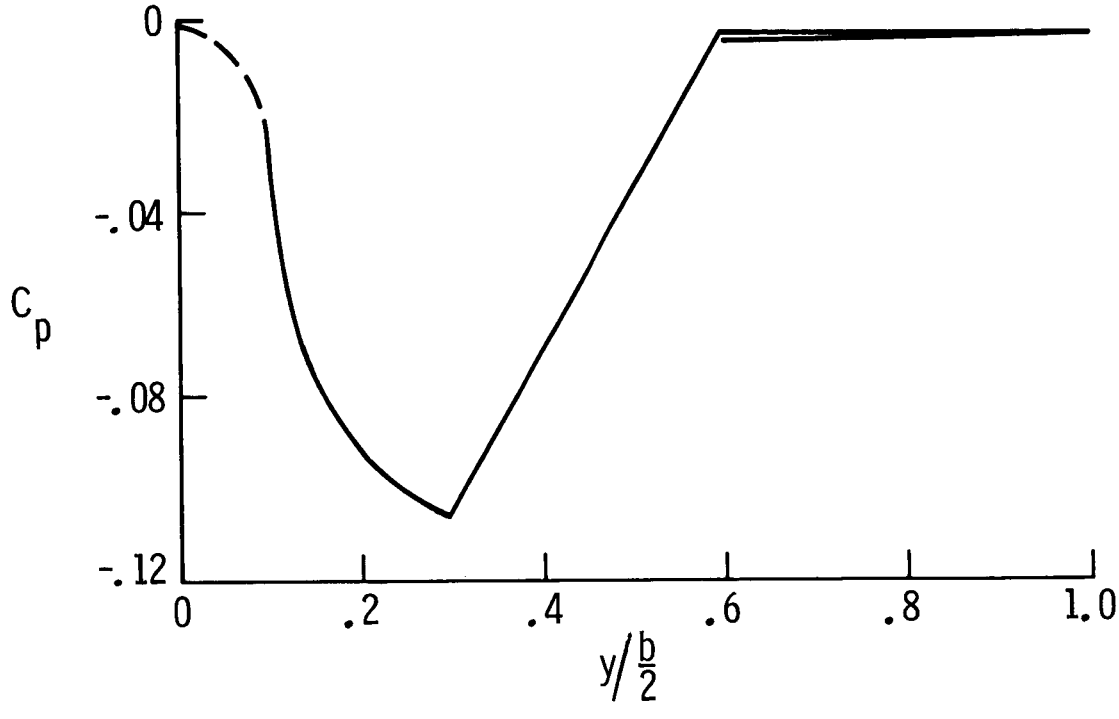

Figure 2. Leading-edge pressure constraints for moderately constrained wing ($M_N < 1$). $M = 2.4$.

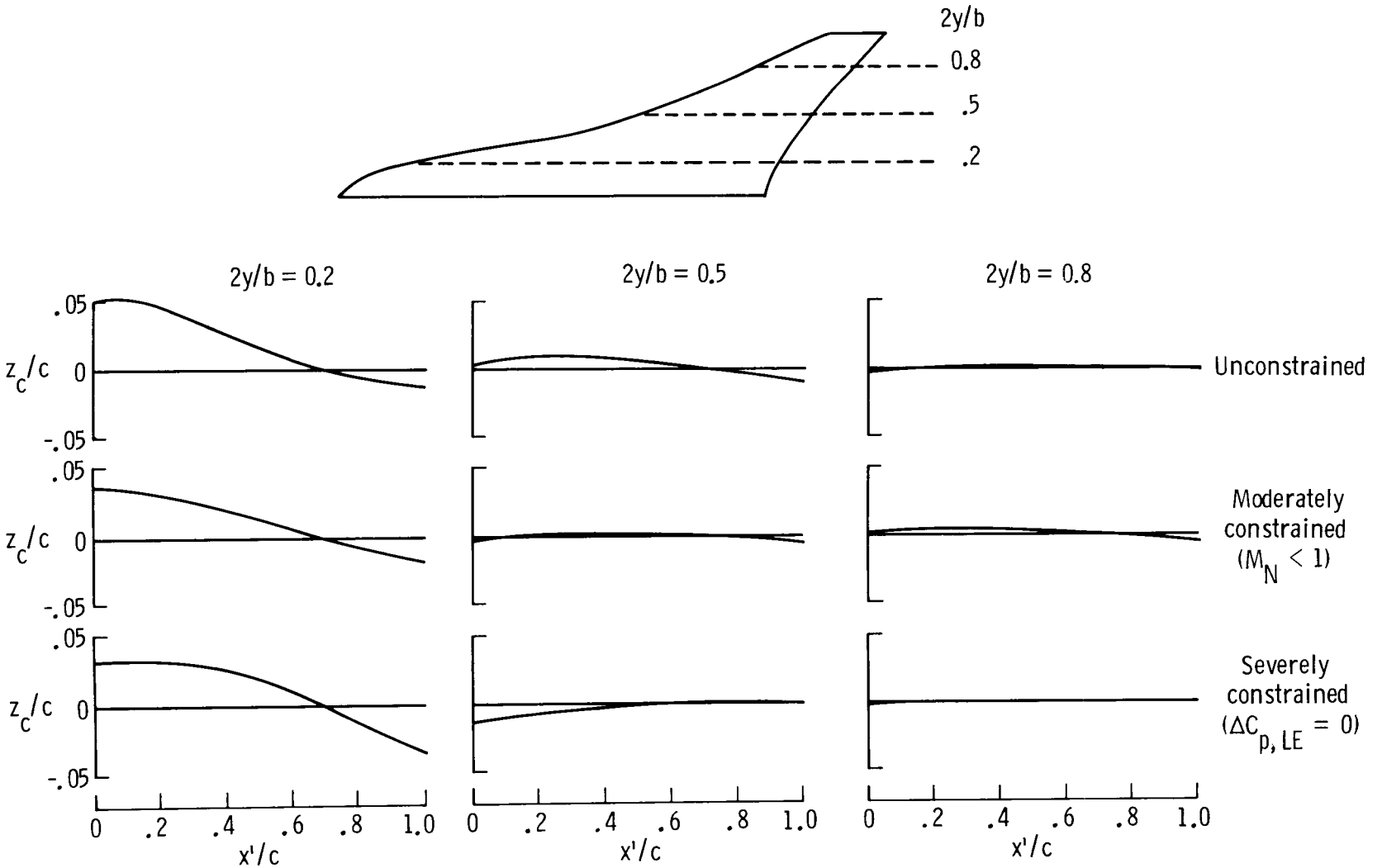

Figure 3. Camber surfaces.

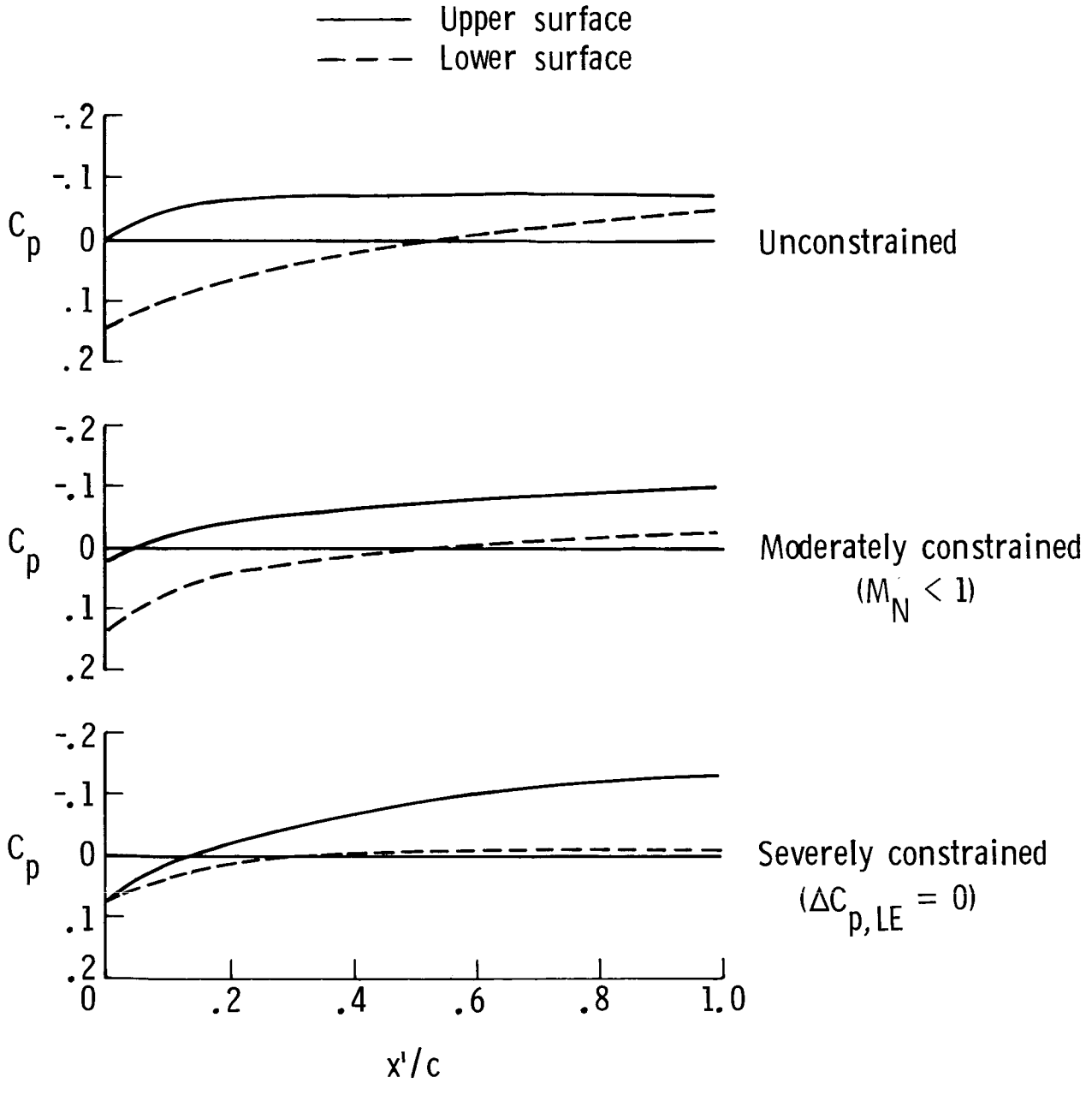

Figure 4. Theoretical pressure coefficients on upper and lower surfaces. $2y/b = 0.5$; $\alpha = 0°$; $C_L = 0.08$.

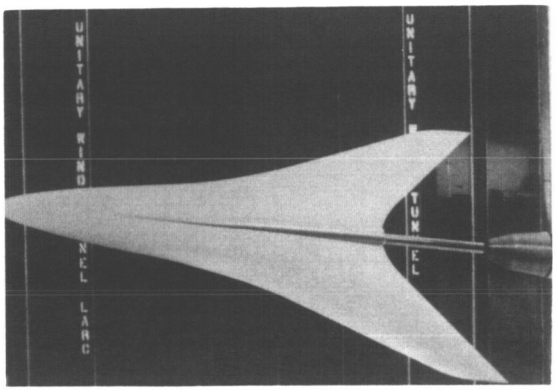

Flat

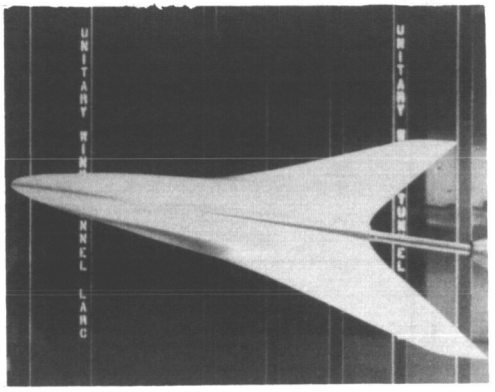

Unconstrained

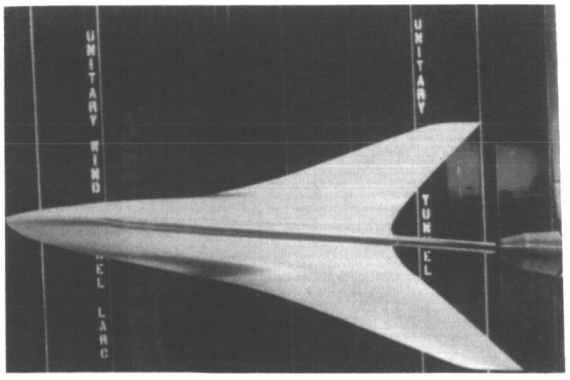

Moderately constrained ($M_N < 1$)

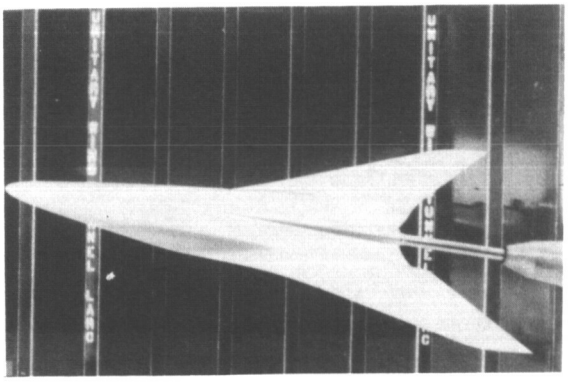

Severely constrained ($\Delta C_{p,\mathrm{LE}} = 0$)

L-85-57

Figure 5. Models in vortex-suppression test series.

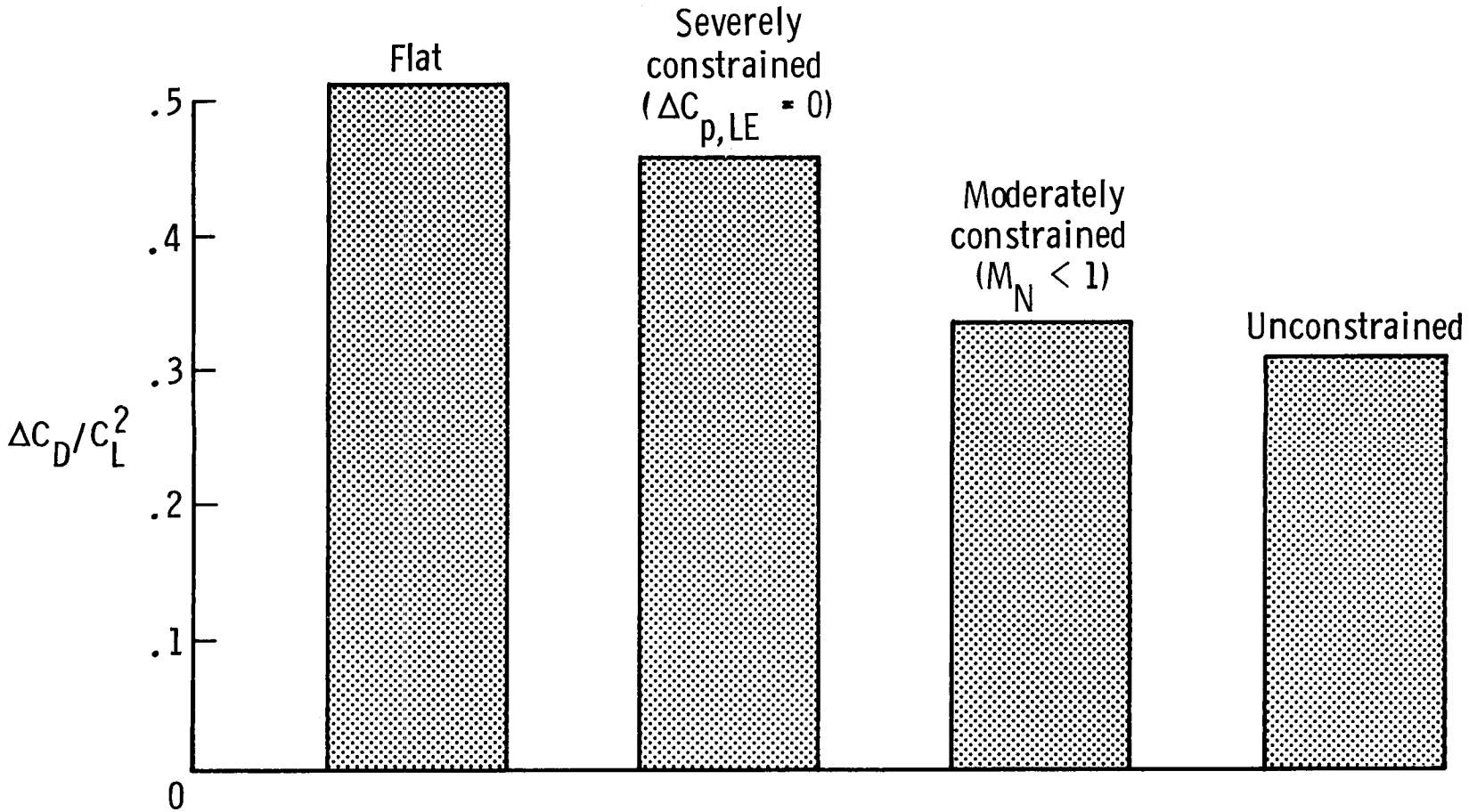

Figure 6. Theoretical drag-due-to-lift factors.

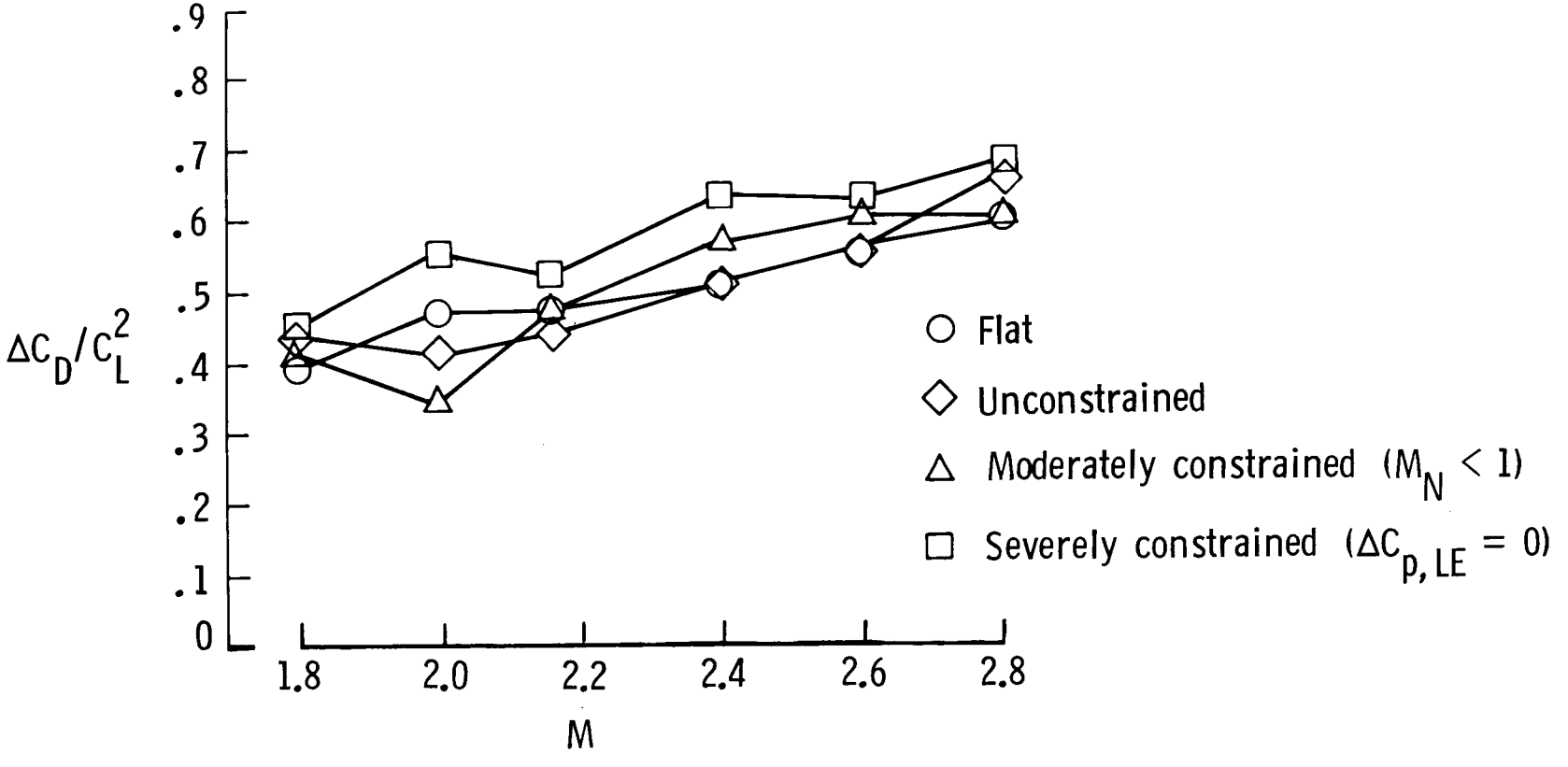

Figure 7. Experimental drag due to lift. $C_L = 0.08$.

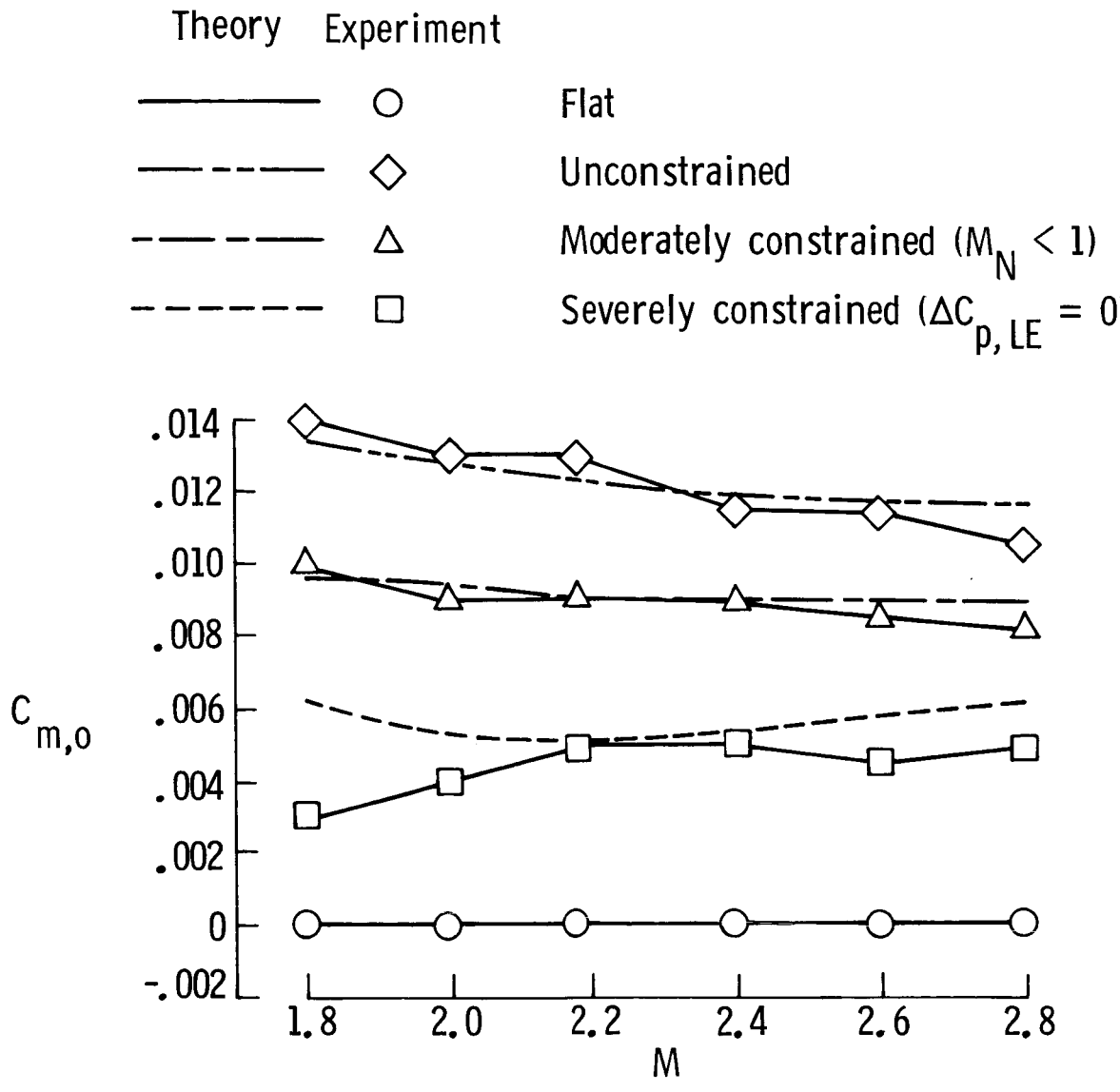

Figure 8. Pitching moment at zero lift.

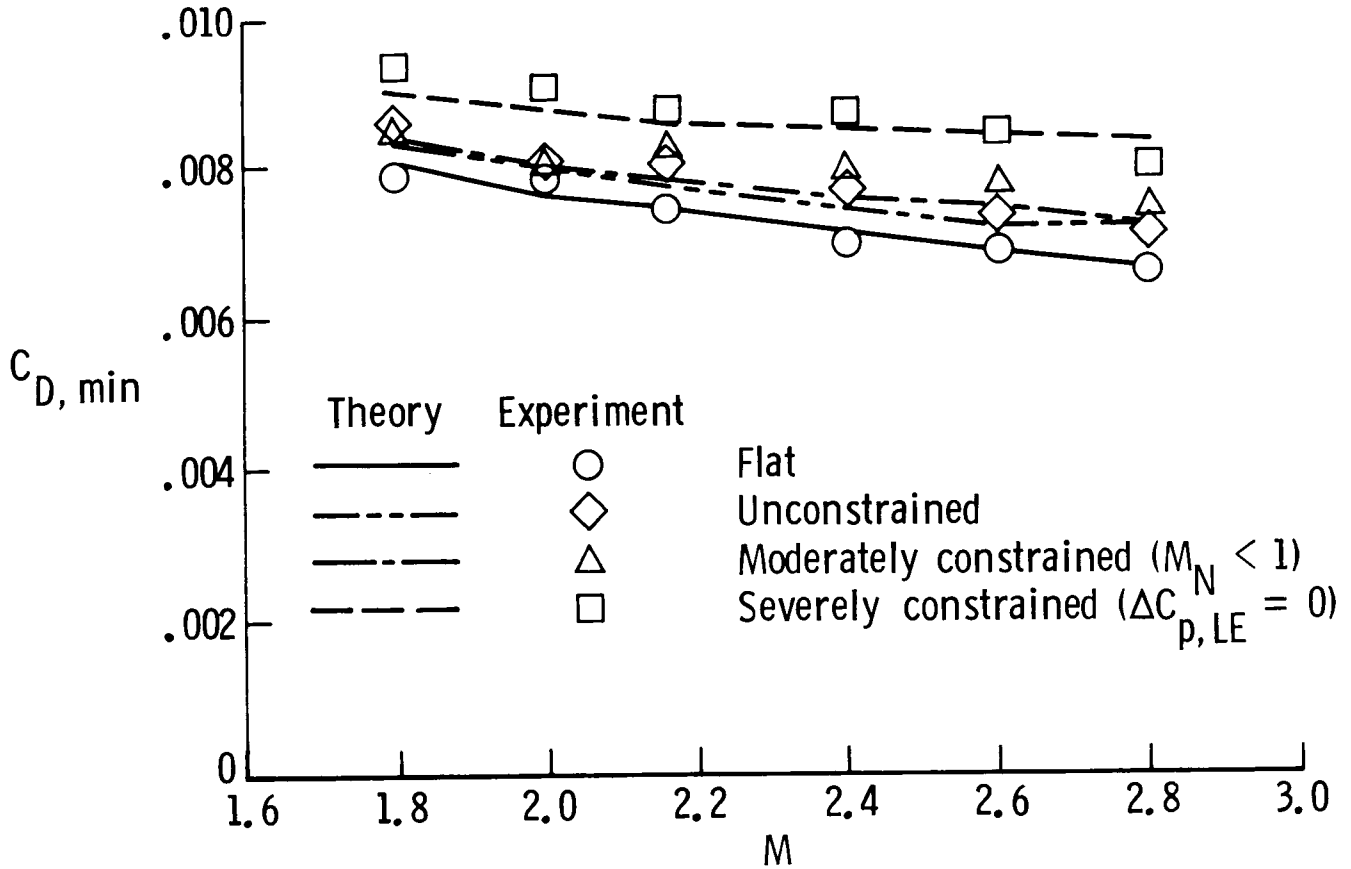

Figure 9. Minimum drag as function of Mach number.

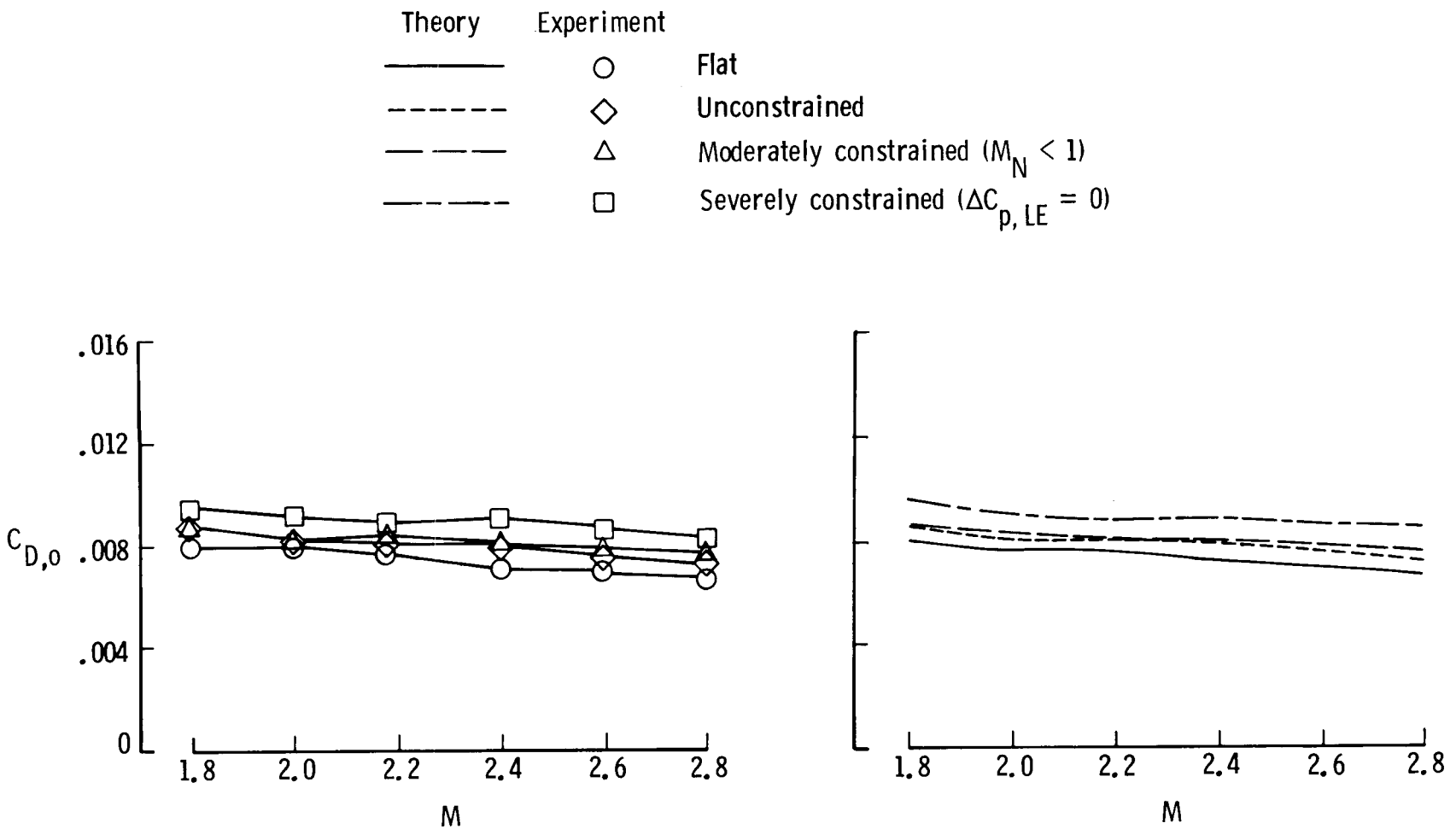

Figure 10. Drag at zero lift.

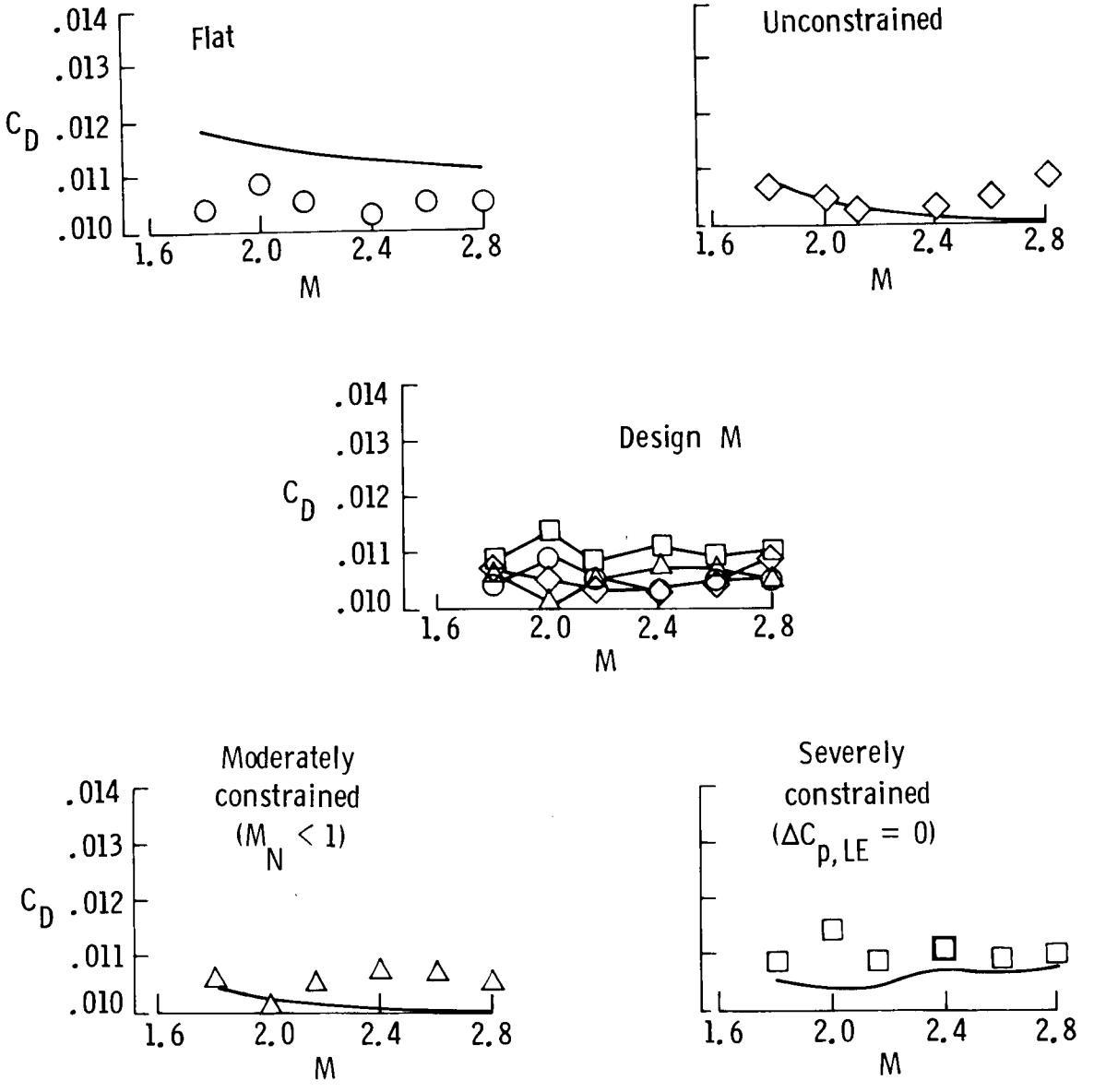

Figure 11. Drag at design lift. The solid-line curve denotes the SDAS prediction.

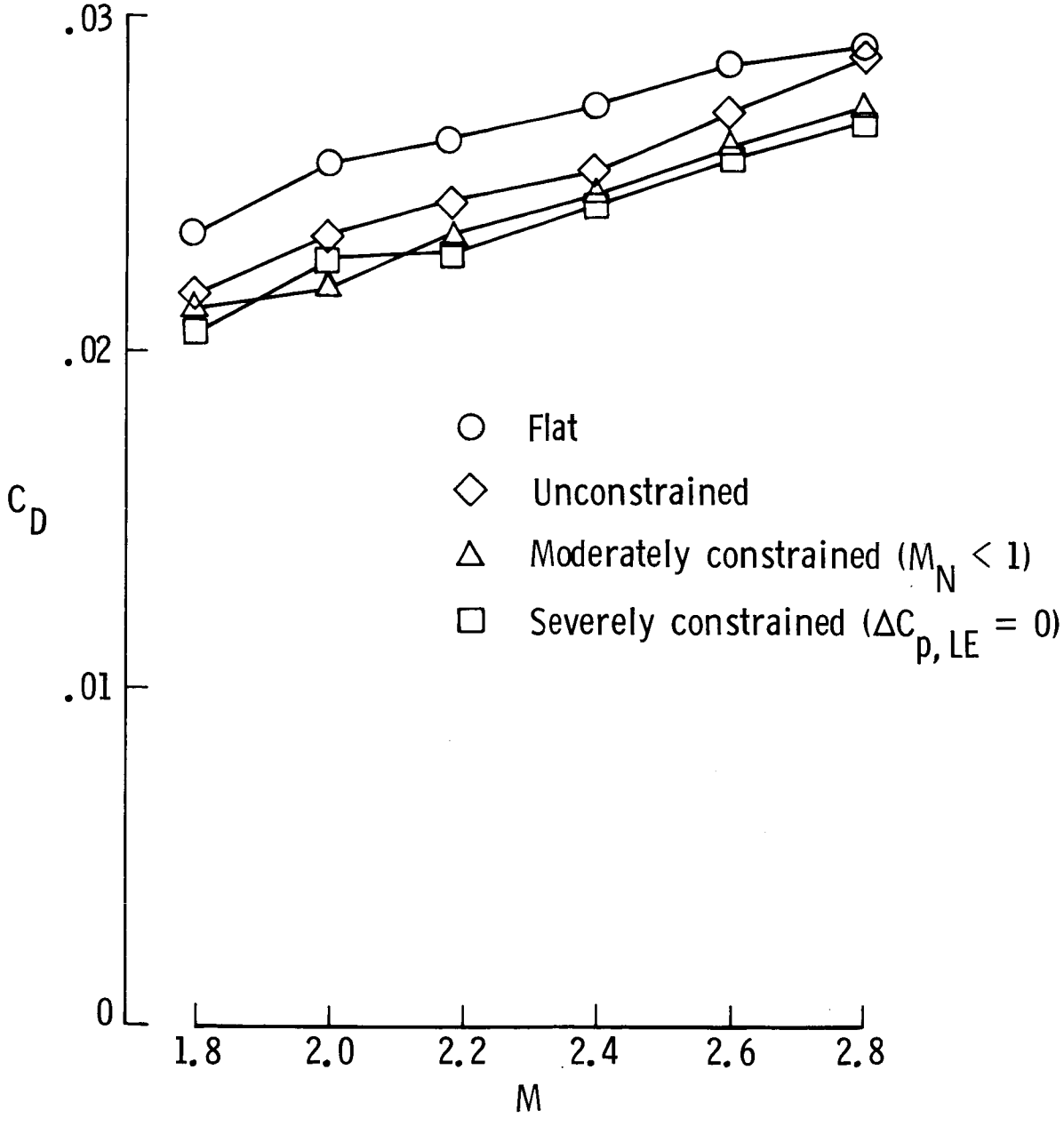

Figure 12. Drag at $C_L = 0.18$.

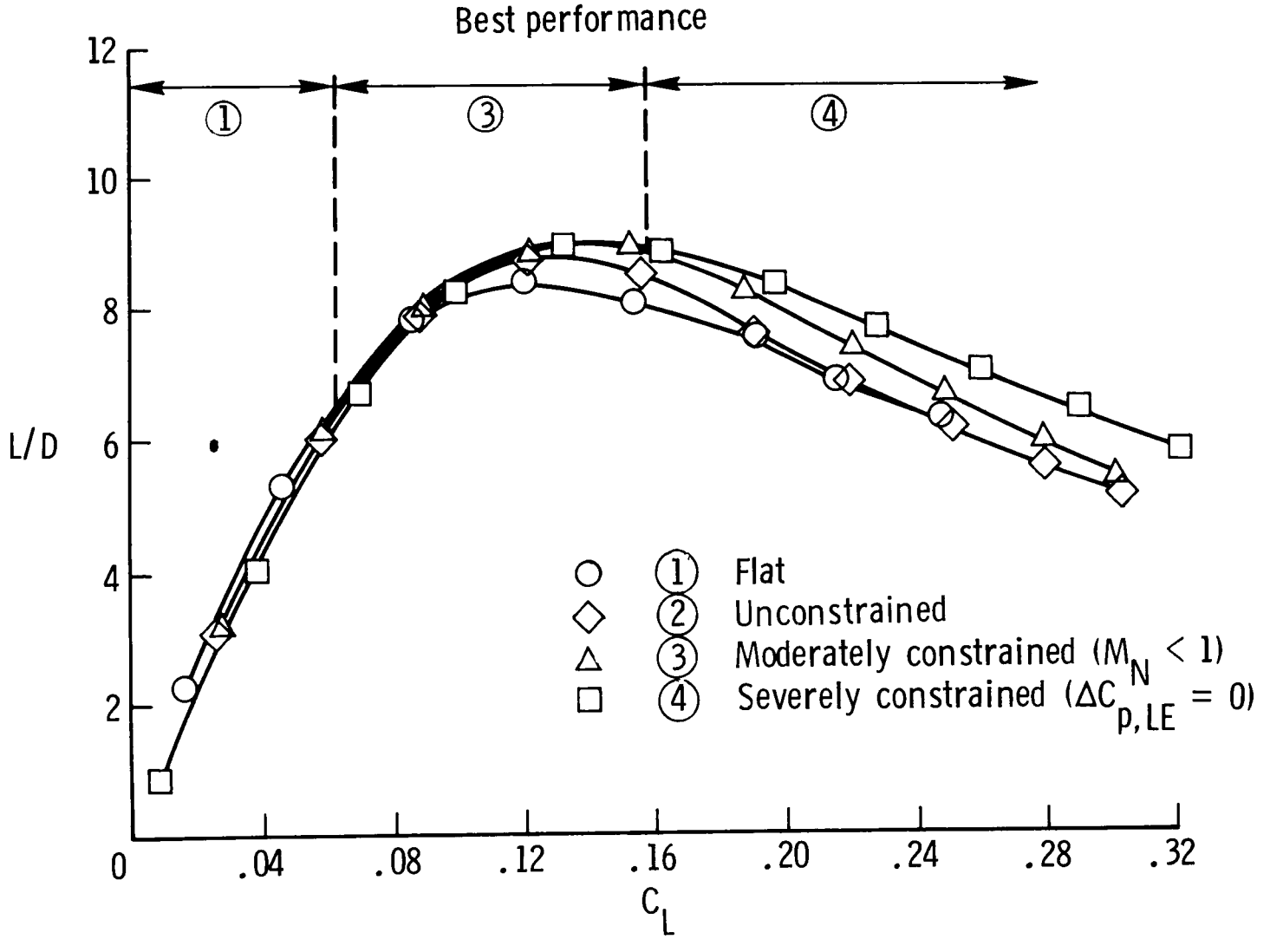

(a) $M = 1.8$.

Figure 13. Experimental performance.

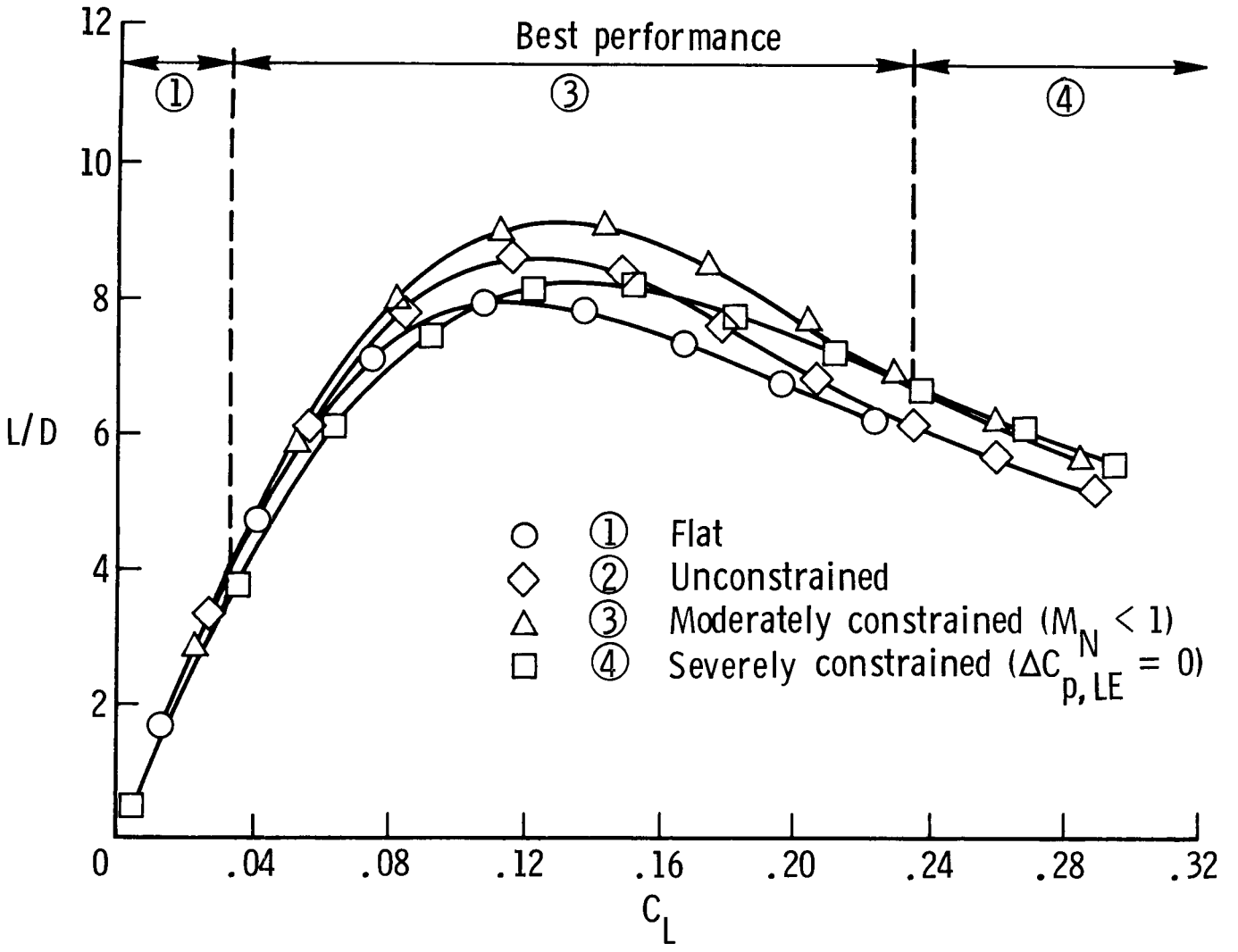

(b) $M = 2.0$.

Figure 13. Continued.

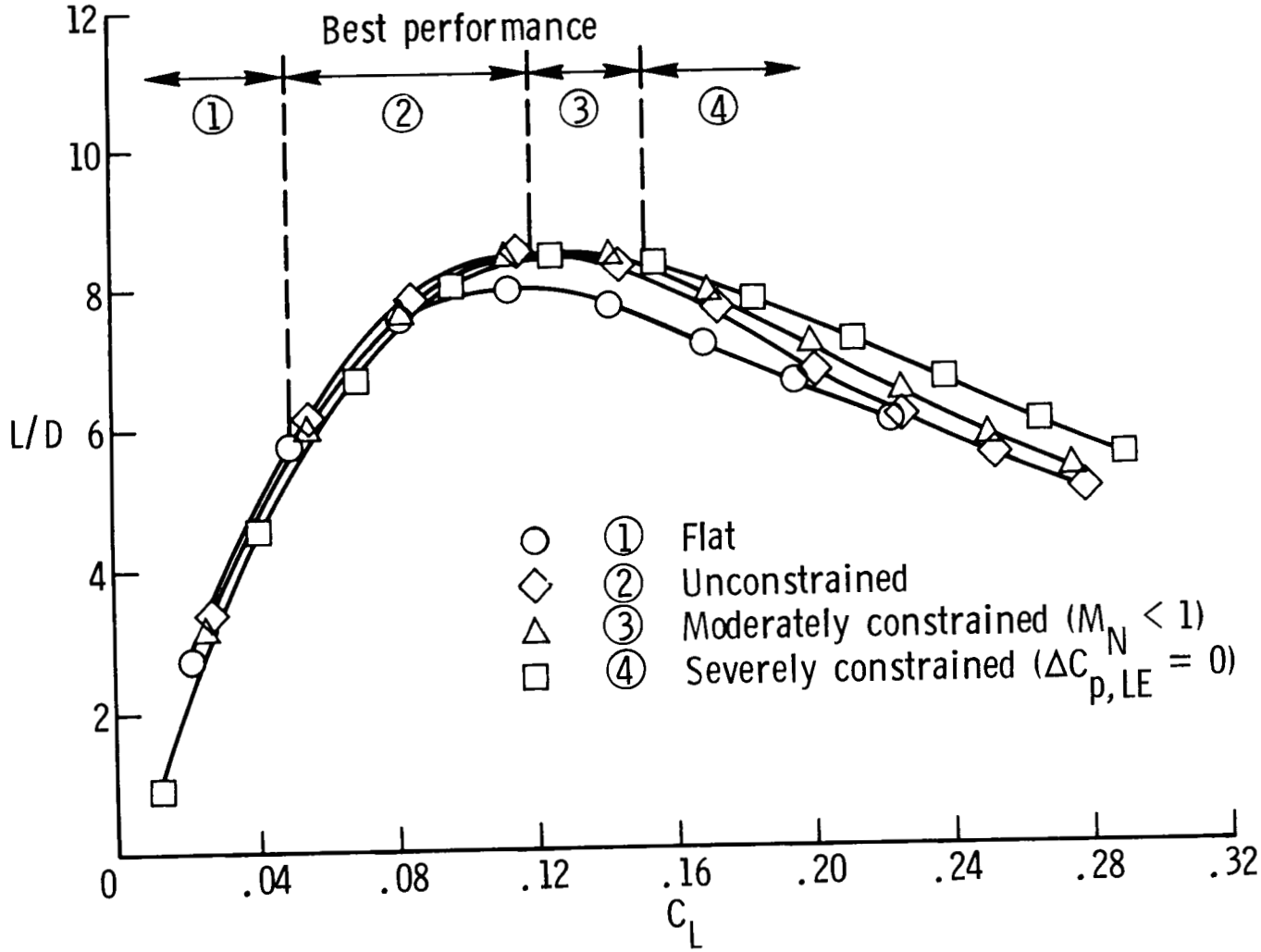

(c) $M = 2.16$.

Figure 13. Continued.

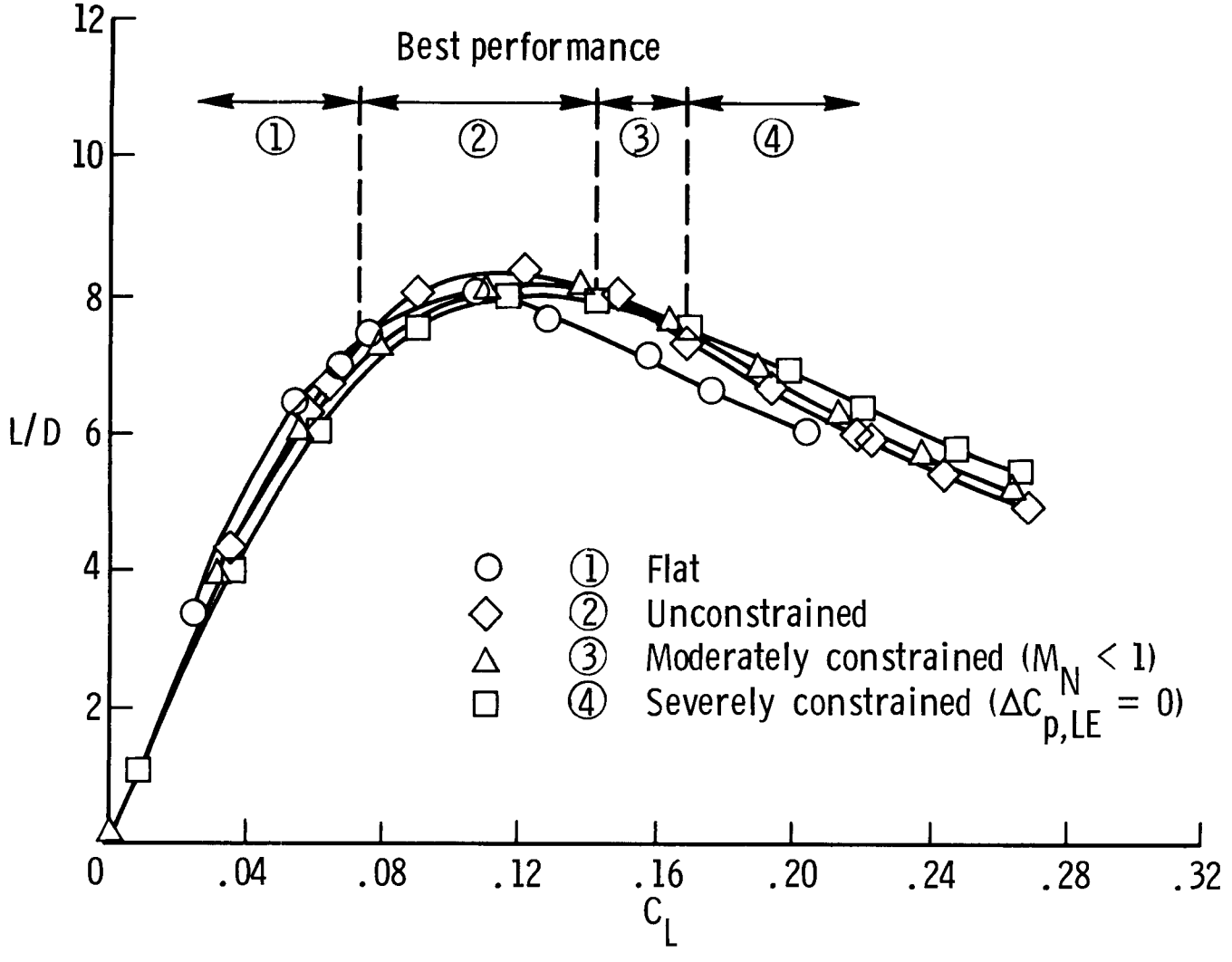

(d) $M = 2.4$.

Figure 13. Continued.

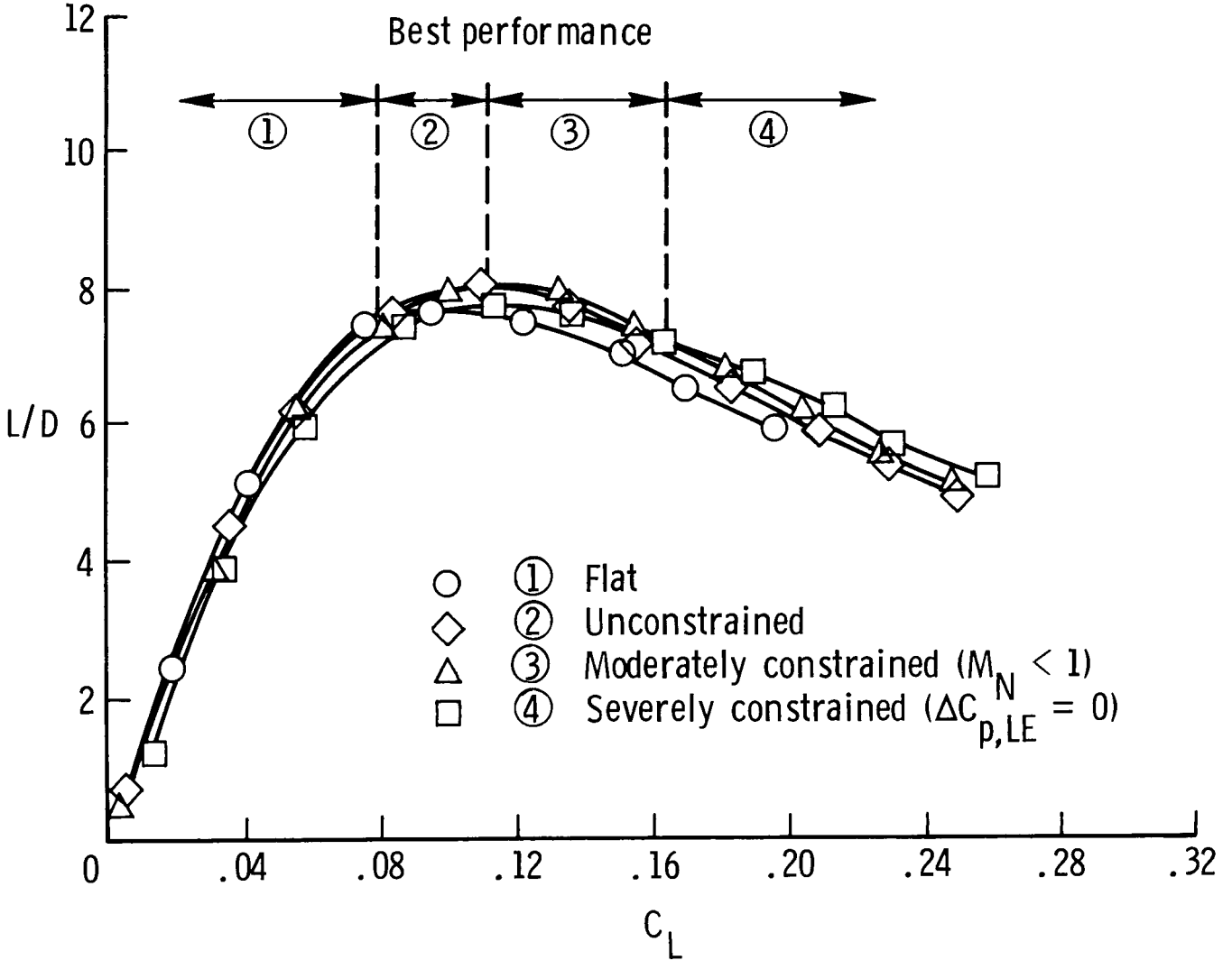

(e) $M = 2.6$.

Figure 13. Continued.

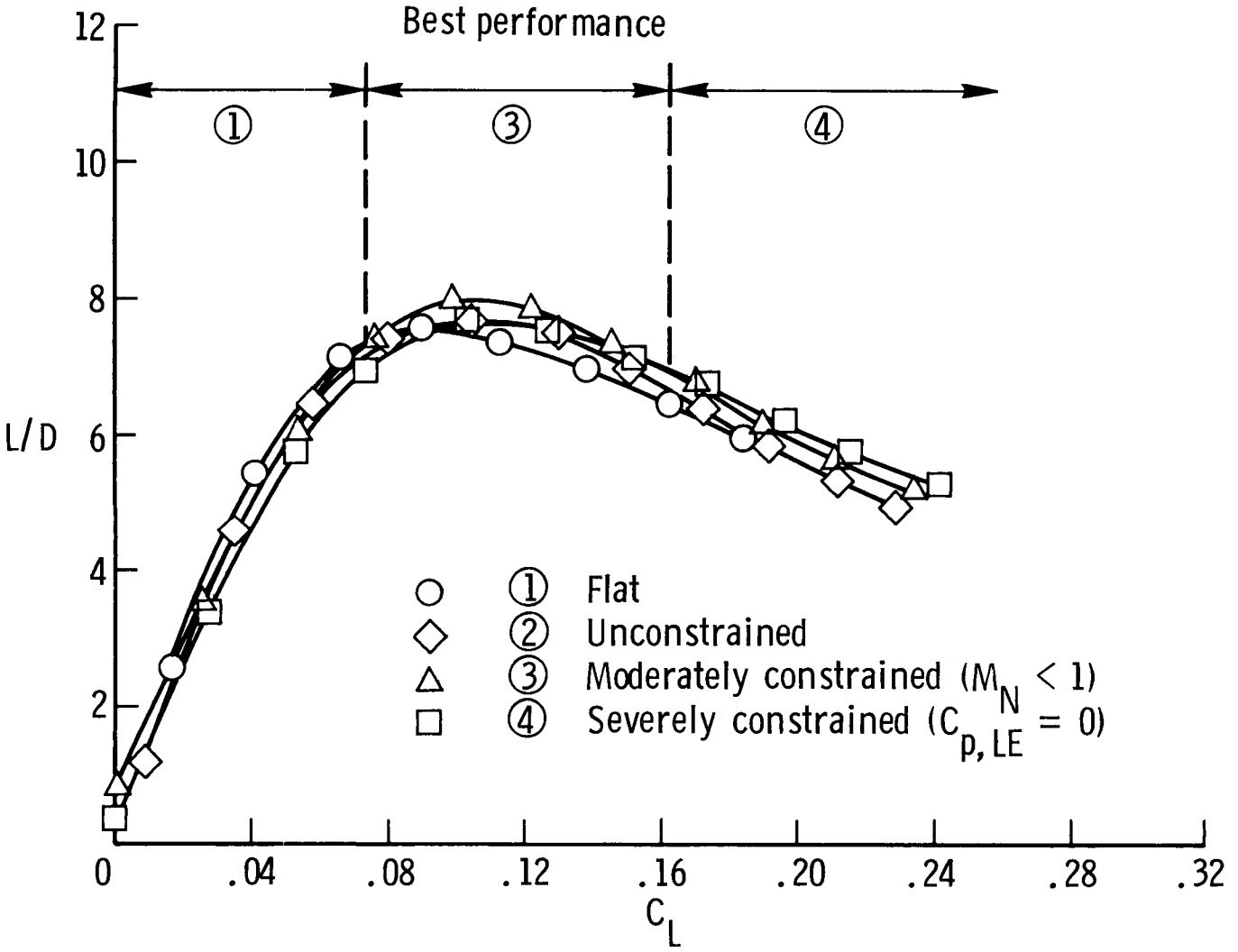

(f) $M = 2.8$.

Figure 13. Concluded.

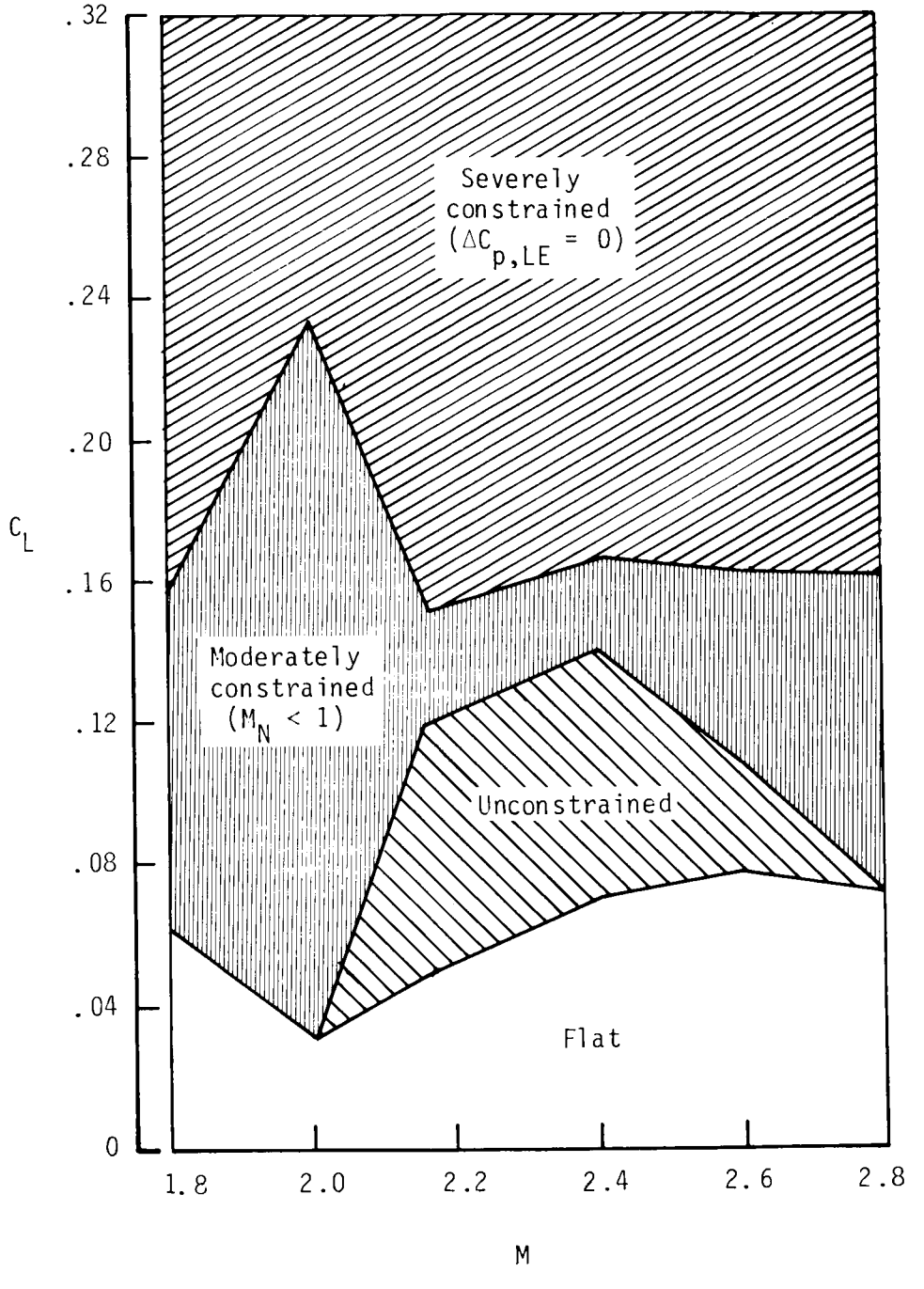

Figure 14. Ranges of best performance.

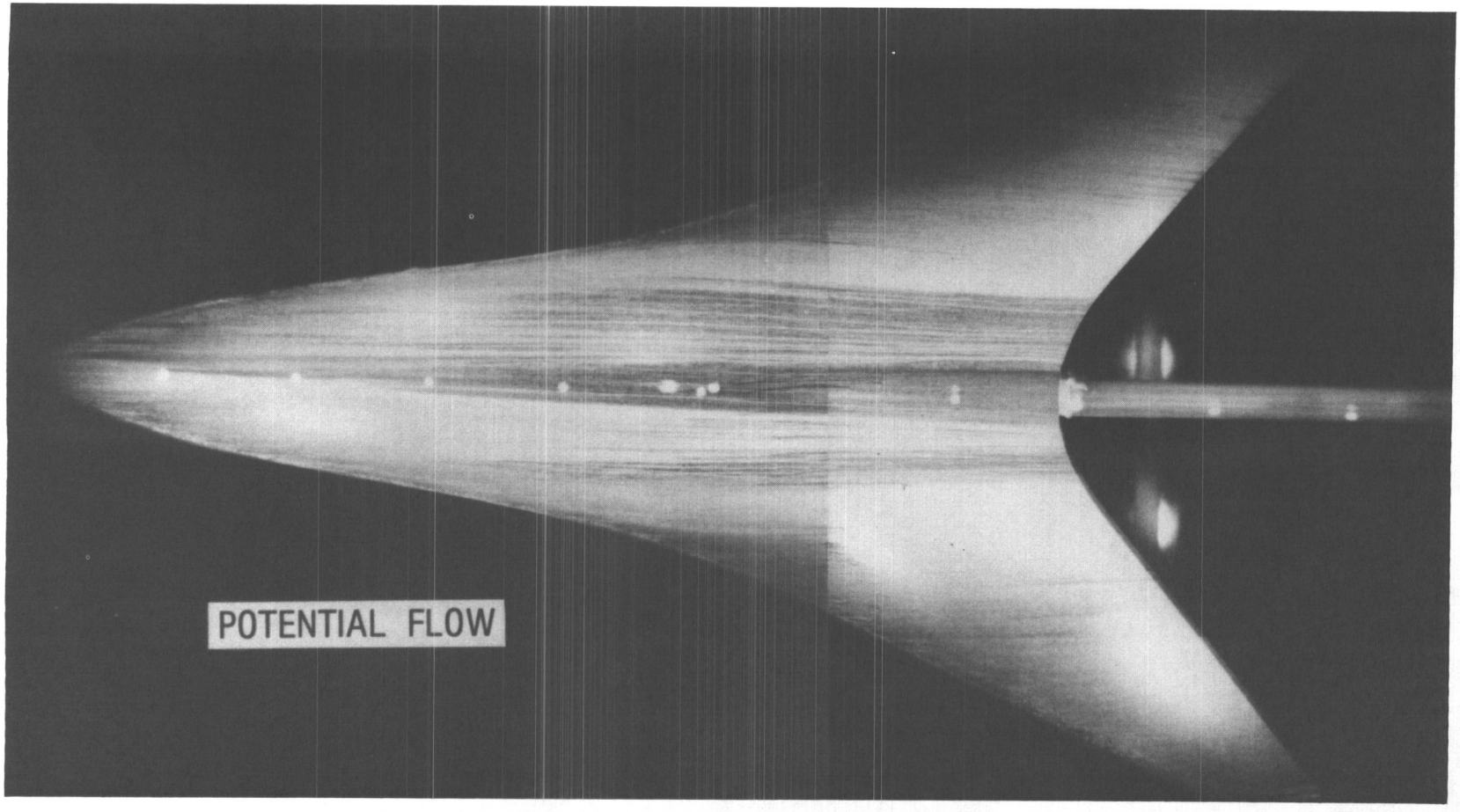

L-85-58

(a) Oil flow at $\alpha = 0°$. $C_L = 0$.

Figure 15. Uncambered flat wing. $M = 2.4$.

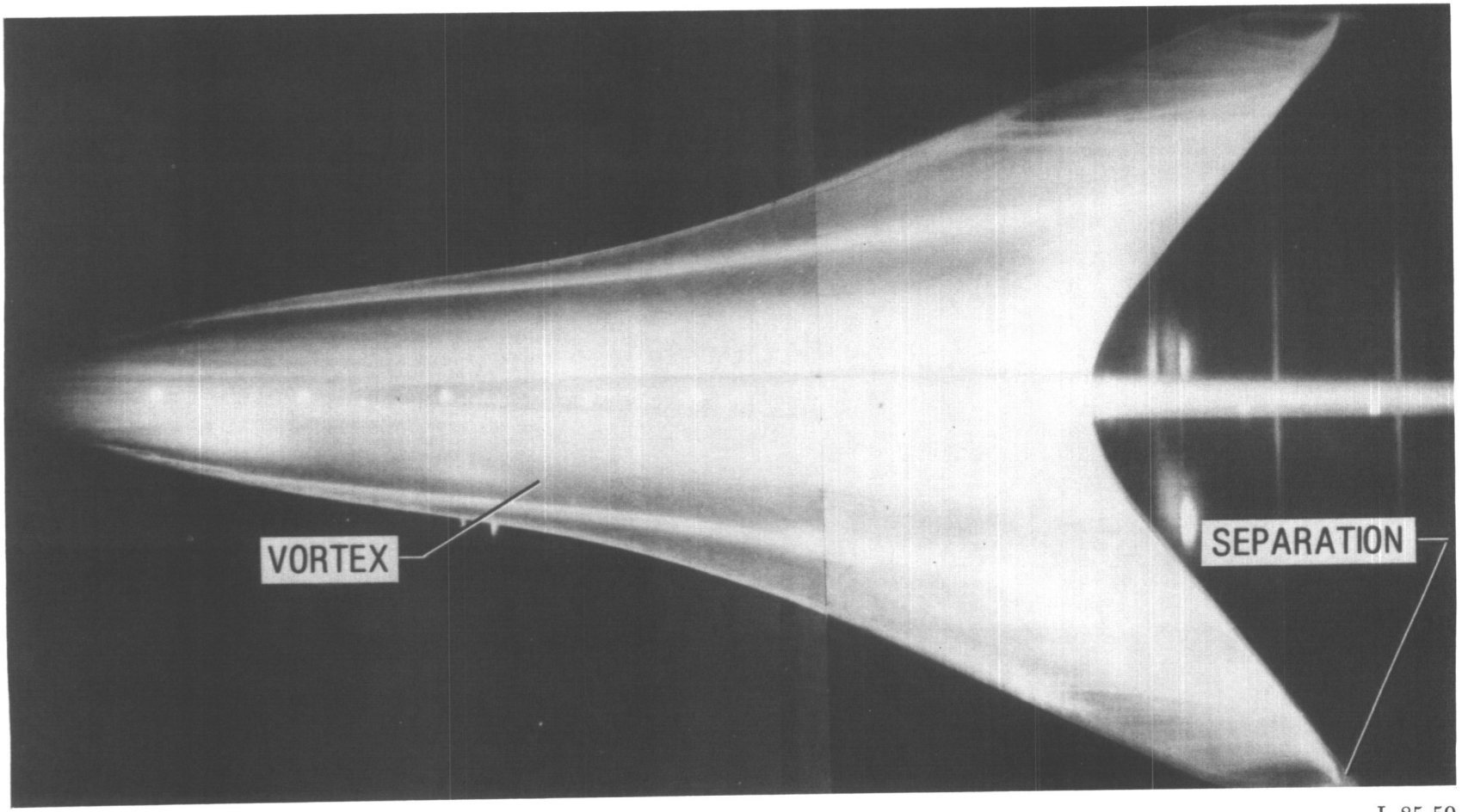

L-85-59

(b) Oil flow at $\alpha = 5°$. $C_L = 0.135$.

Figure 15. Continued.

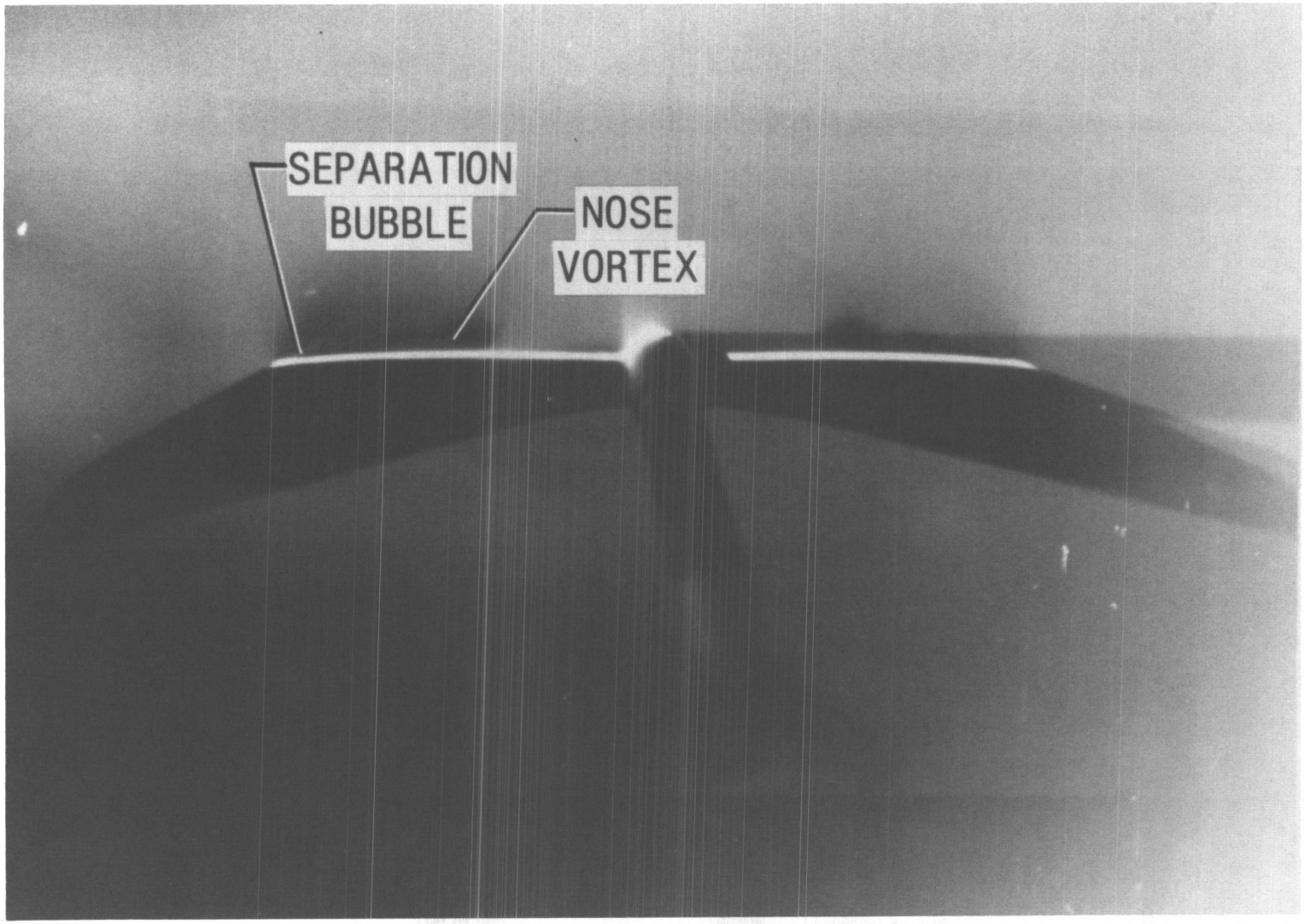

L-85-60

(c) Vapor screen at $\alpha = 5°$.

Figure 15. Concluded.

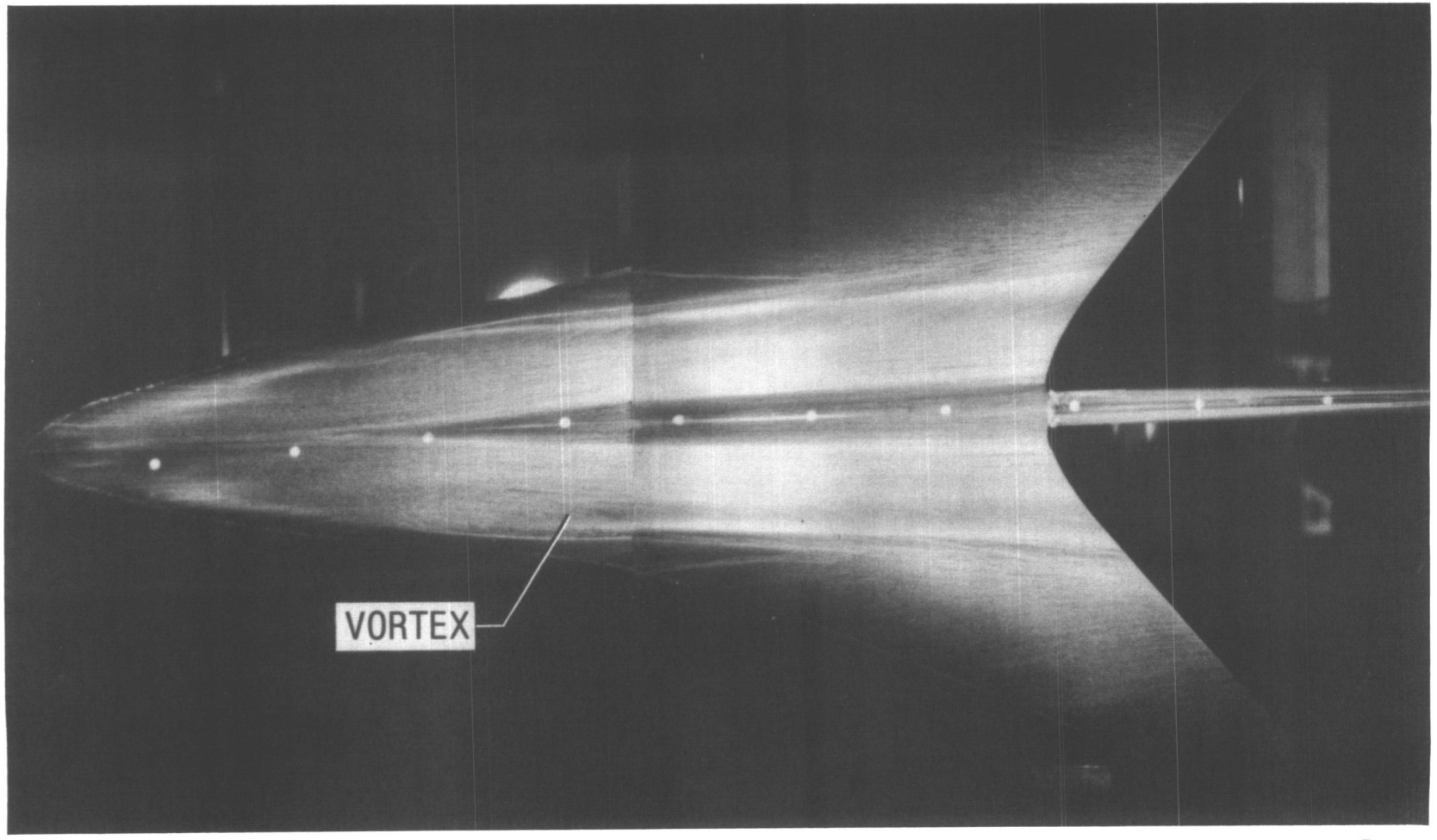

L-85-61

(a) Oil flow at $\alpha = 0°$. $C_L = 0.064$.

Figure 16. Unconstrained wing. $M = 2.4$.

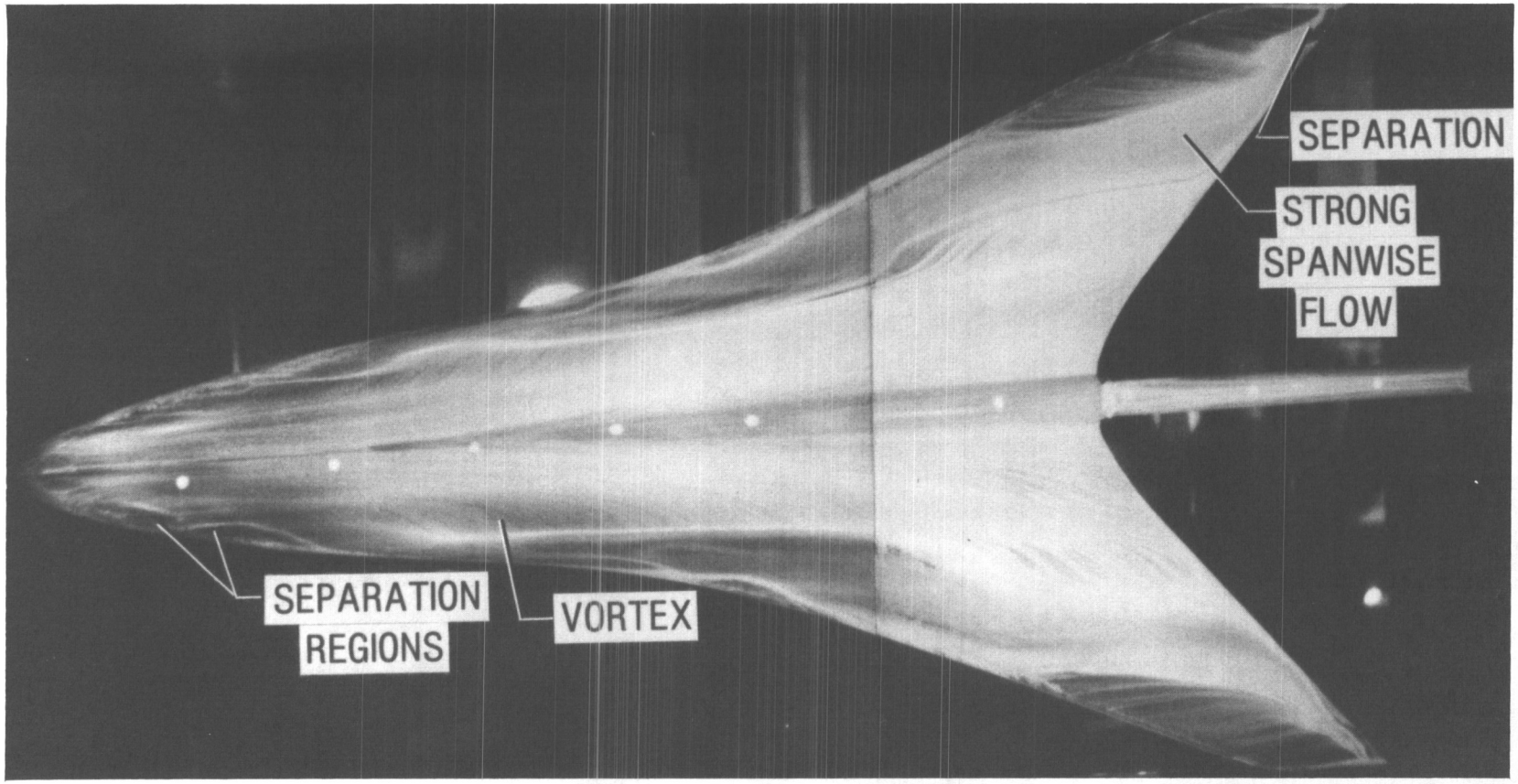

L-85-62

(b) Oil flow at $\alpha = 5°$. $C_L = 0.198$.

Figure 16. Continued.

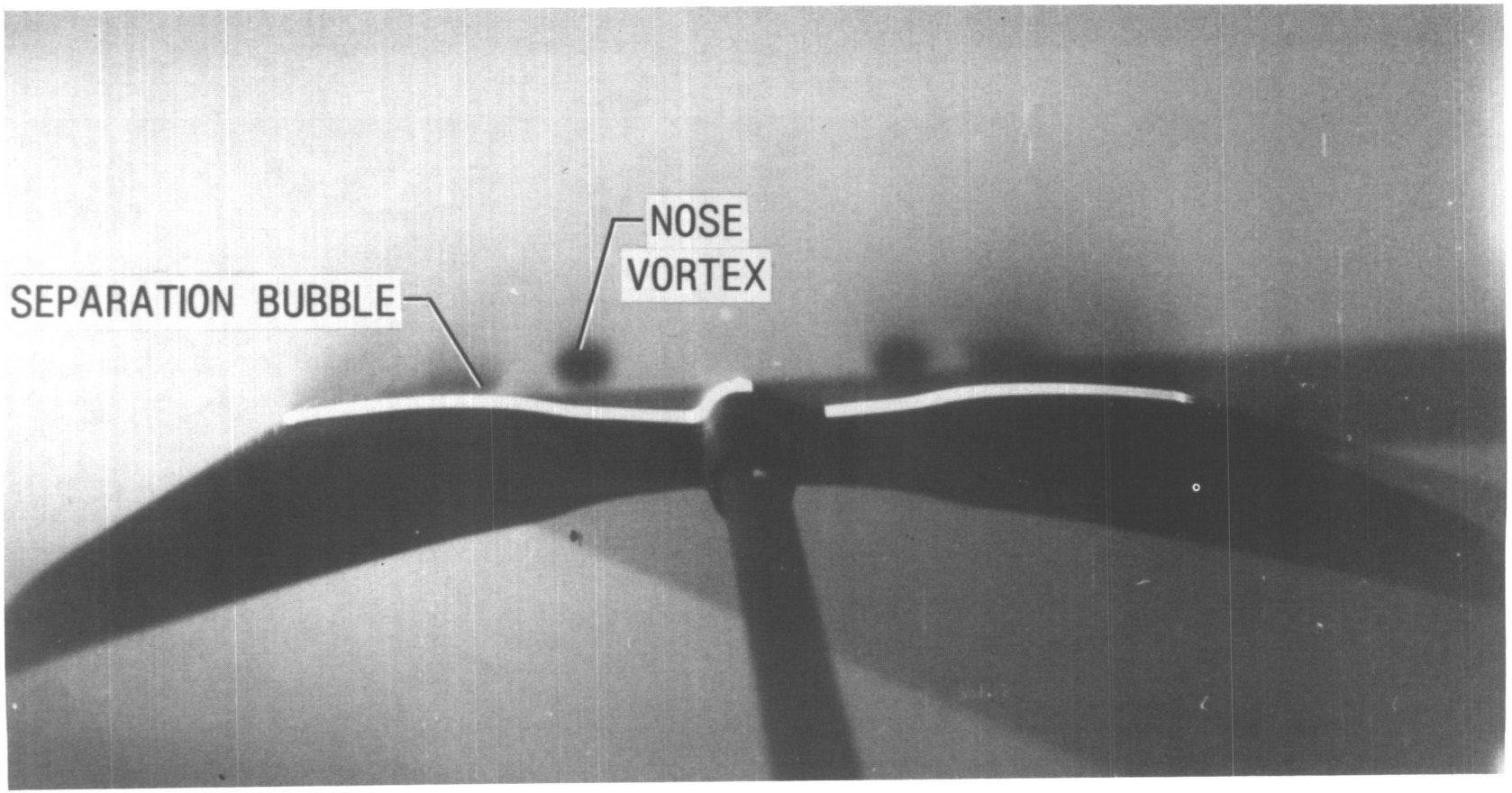

(c) Vapor screen at $\alpha = 5^{\circ}$.

Figure 16. Concluded.

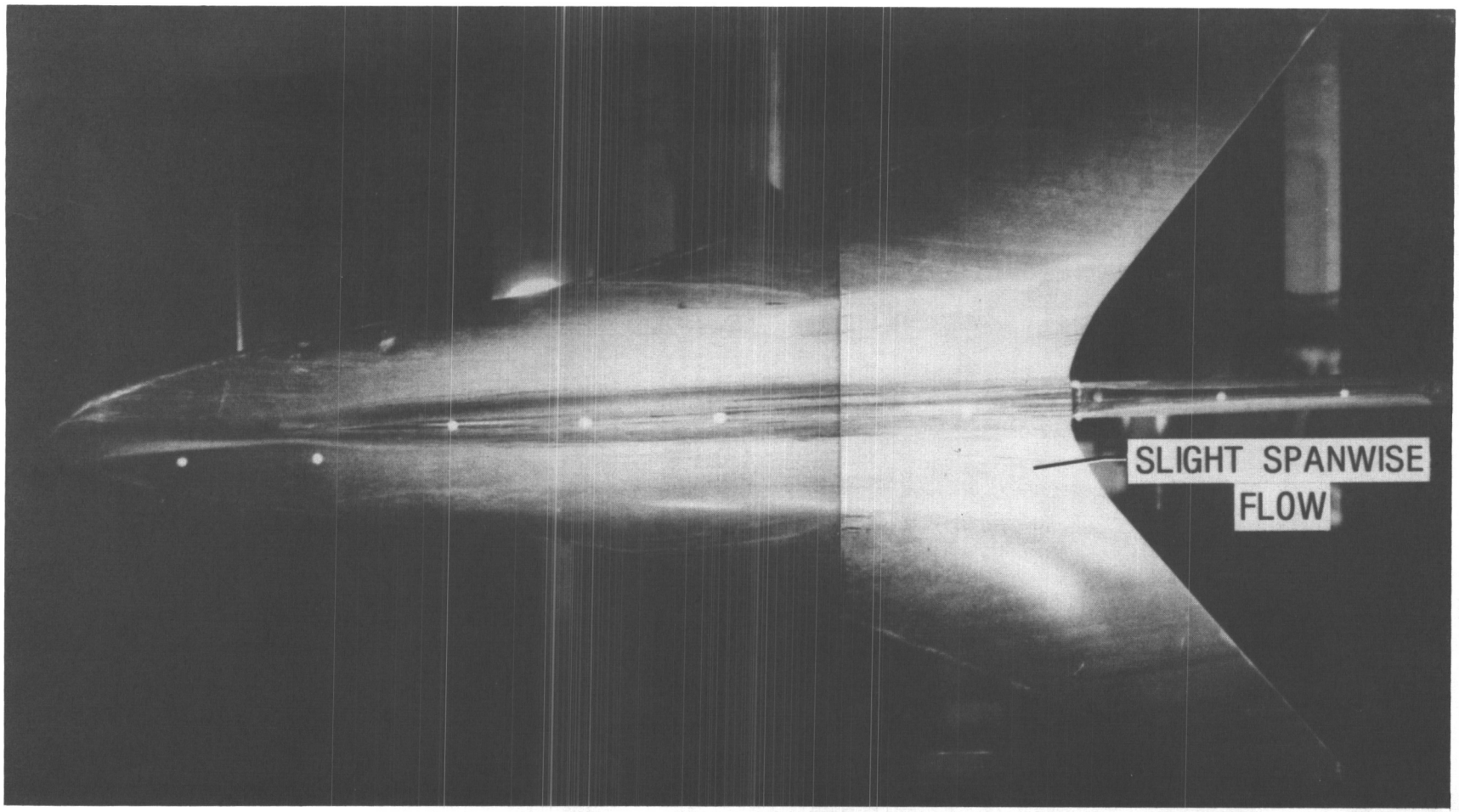

L-85-64

(a) Oil flow at $\alpha = 0°$. $C_L = 0.064$.

Figure 17. Moderately constrained wing ($M_N < 1$). $M = 2.4$.

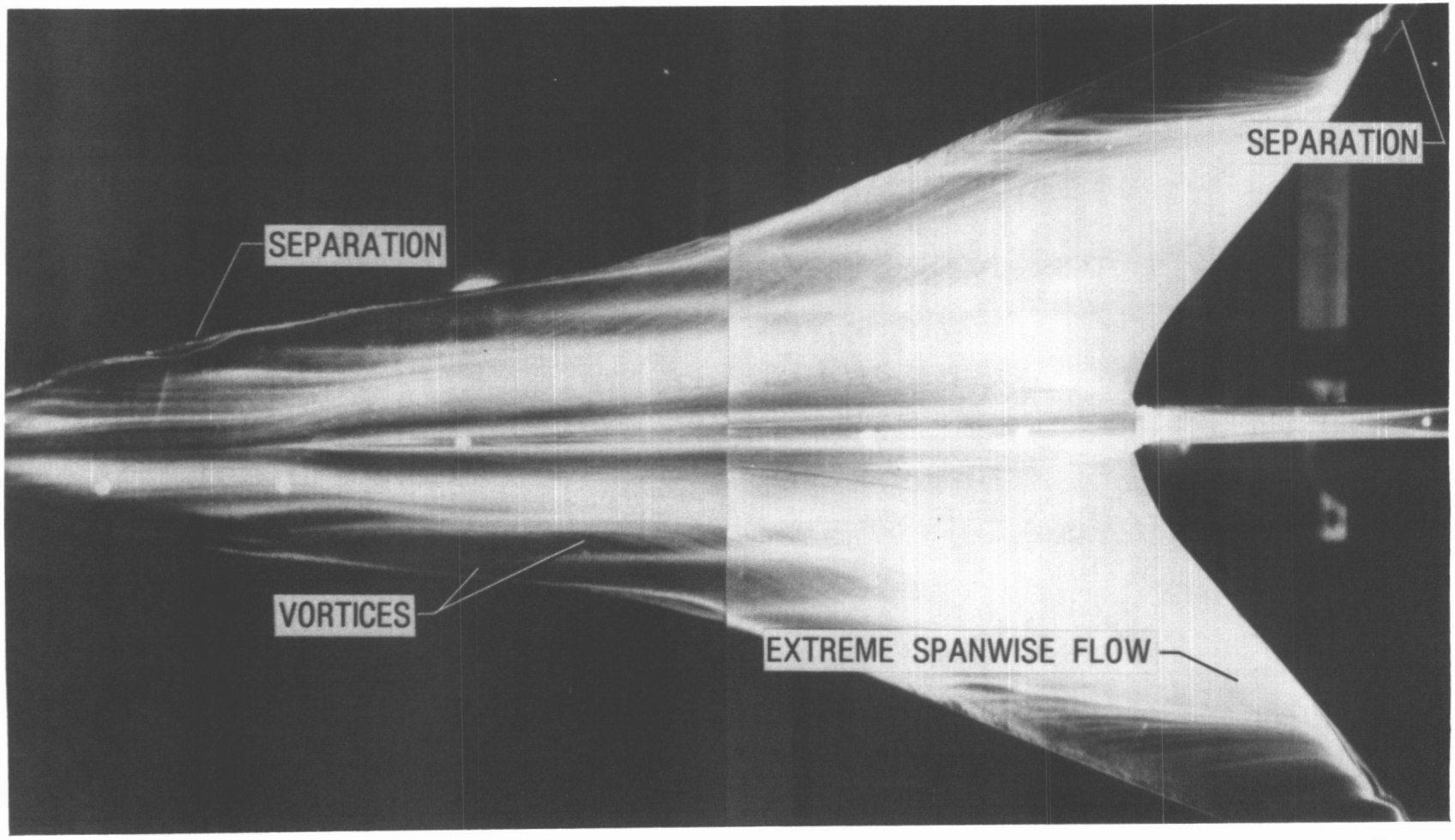

L-85-65

(b) $\alpha = 5°$. $C_L = 0.192$.

Figure 17. Continued.

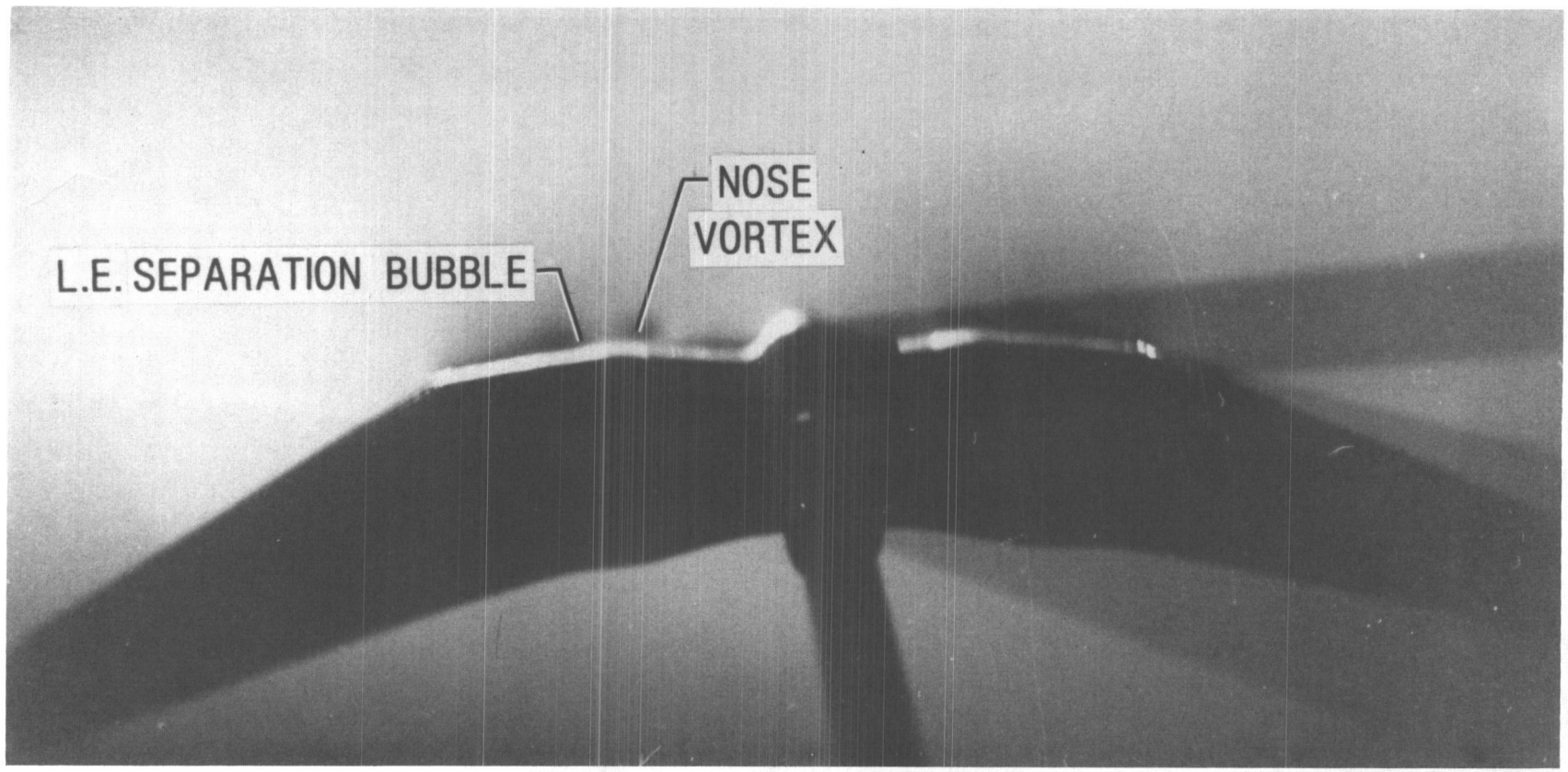

L-85-66

(c) Vapor screen at $\alpha = 5°$.

Figure 17. Concluded.

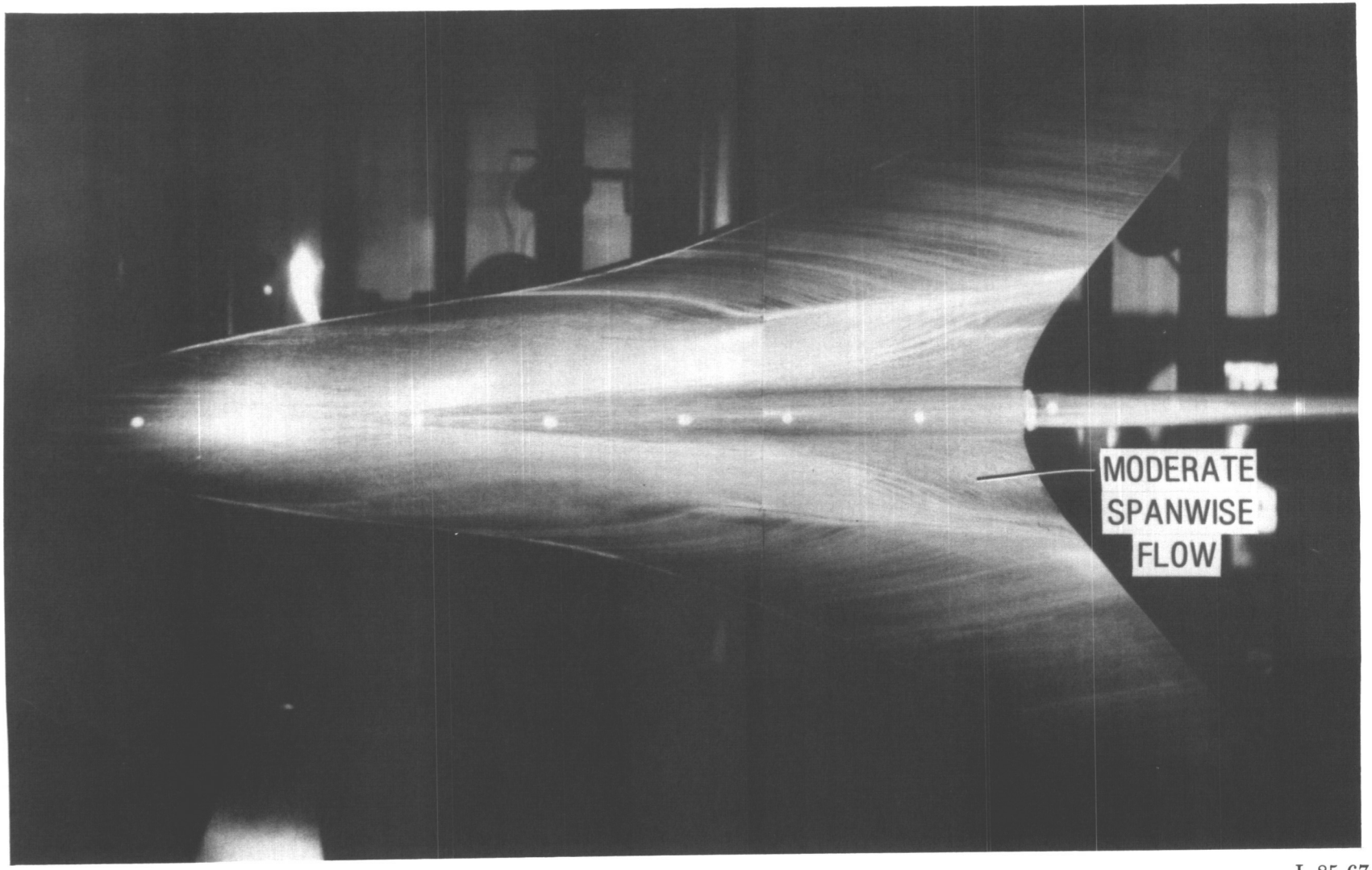

L-85-67

(a) Oil flow at $\alpha = 0°$. $C_L = 0.062$.

Figure 18. Severely constrained wing ($\Delta C_{p,\mathrm{LE}} = 0$). $M = 2.4$.

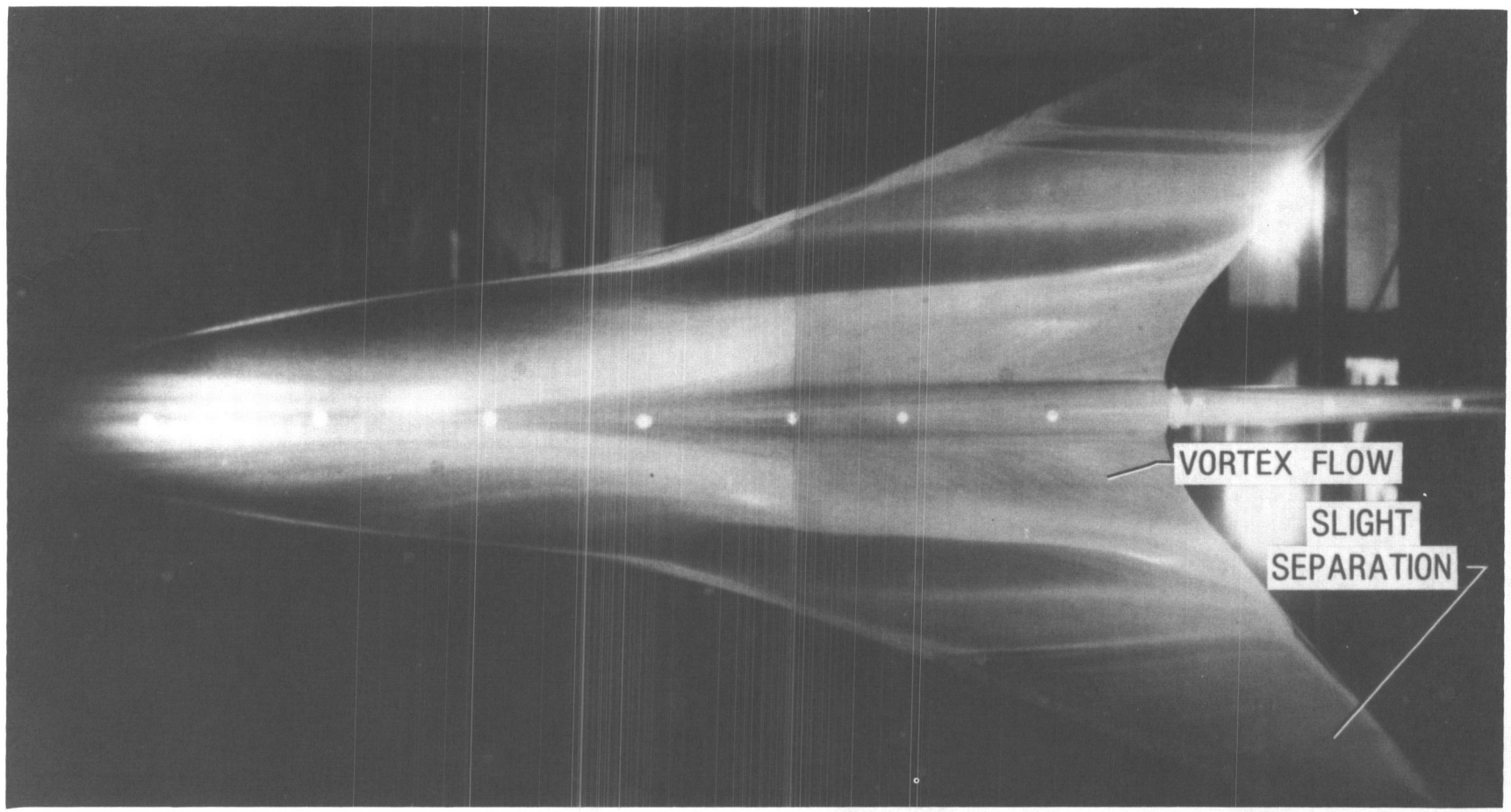

L-85-68

(b) Oil flow at $\alpha = 5°$. $C_L = 0.198$.

Figure 18. Continued.

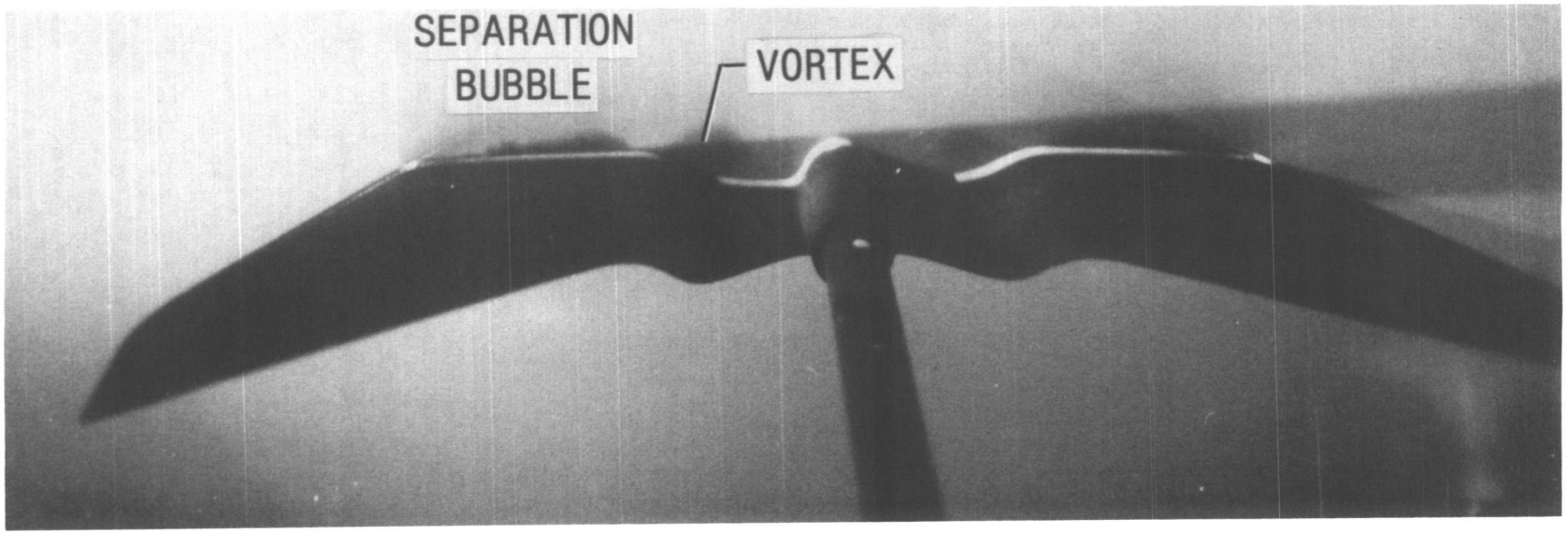

L-85-69

(c) Vapor screen at $\alpha = 5°$.

Figure 18. Concluded.

Appendix A

Tabular Force Data

Force data for the four wing models in this series are presented in appendix A (tables AI to AIV). The lift and drag coefficients have been referred to the stability axis, and the normal and axial forces have been referred to the body axis.

TABLE AI. FORCE DATA FOR FLAT WING

UPWT PROJECT 1298 RUN 66 MACH 1.80

ALPHA	CN	CA	CL	CD	L/D	CM	CAC	CDC	R/FT	DYN PRS
-5.37	-.1731	.0061	-.1718	.0222	-7.7260	.0632	.0008	.0008	2.006	456.81
-4.32	-.1396	.0062	-.1387	.0167	-8.2931	.0524	.0008	.0008	2.005	456.62
-3.34	-.1082	.0065	-.1077	.0128	-8.3809	.0413	.0008	.0008	2.005	456.58
-2.33	-.0741	.0070	-.0738	.0100	-7.3695	.0286	.0008	.0008	2.005	456.66
-1.34	-.0428	.0075	-.0426	.0085	-5.0143	.0169	.0008	.0008	2.006	456.77
-.33	-.0122	.0078	-.0121	.0078	-1.5450	.0054	.0008	.0008	2.006	456.81
.67	.0165	.0078	.0164	.0080	2.0551	-.0056	.0008	.0008	2.005	456.66
1.63	.0467	.0074	.0465	.0087	5.3142	-.0168	.0008	.0008	2.006	456.77
2.66	.0856	.0069	.0852	.0109	7.8060	-.0313	.0008	.0008	2.007	456.93
3.66	.1205	.0066	.1199	.0142	8.4125	-.0434	.0008	.0008	2.004	456.46
4.69	.1549	.0064	.1539	.0190	8.0890	-.0548	.0008	.0008	2.001	455.75
5.67	.1867	.0062	.1851	.0246	7.5230	-.0647	.0008	.0008	2.000	455.47
6.69	.2183	.0060	.2161	.0314	6.8902	-.0740	.0008	.0008	2.000	455.55
7.67	.2497	.0058	.2467	.0391	6.3098	-.0831	.0008	.0008	2.001	455.71
-.34	-.0098	.0079	-.0097	.0079	-1.2287	.0044	.0008	.0008	2.002	455.87

UPWT PROJECT 1298 RUN 77 MACH 2.00

ALPHA	CN	CA	CL	CD	L/D	CM	CAC	CDC	R/FT	DYN PRS
-5.40	-.1627	.0063	-.1614	.0216	-7.4818	.0571	.0008	.0008	2.005	449.53
-4.40	-.1342	.0065	-.1333	.0168	-7.9579	.0485	.0008	.0008	2.005	449.50
-3.41	-.1054	.0067	-.1048	.0130	-8.0592	.0389	.0008	.0008	2.005	449.68
-2.37	-.0736	.0071	-.0733	.0101	-7.2332	.0274	.0008	.0008	2.005	449.57
-1.40	-.0430	.0076	-.0428	.0086	-4.9823	.0163	.0008	.0008	2.005	449.57
-.38	-.0140	.0078	-.0139	.0079	-1.7554	.0056	.0008	.0008	2.005	449.64
.63	.0132	.0078	.0131	.0080	1.6393	-.0045	.0008	.0008	2.005	449.64
1.63	.0412	.0075	.0410	.0087	4.7161	-.0146	.0008	.0008	2.005	449.64
2.61	.0752	.0071	.0748	.0105	7.1175	-.0270	.0008	.0008	2.005	449.61
3.64	.1087	.0068	.1080	.0137	7.9030	-.0386	.0008	.0008	2.005	449.57
4.62	.1388	.0065	.1378	.0177	7.7953	-.0479	.0008	.0008	2.005	449.53
5.61	.1677	.0064	.1662	.0227	7.3155	-.0568	.0008	.0008	2.005	449.50
6.65	.1983	.0062	.1963	.0291	6.7404	-.0655	.0008	.0008	2.005	449.53
7.62	.2258	.0060	.2230	.0359	6.2066	-.0728	.0008	.0008	2.005	449.64
-.40	-.0135	.0078	-.0135	.0079	-1.7013	.0055	.0008	.0008	2.005	449.68

TABLE AI. Continued

UPWT PROJECT 1298 RUN 69 MACH 2.16

ALPHA	CN	CA	CL	CD	L/D	CM	CAC	CDC	R/FT	DYN PRS
-5.12	-.1469	.0061	-.1457	.0191	-7.6206	.0514	.0007	.0007	2.006	439.94
-4.11	-.1183	.0063	-.1175	.0147	-7.9702	.0427	.0007	.0007	2.001	438.84
-3.09	-.0885	.0065	-.0880	.0113	-7.7853	.0328	.0007	.0007	2.000	438.71
-2.09	-.0593	.0069	-.0591	.0090	-6.5407	.0222	.0007	.0007	2.002	439.23
-1.10	-.0311	.0073	-.0309	.0079	-3.9236	.0119	.0007	.0007	2.002	439.10
-.11	-.0048	.0074	-.0048	.0075	-.6415	.0023	.0007	.0007	2.002	439.10
.90	.0213	.0074	.0212	.0077	2.7543	-.0072	.0007	.0007	2.002	439.07
1.91	.0505	.0070	.0502	.0087	5.7981	-.0176	.0007	.0007	2.002	439.10
2.90	.0823	.0067	.0818	.0108	7.5656	-.0292	.0007	.0007	2.002	439.20
3.89	.1136	.0064	.1129	.0141	8.0071	-.0398	.0007	.0007	2.002	439.20
4.90	.1430	.0062	.1419	.0184	7.7286	-.0487	.0007	.0007	2.002	439.10
5.92	.1705	.0060	.1690	.0236	7.1751	-.0566	.0007	.0007	2.002	439.16
6.91	.1977	.0059	.1955	.0296	6.6062	-.0642	.0007	.0007	2.001	439.00
7.93	.2252	.0057	.2223	.0368	6.0449	-.0717	.0007	.0007	2.002	439.20
-.09	-.0035	.0075	-.0035	.0075	-.4630	.0019	.0007	.0007	2.004	439.59

UPWT PROJECT 1298 RUN 61 MACH 2.40

ALPHA	CN	CA	CL	CD	L/D	CM	CAC	CDC	R/FT	DYN PRS
-5.21	-.1416	.0058	-.1404	.0186	-7.5388	.0478	.0006	.0006	2.001	419.20
-4.25	-.1170	.0061	-.1162	.0147	-7.9050	.0403	.0006	.0006	2.001	419.25
-3.19	-.0820	.0062	-.0815	.0108	-7.5561	.0293	.0006	.0006	2.003	419.69
-2.16	-.0538	.0066	-.0535	.0086	-6.2353	.0195	.0006	.0006	2.002	419.44
-1.14	-.0245	.0069	-.0243	.0074	-3.3097	.0097	.0006	.0006	2.000	419.03
-.18	-.0007	.0070	-.0007	.0070	-.0957	.0008	.0006	.0006	2.002	419.47
.85	.0245	.0069	.0244	.0072	3.3744	-.0075	.0006	.0006	2.000	419.03
1.86	.0541	.0066	.0538	.0083	6.4480	-.0187	.0006	.0006	2.000	419.03
2.68	.0671	.0064	.0668	.0095	7.0037	-.0241	.0006	.0006	2.001	419.28
3.93	.1126	.0060	.1119	.0137	8.1637	-.0382	.0006	.0006	2.002	419.53
4.78	.1280	.0059	.1271	.0165	7.6938	-.0438	.0006	.0006	1.999	418.92
5.84	.1580	.0057	.1566	.0218	7.1927	-.0520	.0006	.0006	2.000	419.06
6.75	.1767	.0056	.1749	.0263	6.6402	-.0579	.0006	.0006	2.001	419.28
7.82	.2068	.0055	.2042	.0336	6.0817	-.0656	.0006	.0006	2.001	419.28
3.86	.1082	.0060	.1076	.0133	8.0811	-.0369	.0006	.0006	2.001	419.17
2.78	.0746	.0063	.0742	.0099	7.4924	-.0263	.0006	.0006	2.003	419.58
-.19	-.0044	.0069	-.0044	.0069	-.6338	.0019	.0006	.0006	2.001	419.31

TABLE AI. Concluded

UPWT PROJECT 1298 RUN 79 MACH 2.60

ALPHA	CN	CA	CL	CD	L/D	CM	CAC	CDC	R/FT	DYN PRS
-5.22	-.1339	.0057	-.1328	.0179	-7.4326	.0453	.0006	.0006	2.003	400.32
-4.18	-.1049	.0060	-.1042	.0136	-7.6483	.0368	.0006	.0006	2.000	399.76
-3.15	-.0799	.0061	-.0794	.0105	-7.5787	.0284	.0006	.0006	1.998	399.35
-2.22	-.0595	.0063	-.0592	.0086	-6.8663	.0214	.0006	.0006	2.003	400.28
-1.14	-.0247	.0067	-.0245	.0072	-3.4119	.0098	.0006	.0006	2.002	400.16
-.20	-.0062	.0069	-.0062	.0069	-.8982	.0029	.0006	.0006	2.003	400.21
.83	.0174	.0068	.0173	.0071	2.4470	-.0055	.0005	.0005	2.002	400.16
1.79	.0404	.0066	.0402	.0078	5.1302	-.0140	.0005	.0005	2.003	400.25
2.86	.0746	.0062	.0742	.0099	7.4724	-.0254	.0005	.0005	2.004	400.49
3.80	.0955	.0061	.0948	.0124	7.6348	-.0325	.0006	.0006	2.004	400.56
4.82	.1222	.0060	.1213	.0162	7.4775	-.0408	.0006	.0006	2.003	400.35
5.83	.1512	.0058	.1498	.0211	7.0918	-.0489	.0006	.0006	2.004	400.40
6.81	.1714	.0057	.1695	.0260	6.5151	-.0553	.0006	.0006	2.003	400.30
7.85	.1974	.0056	.1948	.0325	5.9918	-.0621	.0006	.0006	2.005	400.59
-.20	-.0058	.0069	-.0058	.0069	-.8354	.0024	.0006	.0006	2.003	400.30

UPWT PROJECT 1298 RUN 81 MACH 2.80

ALPHA	CN	CA	CL	CD	L/D	CM	CAC	CDC	R/FT	DYN PRS
-5.16	-.1214	.0057	-.1204	.0166	-7.2602	.0406	.0005	.0005	2.002	379.13
-4.16	-.0967	.0057	-.0961	.0127	-7.5513	.0329	.0005	.0005	2.002	379.13
-3.12	-.0739	.0059	-.0734	.0099	-7.4353	.0258	.0005	.0005	2.004	379.61
-2.16	-.0516	.0061	-.0513	.0080	-6.3986	.0184	.0005	.0005	2.001	378.91
-1.14	-.0260	.0064	-.0258	.0069	-3.7495	.0097	.0005	.0005	2.003	379.29
-.17	-.0071	.0066	-.0071	.0066	-1.0766	.0027	.0005	.0005	2.004	379.61
.86	.0175	.0065	.0174	.0068	2.5668	-.0059	.0005	.0005	2.003	379.35
1.83	.0411	.0062	.0408	.0075	5.4332	-.0140	.0005	.0005	2.000	378.83
2.86	.0672	.0060	.0668	.0093	7.1464	-.0230	.0005	.0005	2.002	379.07
3.83	.0907	.0059	.0901	.0119	7.5693	-.0307	.0005	.0005	2.002	379.21
4.83	.1138	.0058	.1129	.0153	7.3623	-.0381	.0005	.0005	2.005	379.67
5.84	.1393	.0056	.1380	.0198	6.9815	-.0453	.0005	.0005	2.001	378.99
6.86	.1643	.0056	.1625	.0251	6.4611	-.0524	.0005	.0005	2.002	379.07
7.89	.1870	.0055	.1845	.0311	5.9338	-.0588	.0005	.0005	2.004	379.57
-.14	-.0025	.0066	-.0025	.0066	-.3770	.0016	.0005	.0005	2.003	379.41

TABLE AII. FORCE DATA FOR UNCONSTRAINED WING

UPWT PROJECT 1298 RUN 194 MACH 1.80

ALPHA	CN	CA	CL	CD	L/D	CM	CAC	CDC	R/FT	DYN PRS
-5.33	-.1007	.0054	-.0997	.0147	-6.7733	.0520	.0008	.0008	2.000	455.51
-4.39	-.0700	.0064	-.0693	.0117	-5.9097	.0404	.0008	.0008	2.001	455.75
-3.33	-.0350	.0075	-.0345	.0096	-3.6047	.0270	.0008	.0008	2.006	456.73
-2.34	-.0028	.0086	-.0025	.0087	-.2854	.0147	.0009	.0009	2.003	456.22
-1.37	.0263	.0093	.0265	.0087	3.0533	.0038	.0009	.0009	2.006	456.77
-.37	.0578	.0100	.0579	.0096	6.0430	-.0076	.0009	.0009	2.004	456.38
.64	.0891	.0103	.0890	.0113	7.9095	-.0186	.0009	.0009	2.001	455.67
1.63	.1220	.0105	.1216	.0139	8.7294	-.0298	.0009	.0009	2.004	456.38
2.62	.1567	.0112	.1560	.0183	8.5123	-.0413	.0009	.0009	2.001	455.71
3.66	.1894	.0126	.1882	.0247	7.6185	-.0496	.0009	.0009	2.004	456.38
4.63	.2209	.0141	.2191	.0319	6.8771	-.0582	.0009	.0009	2.003	456.14
5.67	.2531	.0156	.2503	.0405	6.1767	-.0665	.0009	.0009	2.002	455.87
6.65	.2836	.0171	.2797	.0498	5.6155	-.0742	.0009	.0009	2.002	455.83
7.63	.3140	.0184	.3088	.0600	5.1498	-.0820	.0009	.0009	2.001	455.79
-.34	.0589	.0100	.0590	.0096	6.1400	-.0078	.0009	.0009	2.003	456.02

UPWT PROJECT 1298 RUN 201 MACH 2.00

ALPHA	CN	CA	CL	CD	L/D	CM	CAC	CDC	R/FT	DYN PRS
-5.46	-.0938	.0053	-.0929	.0142	-6.5458	.0473	.0008	.0008	1.999	448.35
-4.42	-.0634	.0063	-.0628	.0112	-5.6089	.0364	.0008	.0008	1.999	448.35
-3.46	-.0339	.0073	-.0334	.0093	-3.5969	.0253	.0008	.0008	2.001	448.75
-2.43	-.0026	.0082	-.0022	.0083	-.2647	.0135	.0008	.0008	1.999	448.17
-1.42	.0272	.0090	.0274	.0084	3.2746	.0028	.0008	.0008	1.999	448.35
-.44	.0563	.0097	.0564	.0092	6.1029	-.0073	.0008	.0008	2.001	448.64
.54	.0845	.0100	.0844	.0108	7.8065	-.0170	.0008	.0008	1.997	447.85
1.55	.1165	.0103	.1162	.0135	8.6156	-.0279	.0008	.0008	1.997	447.89
2.60	.1500	.0110	.1494	.0178	8.3838	-.0389	.0008	.0008	1.997	447.85
3.59	.1798	.0123	.1787	.0235	7.6015	-.0464	.0008	.0008	2.001	448.71
4.59	.2081	.0136	.2063	.0303	6.8189	-.0532	.0008	.0008	2.000	448.46
5.61	.2380	.0151	.2353	.0383	6.1372	-.0606	.0008	.0008	1.998	448.03
6.53	.2637	.0164	.2601	.0463	5.6241	-.0673	.0008	.0008	1.998	448.07
7.57	.2938	.0178	.2889	.0563	5.1296	-.0746	.0008	.0008	2.001	448.68
-.43	.0569	.0097	.0570	.0092	6.1685	-.0078	.0008	.0008	2.001	448.68

TABLE AII. Continued

UPWT PROJECT 1298 RUN 203 MACH 2.16

ALPHA	CN	CA	CL	CD	L/D	CM	CAC	CDC	R/FT	DYN PRS
-5.42	-.0864	.0054	-.0855	.0135	-6.3224	.0434	.0007	.0007	1.999	438.45
-4.40	-.0579	.0064	-.0572	.0108	-5.3122	.0335	.0007	.0007	2.000	438.68
-3.38	-.0282	.0073	-.0277	.0089	-3.1059	.0227	.0007	.0007	1.998	438.25
-2.45	-.0013	.0081	-.0009	.0081	-.1165	.0128	.0007	.0007	2.002	439.03
-1.45	.0272	.0089	.0274	.0082	3.3423	.0026	.0008	.0008	2.002	439.20
-.44	.0559	.0095	.0560	.0091	6.1478	-.0074	.0008	.0008	1.998	438.29
.57	.0848	.0099	.0847	.0108	7.8544	-.0172	.0008	.0008	1.997	437.93
1.55	.1145	.0103	.1141	.0134	8.5142	-.0271	.0008	.0008	1.999	438.55
2.59	.1454	.0109	.1447	.0174	8.2991	-.0371	.0008	.0008	2.000	438.74
3.55	.1734	.0119	.1723	.0226	7.6220	-.0449	.0008	.0008	1.999	438.38
4.60	.2022	.0134	.2005	.0296	6.7797	-.0515	.0008	.0008	1.998	438.19
5.58	.2282	.0147	.2257	.0368	6.1341	-.0576	.0008	.0008	2.000	438.68
6.61	.2552	.0160	.2516	.0452	5.5662	-.0646	.0008	.0008	2.002	439.20
7.58	.2817	.0173	.2769	.0543	5.1029	-.0713	.0008	.0008	2.000	438.68
-.46	.0564	.0096	.0565	.0091	6.2007	-.0075	.0008	.0008	2.001	438.97

UPWT PROJECT 1298 RUN 206 MACH 2.40

ALPHA	CN	CA	CL	CD	L/D	CM	CAC	CDC	R/FT	DYN PRS
-5.21	-.0736	.0056	-.0728	.0122	-5.9437	.0377	.0006	.0006	2.004	419.80
-4.23	-.0497	.0064	-.0490	.0100	-4.8869	.0294	.0006	.0006	2.002	419.42
-3.21	-.0225	.0071	-.0220	.0084	-2.6240	.0196	.0006	.0006	2.003	419.58
-2.32	-.0005	.0078	-.0002	.0078	-.0277	.0113	.0006	.0006	2.003	419.77
-1.22	.0350	.0089	.0352	.0081	4.3205	-.0009	.0006	.0006	2.004	419.83
-.13	.0633	.0095	.0633	.0094	6.7629	-.0106	.0007	.0007	2.005	420.11
.77	.0892	.0098	.0890	.0110	8.0825	-.0192	.0007	.0007	2.006	420.22
1.87	.1205	.0104	.1201	.0143	8.4100	-.0295	.0007	.0007	2.006	420.35
2.74	.1383	.0108	.1376	.0174	7.9211	-.0355	.0007	.0007	2.007	420.52
3.78	.1690	.0115	.1678	.0226	7.4173	-.0440	.0007	.0007	2.007	420.46
4.77	.1943	.0126	.1925	.0287	6.7015	-.0508	.0007	.0007	2.008	420.71
5.89	.2245	.0142	.2218	.0372	5.9654	-.0578	.0007	.0007	2.007	420.60
6.82	.2466	.0153	.2430	.0444	5.4688	-.0636	.0007	.0007	2.008	420.66
7.88	.2732	.0167	.2683	.0540	4.9726	-.0697	.0007	.0007	2.008	420.79
-.23	.0569	.0093	.0569	.0091	6.2907	-.0087	.0007	.0007	2.008	420.79

TABLE AII. Concluded

UPWT PROJECT 1298 RUN 210 MACH 2.60

ALPHA	CN	CA	CL	CD	L/D	CM	CAC	CDC	R/FT	DYN PRS
-5.20	-.0688	.0054	-.0680	.0116	-5.8705	.0353	.0006	.0005	2.001	399.90
-4.17	-.0414	.0063	-.0408	.0093	-4.3783	.0268	.0006	.0006	2.000	399.71
-3.15	-.0156	.0071	-.0152	.0080	-1.9062	.0176	.0006	.0006	2.001	399.83
-2.22	.0047	.0077	.0050	.0075	.6677	.0099	.0006	.0006	2.002	399.99
-1.16	.0353	.0086	.0354	.0079	4.5102	-.0010	.0006	.0006	2.001	399.92
-.22	.0547	.0091	.0547	.0088	6.1864	-.0077	.0006	.0006	2.001	399.92
.80	.0825	.0096	.0824	.0108	7.6458	-.0172	.0006	.0006	2.001	399.87
1.83	.1097	.0101	.1093	.0136	8.0500	-.0258	.0006	.0006	2.002	399.99
2.83	.1350	.0106	.1343	.0172	7.8009	-.0336	.0006	.0006	2.002	400.04
3.77	.1560	.0112	.1549	.0214	7.2339	-.0398	.0006	.0006	2.004	400.49
4.82	.1841	.0122	.1824	.0276	6.6012	-.0471	.0006	.0006	2.001	399.85
5.91	.2111	.0135	.2086	.0352	5.9318	-.0538	.0006	.0006	2.002	400.09
6.84	.2315	.0145	.2281	.0419	5.4398	-.0595	.0006	.0006	2.001	399.87
7.84	.2535	.0155	.2490	.0500	4.9811	-.0651	.0006	.0006	2.002	400.04
-.17	.0572	.0091	.0572	.0090	6.3782	-.0085	.0006	.0006	2.001	399.95

UPWT PROJECT 1298 RUN 212 MACH 2.80

ALPHA	CN	CA	CL	CD	L/D	CM	CAC	CDC	R/FT	DYN PRS
-5.13	-.0642	.0053	-.0635	.0110	-5.7746	.0329	.0005	.0005	2.000	378.68
-4.11	-.0401	.0060	-.0395	.0089	-4.4462	.0249	.0005	.0005	2.001	378.87
-3.11	-.0166	.0068	-.0162	.0077	-2.1142	.0171	.0005	.0005	2.001	378.91
-2.11	.0083	.0075	.0086	.0072	1.1820	.0080	.0005	.0005	2.001	378.93
-1.08	.0349	.0084	.0351	.0077	4.5568	-.0006	.0005	.0005	2.000	378.85
-.08	.0578	.0090	.0578	.0089	6.4948	-.0087	.0005	.0005	2.000	378.83
.92	.0796	.0095	.0794	.0108	7.3855	-.0161	.0005	.0005	2.000	378.76
1.91	.1035	.0100	.1031	.0134	7.6780	-.0237	.0005	.0005	1.999	378.66
2.96	.1293	.0105	.1286	.0172	7.4693	-.0311	.0005	.0005	2.000	378.78
3.90	.1509	.0111	.1498	.0214	7.0074	-.0372	.0005	.0005	1.999	378.62
4.93	.1737	.0120	.1720	.0269	6.3939	-.0433	.0005	.0005	2.000	378.83
5.92	.1937	.0128	.1914	.0328	5.8423	-.0488	.0005	.0005	2.000	378.70
6.89	.2139	.0138	.2107	.0393	5.3553	-.0541	.0005	.0005	2.000	378.76
7.83	.2334	.0147	.2292	.0463	4.9466	-.0597	.0005	.0005	1.999	378.64
-.11	.0546	.0089	.0546	.0088	6.2100	-.0079	.0005	.0005	1.999	378.66

TABLE AIII. FORCE DATA FOR MODERATELY CONSTRAINED WING ($M_N < 1$)

UPWT PROJECT 1298 RUN 170 MACH 1.80

ALPHA	CN	CA	CL	CD	L/D	CM	CAC	CDC	R/FT	DYN PRS
-5.36	-.1010	.0056	-.1001	.0151	-6.6484	.0474	.0008	.0008	2.006	456.81
-4.35	-.0672	.0066	-.0665	.0117	-5.6870	.0350	.0008	.0008	2.004	456.38
-3.36	-.0351	.0076	-.0346	.0096	-3.6022	.0228	.0008	.0008	2.001	455.71
-2.33	-.0026	.0085	-.0023	.0086	-.2665	.0104	.0008	.0008	2.004	456.38
-1.37	.0270	.0093	.0272	.0086	3.1612	-.0007	.0008	.0008	2.003	456.02
-.35	.0586	.0099	.0587	.0095	6.1700	-.0123	.0008	.0008	2.002	455.87
.69	.0903	.0101	.0901	.0112	8.0564	-.0234	.0008	.0008	2.003	456.14
1.66	.1228	.0103	.1224	.0138	8.8526	-.0348	.0008	.0008	2.001	455.59
2.62	.1535	.0101	.1529	.0171	8.9172	-.0454	.0008	.0008	2.002	455.98
3.65	.1882	.0107	.1872	.0226	8.2646	-.0556	.0008	.0008	2.003	456.10
4.68	.2225	.0117	.2208	.0298	7.3979	-.0650	.0008	.0008	2.004	456.46
5.67	.2522	.0127	.2497	.0376	6.6454	-.0729	.0008	.0008	2.001	455.67
6.66	.2826	.0139	.2791	.0466	5.9942	-.0804	.0008	.0008	2.004	456.34
7.68	.3142	.0151	.3093	.0569	5.4352	-.0881	.0008	.0007	2.002	455.94
-.35	.0583	.0098	.0584	.0095	6.1790	-.0122	.0008	.0008	2.003	456.18

UPWT PROJECT 1298 RUN 177 MACH 2.00

ALPHA	CN	CA	CL	CD	L/D	CM	CAC	CDC	R/FT	DYN PRS
-5.74	-.0956	.0056	-.0946	.0152	-6.2427	.0438	.0008	.0008	1.998	448.00
-4.76	-.0671	.0064	-.0664	.0120	-5.5336	.0338	.0008	.0008	1.997	447.85
-3.74	-.0366	.0074	-.0361	.0097	-3.7087	.0225	.0008	.0008	1.997	447.89
-2.75	-.0059	.0083	-.0055	.0086	-.6440	.0111	.0008	.0008	1.999	448.14
-1.77	.0225	.0090	.0228	.0083	2.7437	.0006	.0008	.0008	1.998	448.03
-.76	.0517	.0096	.0518	.0089	5.8212	-.0098	.0008	.0008	1.998	447.92
.25	.0814	.0098	.0813	.0102	7.9827	-.0200	.0008	.0008	1.997	447.85
1.26	.1123	.0101	.1121	.0125	8.9496	-.0306	.0008	.0008	1.998	448.03
2.24	.1434	.0102	.1429	.0158	9.0577	-.0412	.0008	.0008	1.998	448.00
3.25	.1741	.0107	.1732	.0205	8.4417	-.0501	.0008	.0008	1.997	447.82
4.27	.2044	.0114	.2030	.0266	7.6307	-.0580	.0007	.0007	1.998	447.96
5.23	.2313	.0124	.2292	.0334	6.8612	-.0647	.0007	.0007	1.998	448.10
6.27	.2614	.0135	.2584	.0420	6.1523	-.0717	.0007	.0007	1.997	447.85
7.24	.2884	.0146	.2843	.0509	5.5874	-.0782	.0007	.0007	1.997	447.85
-.75	.0532	.0096	.0533	.0089	5.9857	-.0103	.0008	.0008	1.999	448.17

TABLE AIII. Continued

UPWT PROJECT 1298 RUN 179 MACH 2.16

ALPHA	CN	CA	CL	CD	L/D	CM	CAC	CDC	R/FT	DYN PRS
-5.36	-.0862	.0059	-.0853	.0139	-6.1397	.0391	.0007	.0007	2.007	440.14
-4.35	-.0583	.0067	-.0576	.0111	-5.1927	.0299	.0007	.0007	2.004	439.46
-3.37	-.0308	.0075	-.0303	.0093	-3.2641	.0199	.0007	.0007	1.999	438.48
-2.35	-.0005	.0083	-.0002	.0084	-.0201	.0090	.0007	.0007	2.001	438.90
-1.38	.0260	.0090	.0263	.0084	3.1333	-.0005	.0007	.0007	2.002	439.13
-.36	.0550	.0096	.0550	.0092	5.9745	-.0106	.0007	.0007	2.002	439.10
.65	.0827	.0098	.0826	.0108	7.6684	-.0199	.0007	.0007	2.001	439.00
1.65	.1122	.0100	.1119	.0132	8.4733	-.0300	.0007	.0007	2.002	439.23
2.65	.1425	.0103	.1419	.0168	8.4229	-.0398	.0007	.0007	2.000	438.74
3.63	.1709	.0107	.1699	.0215	7.9053	-.0482	.0007	.0007	2.001	438.87
4.64	.2001	.0115	.1985	.0277	7.1735	-.0555	.0007	.0007	2.002	439.10
5.64	.2271	.0124	.2248	.0347	6.4765	-.0619	.0007	.0007	2.000	438.61
6.66	.2542	.0135	.2509	.0429	5.8517	-.0680	.0007	.0007	2.001	438.90
7.62	.2792	.0145	.2748	.0514	5.3426	-.0739	.0007	.0007	2.001	438.90
-.36	.0550	.0096	.0551	.0092	5.9683	-.0106	.0007	.0007	2.002	439.03

UPWT PROJECT 1298 RUN 182 MACH 2.40

ALPHA	CN	CA	CL	CD	L/D	CM	CAC	CDC	R/FT	DYN PRS
-5.19	-.0746	.0059	-.0737	.0126	-5.8335	.0344	.0006	.0006	1.990	393.99
-4.18	-.0528	.0066	-.0522	.0104	-5.0139	.0270	.0006	.0006	1.990	394.07
-3.17	-.0217	.0074	-.0213	.0086	-2.4686	.0169	.0006	.0006	1.988	393.74
-2.23	.0013	.0081	.0016	.0080	.2020	.0082	.0006	.0006	1.992	394.37
-1.15	.0313	.0088	.0315	.0081	3.8713	-.0025	.0006	.0006	1.989	393.77
-.19	.0549	.0093	.0549	.0091	6.0100	-.0108	.0006	.0006	1.990	393.99
.79	.0777	.0096	.0776	.0106	7.2893	-.0185	.0006	.0006	1.990	394.13
1.82	.1089	.0099	.1086	.0134	8.1210	-.0288	.0006	.0006	1.990	393.96
2.77	.1381	.0101	.1375	.0168	8.1969	-.0380	.0006	.0006	1.989	393.85
3.78	.1644	.0106	.1634	.0214	7.6367	-.0460	.0006	.0006	1.991	394.21
4.78	.1909	.0112	.1893	.0271	6.9990	-.0531	.0006	.0006	1.991	394.24
5.78	.2149	.0121	.2125	.0337	6.3049	-.0594	.0006	.0006	1.990	394.02
6.78	.2394	.0129	.2362	.0411	5.7455	-.0649	.0006	.0006	1.989	393.85
7.81	.2678	.0142	.2634	.0504	5.2238	-.0713	.0006	.0006	1.991	394.21
-.23	.0537	.0094	.0538	.0092	5.8687	-.0106	.0006	.0006	1.989	393.82

TABLE AIII. Concluded

UPWT PROJECT 1298 RUN 186 MACH 2.60

ALPHA	CN	CA	CL	CD	L/D	CM	CAC	CDC	R/FT	DYN PRS
-5.10	-.0721	.0057	-.0713	.0121	-5.9038	.0329	.0005	.0005	2.001	375.28
-4.15	-.0496	.0065	-.0490	.0101	-4.8428	.0255	.0005	.0005	2.000	375.07
-3.14	-.0218	.0071	-.0214	.0083	-2.5764	.0161	.0005	.0005	2.003	375.78
-2.15	.0030	.0079	.0033	.0078	.4211	.0074	.0005	.0005	2.001	375.31
-1.09	.0308	.0086	.0309	.0080	3.8458	-.0022	.0005	.0005	2.000	375.16
-.13	.0557	.0090	.0557	.0089	6.2543	-.0108	.0005	.0005	1.999	374.97
.90	.0800	.0095	.0798	.0108	7.4105	-.0191	.0005	.0005	2.001	375.28
1.76	.0987	.0093	.0984	.0124	7.9481	-.0257	.0005	.0005	2.001	375.28
2.88	.1317	.0098	.1311	.0164	7.9929	-.0358	.0005	.0005	1.999	374.95
3.83	.1551	.0105	.1541	.0208	7.4119	-.0428	.0005	.0005	2.000	375.16
4.87	.1820	.0109	.1804	.0263	6.8572	-.0501	.0005	.0005	2.000	375.21
5.83	.2052	.0118	.2030	.0325	6.2379	-.0562	.0005	.0005	2.001	375.23
6.89	.2297	.0126	.2266	.0401	5.6527	-.0625	.0005	.0005	2.003	375.61
7.82	.2511	.0135	.2469	.0475	5.1971	-.0676	.0005	.0005	2.001	375.33
-.16	.0519	.0088	.0519	.0087	5.9720	-.0099	.0005	.0005	1.999	374.97

UPWT PROJECT 1298 RUN 188 MACH 2.80

ALPHA	CN	CA	CL	CD	L/D	CM	CAC	CDC	R/FT	DYN PRS
-5.25	-.0713	.0054	-.0705	.0119	-5.9284	.0317	.0005	.0005	1.999	355.04
-4.24	-.0453	.0062	-.0447	.0095	-4.6960	.0240	.0005	.0005	2.001	355.39
-3.20	-.0225	.0068	-.0221	.0080	-2.7508	.0159	.0005	.0005	2.001	355.29
-2.21	.0003	.0075	.0006	.0075	.0838	.0082	.0005	.0005	2.000	355.19
-1.21	.0268	.0082	.0269	.0076	3.5236	-.0007	.0005	.0005	1.999	355.06
-.17	.0527	.0088	.0527	.0087	6.0727	-.0094	.0005	.0005	2.000	355.21
.80	.0756	.0091	.0754	.0102	7.4240	-.0172	.0005	.0005	2.000	355.12
1.82	.0989	.0092	.0986	.0124	7.9768	-.0249	.0005	.0005	2.001	355.35
2.82	.1234	.0096	.1227	.0157	7.8268	-.0322	.0005	.0005	2.000	355.21
3.78	.1464	.0102	.1454	.0199	7.3168	-.0391	.0005	.0004	2.000	355.25
4.81	.1703	.0108	.1688	.0250	6.7498	-.0454	.0004	.0004	1.998	354.84
5.80	.1918	.0114	.1897	.0308	6.1630	-.0509	.0004	.0004	2.003	355.67
6.78	.2134	.0123	.2104	.0375	5.6181	-.0567	.0004	.0004	2.000	355.14
7.83	.2385	.0133	.2345	.0456	5.1396	-.0628	.0004	.0004	2.000	355.25
-.23	.0477	.0085	.0477	.0083	5.7368	-.0082	.0005	.0005	2.000	355.17

TABLE AIV. FORCE DATA FOR SEVERELY CONSTRAINED WING ($\Delta C_{p,\mathrm{LE}} = 0$)

UPWT PROJECT 1298 RUN 116 MACH 1.80

ALPHA	CN	CA	CL	CD	L/D	CM	CAC	CDC	R/FT	DYN PRS
-5.40	-.0938	.0075	-.0927	.0163	-5.6953	.0369	.0007	.0007	2.015	458.87
-4.40	-.0608	.0081	-.0600	.0128	-4.7021	.0255	.0007	.0007	2.020	459.97
-3.40	-.0274	.0088	-.0268	.0104	-2.5858	.0133	.0007	.0007	2.013	458.39
-2.37	.0077	.0097	.0081	.0094	.8611	.0008	.0007	.0007	2.010	457.64
-1.39	.0378	.0104	.0380	.0095	4.0141	-.0102	.0007	.0007	2.013	458.35
-.38	.0692	.0109	.0693	.0104	6.6656	-.0214	.0008	.0008	2.012	458.19
.61	.0991	.0110	.0989	.0120	8.2137	-.0323	.0008	.0008	2.007	457.01
1.64	.1323	.0109	.1319	.0147	8.9660	-.0442	.0008	.0008	2.002	455.91
2.58	.1626	.0109	.1620	.0182	8.8759	-.0551	.0008	.0008	1.999	455.19
3.65	.1977	.0109	.1966	.0234	8.3884	-.0665	.0008	.0008	2.006	456.81
4.65	.2295	.0111	.2278	.0296	7.6920	-.0759	.0008	.0008	2.012	458.23
5.65	.2620	.0112	.2596	.0369	7.0298	-.0853	.0008	.0008	2.013	458.31
6.63	.2937	.0113	.2904	.0452	6.4282	-.0940	.0008	.0008	2.010	457.76
7.65	.3253	.0120	.3208	.0551	5.8181	-.1019	.0008	.0008	2.008	457.33
-.38	.0702	.0109	.0703	.0104	6.7513	-.0219	.0008	.0008	2.012	458.08

UPWT PROJECT 1298 RUN 119 MACH 2.00

ALPHA	CN	CA	CL	CD	L/D	CM	CAC	CDC	R/FT	DYN PRS
-5.04	-.0853	.0074	-.0844	.0148	-5.6928	.0332	.0007	.0007	2.008	450.21
-4.06	-.0579	.0079	-.0572	.0120	-4.7722	.0239	.0007	.0007	2.008	450.21
-3.05	-.0281	.0085	-.0276	.0100	-2.7576	.0135	.0007	.0007	2.009	450.43
-2.04	.0037	.0092	.0040	.0091	.4373	.0022	.0008	.0008	2.009	450.54
-1.03	.0344	.0100	.0345	.0093	3.6989	-.0085	.0008	.0008	2.010	450.61
-.03	.0638	.0105	.0638	.0105	6.0840	-.0188	.0008	.0008	2.008	450.25
.97	.0917	.0107	.0915	.0123	7.4573	-.0284	.0008	.0008	2.006	449.82
1.97	.1220	.0108	.1215	.0150	8.1010	-.0388	.0008	.0008	2.007	450.00
2.96	.1523	.0108	.1515	.0186	8.1520	-.0492	.0008	.0008	2.008	450.25
3.99	.1838	.0109	.1826	.0237	7.7178	-.0593	.0008	.0008	2.008	450.29
4.99	.2130	.0109	.2112	.0294	7.1728	-.0674	.0008	.0008	2.008	450.32
5.94	.2401	.0110	.2377	.0358	6.6359	-.0746	.0008	.0008	2.008	450.36
7.00	.2712	.0114	.2678	.0444	6.0335	-.0823	.0009	.0008	2.009	450.50
7.98	.2991	.0122	.2945	.0536	5.4946	-.0886	.0009	.0009	2.009	450.50
-.04	.0645	.0105	.0645	.0104	6.1756	-.0190	.0008	.0008	2.009	450.43

TABLE AIV. Continued

UPWT PROJECT 1298 RUN 120 MACH 2.16

ALPHA	CN	CA	CL	CD	L/D	CM	CAC	CDC	R/FT	DYN PRS
-5.12	-.0737	.0075	-.0727	.0140	-5.1905	.0297	.0007	.0007	2.005	439.85
-4.15	-.0469	.0080	-.0462	.0114	-4.0475	.0208	.0007	.0007	2.005	439.88
-3.14	-.0174	.0087	-.0169	.0096	-1.7535	.0105	.0007	.0007	2.006	439.91
-2.14	.0120	.0093	.0124	.0088	1.4010	.0002	.0007	.0007	2.005	439.81
-1.13	.0407	.0099	.0409	.0091	4.5067	-.0096	.0007	.0007	2.005	439.85
-.14	.0688	.0104	.0688	.0102	6.7299	-.0193	.0007	.0007	2.005	439.88
.89	.0975	.0106	.0973	.0121	8.0252	-.0290	.0008	.0008	2.005	439.85
1.90	.1260	.0107	.1256	.0149	8.4321	-.0387	.0008	.0008	2.006	439.98
2.89	.1556	.0108	.1548	.0186	8.3242	-.0486	.0008	.0008	2.006	440.01
3.89	.1839	.0110	.1828	.0234	7.8083	-.0573	.0008	.0008	2.006	440.01
4.91	.2135	.0111	.2118	.0293	7.2177	-.0659	.0008	.0008	2.006	440.04
5.87	.2401	.0113	.2377	.0358	6.6429	-.0730	.0008	.0008	2.007	440.14
6.89	.2675	.0118	.2642	.0438	6.0369	-.0793	.0008	.0008	2.006	440.11
7.88	.2933	.0123	.2888	.0524	5.5112	-.0849	.0008	.0008	2.006	440.04

UPWT PROJECT 1298 RUN 122 MACH 2.40

ALPHA	CN	CA	CL	CD	L/D	CM	CAC	CDC	R/FT	DYN PRS
-5.04	-.0683	.0075	-.0674	.0135	-4.9890	.0276	.0006	.0006	2.008	420.63
-4.09	-.0444	.0079	-.0437	.0111	-3.9505	.0200	.0006	.0006	2.007	420.55
-3.09	-.0200	.0082	-.0195	.0092	-2.1085	.0113	.0006	.0006	2.006	420.24
-2.08	.0089	.0092	.0092	.0088	1.0411	.0016	.0006	.0006	2.007	420.41
-1.08	.0349	.0094	.0351	.0088	3.9940	-.0073	.0006	.0006	2.002	419.42
-.14	.0604	.0101	.0604	.0100	6.0521	-.0160	.0007	.0007	2.000	419.11
.91	.0898	.0104	.0897	.0119	7.5667	-.0258	.0007	.0007	2.001	419.17
1.91	.1148	.0104	.1144	.0142	8.0671	-.0339	.0007	.0007	2.003	419.66
2.88	.1419	.0107	.1412	.0179	7.9070	-.0428	.0007	.0007	2.002	419.55
3.93	.1707	.0108	.1696	.0225	7.5421	-.0517	.0007	.0007	2.002	419.44
4.90	.1987	.0113	.1970	.0282	6.9838	-.0592	.0007	.0007	2.002	419.53
5.87	.2225	.0116	.2202	.0343	6.4226	-.0658	.0007	.0007	2.001	419.20
6.91	.2502	.0122	.2469	.0422	5.8501	-.0730	.0007	.0007	2.003	419.66
7.78	.2697	.0124	.2655	.0488	5.4437	-.0775	.0007	.0007	2.003	419.69
-.12	.0626	.0100	.0626	.0099	6.3462	-.0167	.0007	.0007	2.003	419.61

TABLE AIV. Concluded

UPWT PROJECT 1298 RUN 125 MACH 2.60

ALPHA	CN	CA	CL	CD	L/D	CM	CAC	CDC	R/FT	DYN PRS
-5.08	-.0688	.0072	-.0679	.0133	-5.1002	.0269	.0005	.0005	2.001	399.87
-4.02	-.0427	.0075	-.0420	.0105	-4.0026	.0190	.0005	.0005	2.001	399.85
-3.04	-.0202	.0082	-.0197	.0093	-2.1220	.0111	.0005	.0005	2.001	399.78
-1.97	.0103	.0088	.0106	.0085	1.2503	.0014	.0006	.0006	2.001	399.87
-1.05	.0328	.0092	.0330	.0086	3.8179	-.0066	.0006	.0006	2.000	399.76
-.02	.0567	.0095	.0567	.0094	6.0091	-.0147	.0006	.0006	2.002	400.06
.97	.0850	.0100	.0848	.0114	7.4296	-.0243	.0006	.0006	2.001	399.92
2.07	.1130	.0104	.1125	.0145	7.7564	-.0331	.0006	.0006	2.001	399.80
2.99	.1367	.0106	.1359	.0177	7.6787	-.0408	.0006	.0006	2.001	399.90
4.01	.1636	.0110	.1624	.0224	7.2647	-.0490	.0006	.0006	2.001	399.78
4.99	.1896	.0112	.1880	.0276	6.7983	-.0564	.0006	.0006	2.001	399.92
5.98	.2147	.0114	.2124	.0337	6.3047	-.0630	.0006	.0006	2.002	400.09
6.90	.2335	.0118	.2303	.0398	5.7871	-.0682	.0006	.0006	2.000	399.59
7.96	.2614	.0124	.2572	.0485	5.3043	-.0751	.0006	.0006	2.001	399.85
.01	.0618	.0099	.0618	.0099	6.2269	-.0165	.0006	.0006	2.001	399.90

UPWT PROJECT 1298 RUN 126 MACH 2.80

ALPHA	CN	CA	CL	CD	L/D	CM	CAC	CDC	R/FT	DYN PRS
-5.04	-.0621	.0070	-.0612	.0124	-4.9403	.0252	.0005	.0005	1.995	377.79
-4.11	-.0453	.0074	-.0447	.0106	-4.1926	.0194	.0005	.0005	1.998	378.30
-3.11	-.0233	.0076	-.0229	.0088	-2.5889	.0123	.0005	.0005	1.997	378.14
-2.15	-.0000	.0081	.0003	.0081	.0356	.0047	.0005	.0005	1.998	378.40
-1.08	.0269	.0087	.0271	.0082	3.3191	-.0044	.0005	.0005	1.999	378.54
-.08	.0535	.0094	.0535	.0093	5.7522	-.0129	.0005	.0005	1.998	378.46
.87	.0731	.0094	.0730	.0105	6.9556	-.0197	.0005	.0005	1.998	378.44
1.95	.1038	.0100	.1034	.0135	7.6581	-.0294	.0005	.0005	1.999	378.66
2.90	.1268	.0103	.1262	.0167	7.5699	-.0366	.0005	.0005	1.999	378.66
3.95	.1528	.0106	.1517	.0211	7.1839	-.0441	.0005	.0005	1.998	378.40
4.88	.1747	.0110	.1732	.0258	6.7158	-.0506	.0005	.0005	1.999	378.58
5.91	.1989	.0113	.1967	.0318	6.1910	-.0575	.0005	.0005	1.999	378.62
6.87	.2185	.0115	.2155	.0375	5.7438	-.0628	.0005	.0005	2.000	378.72
7.92	.2458	.0123	.2417	.0461	5.2477	-.0692	.0005	.0005	1.999	378.62
-.09	.0557	.0093	.0557	.0092	6.0679	-.0137	.0005	.0005	1.999	378.62

Appendix B

Lateral Force Data and Derivatives

Lateral force data and derivatives for the models in this series are not included in the tabular data. These coefficients are therefore presented graphically in figures B1 to B5.

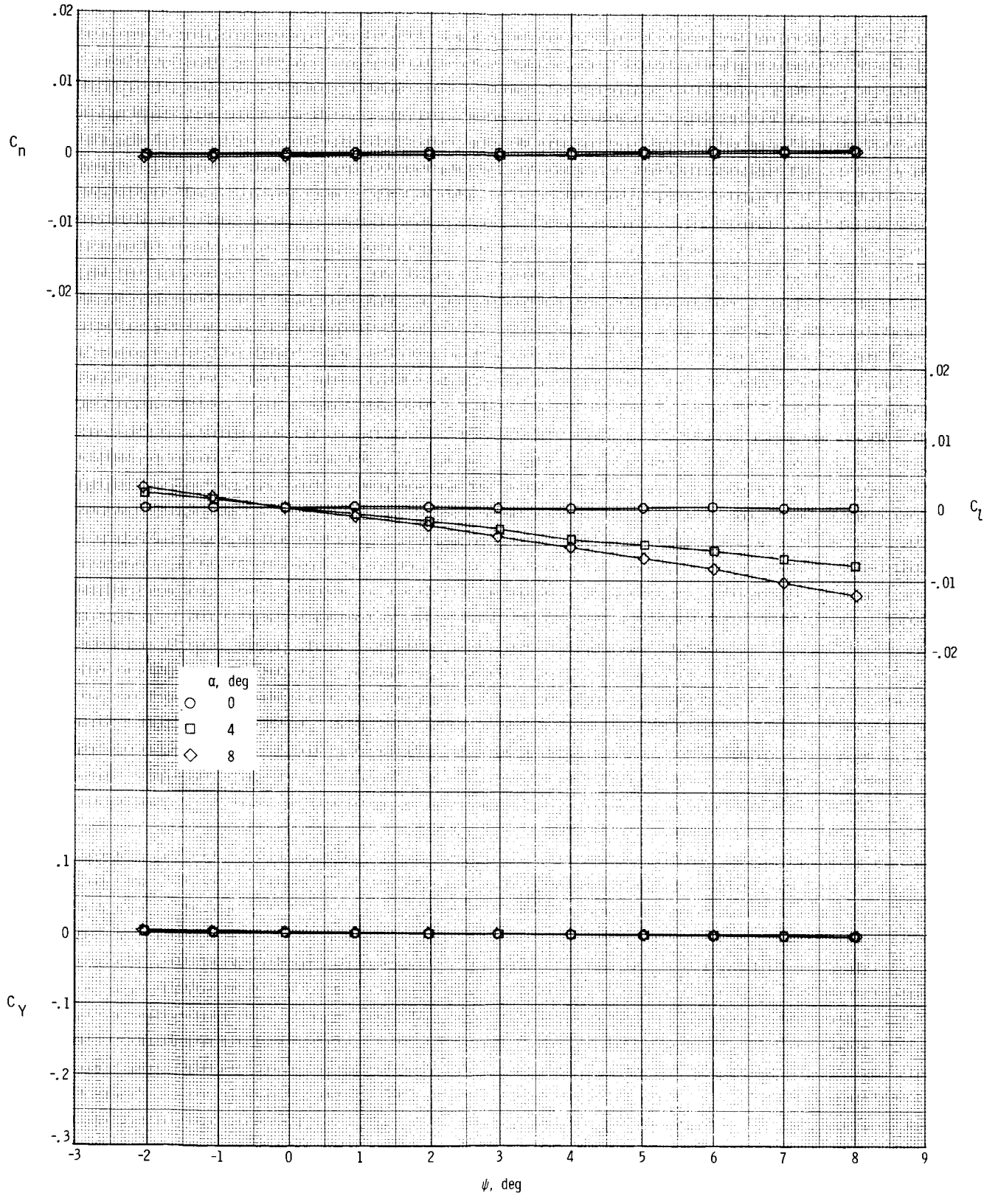

(a) $M = 1.8$.

Figure B1. Lateral coefficients plotted against ψ for flat wing model.

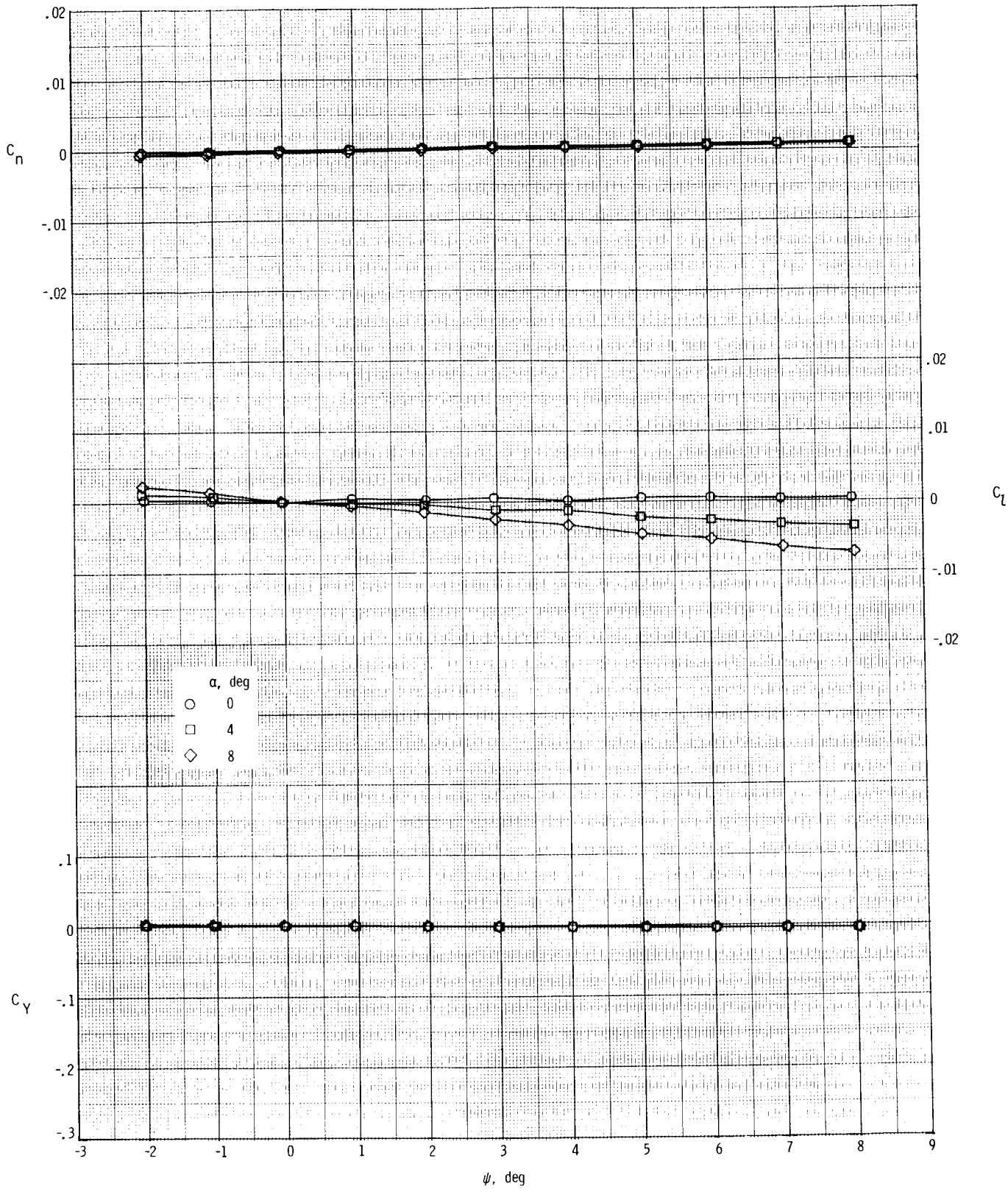

(b) $M = 2.8$.

Figure B1. Concluded.

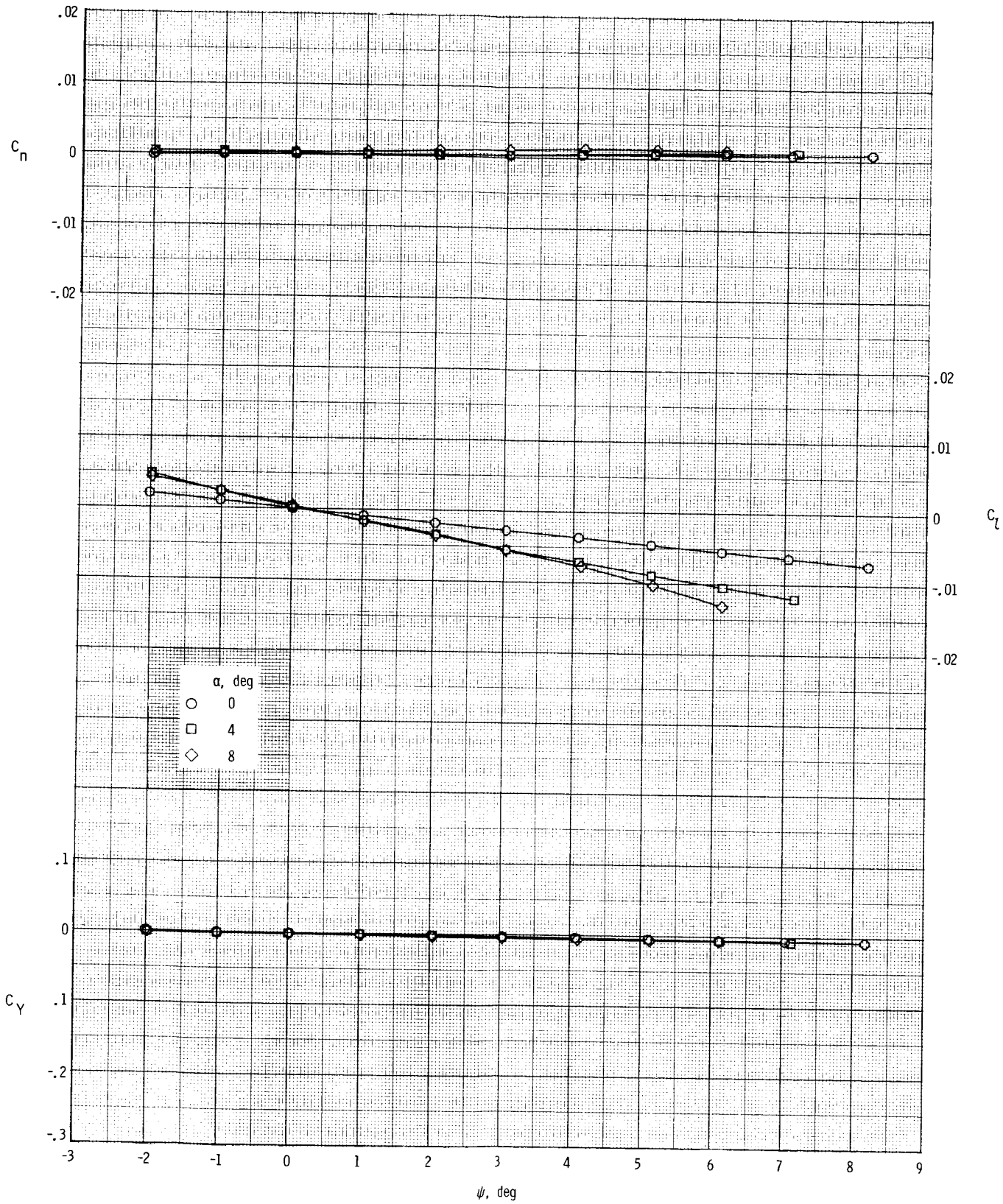

(a) $M = 1.8$.

Figure B2. Lateral coefficients plotted against ψ for unconstrained wing model.

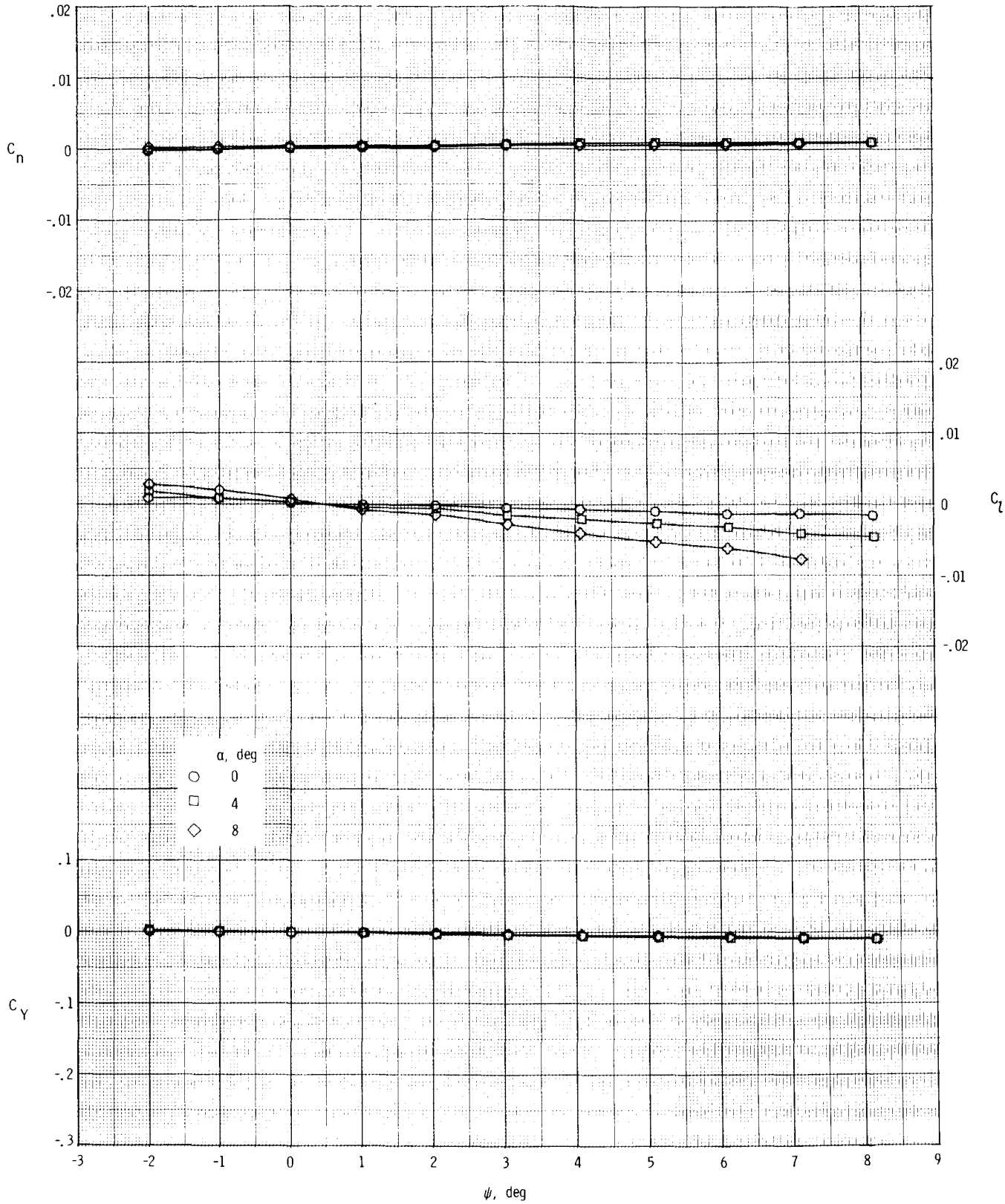

(b) $M = 2.8$.

Figure B2. Concluded.

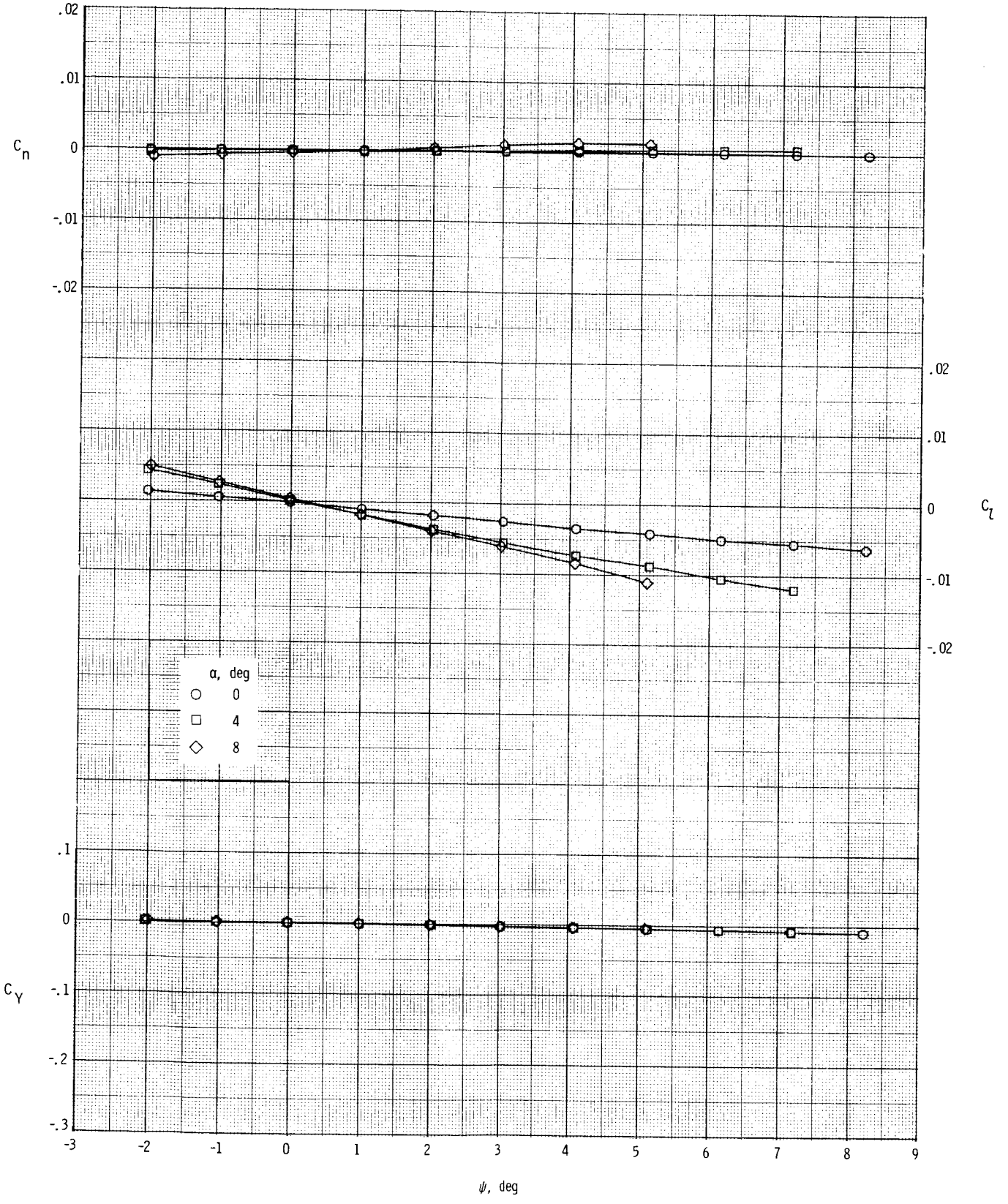

(a) $M = 1.8$.

Figure B3. Lateral coefficients plotted against ψ for moderately constrained wing model ($M_N < 1$).

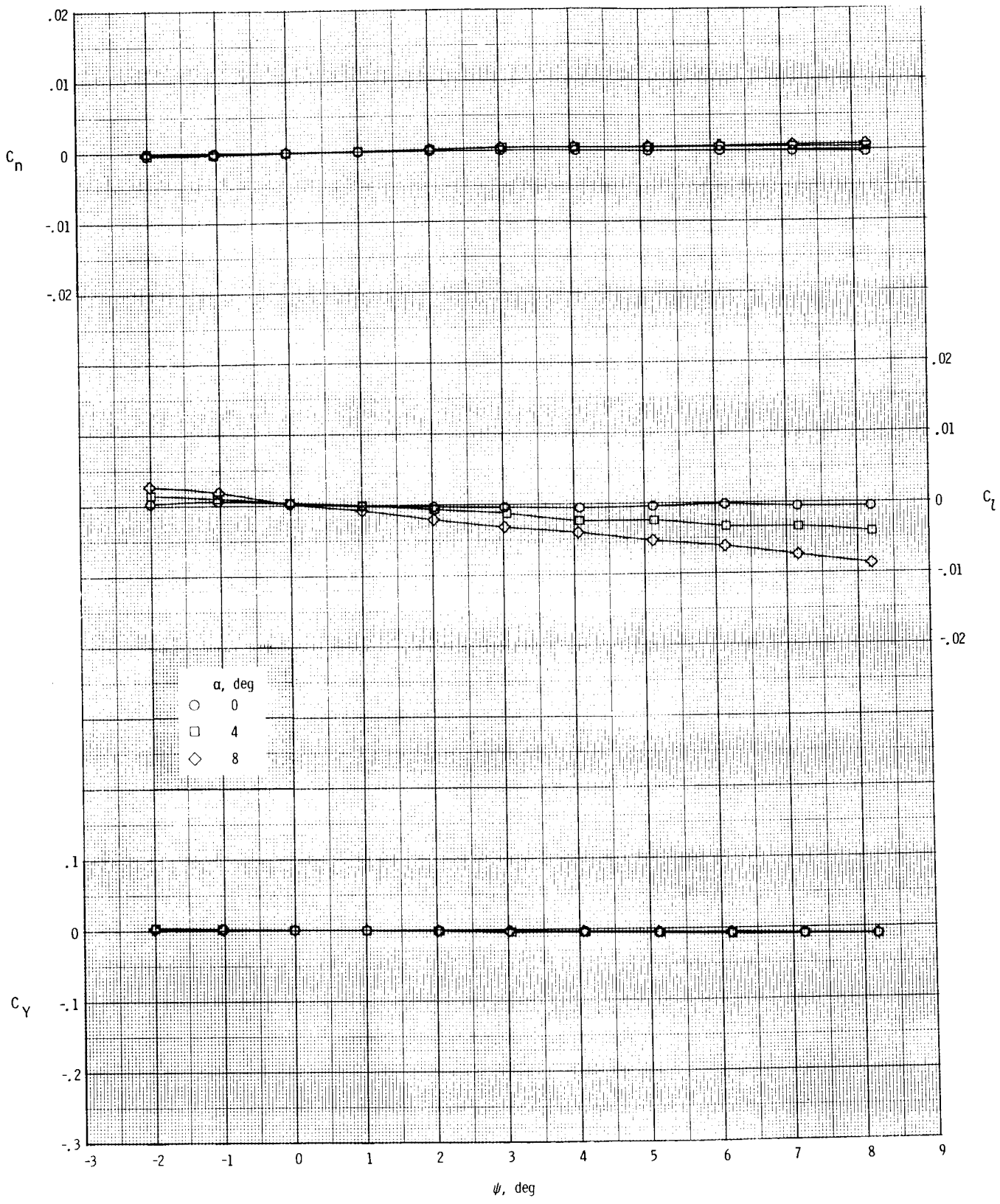

(b) $M = 2.8$.

Figure B3. Concluded.

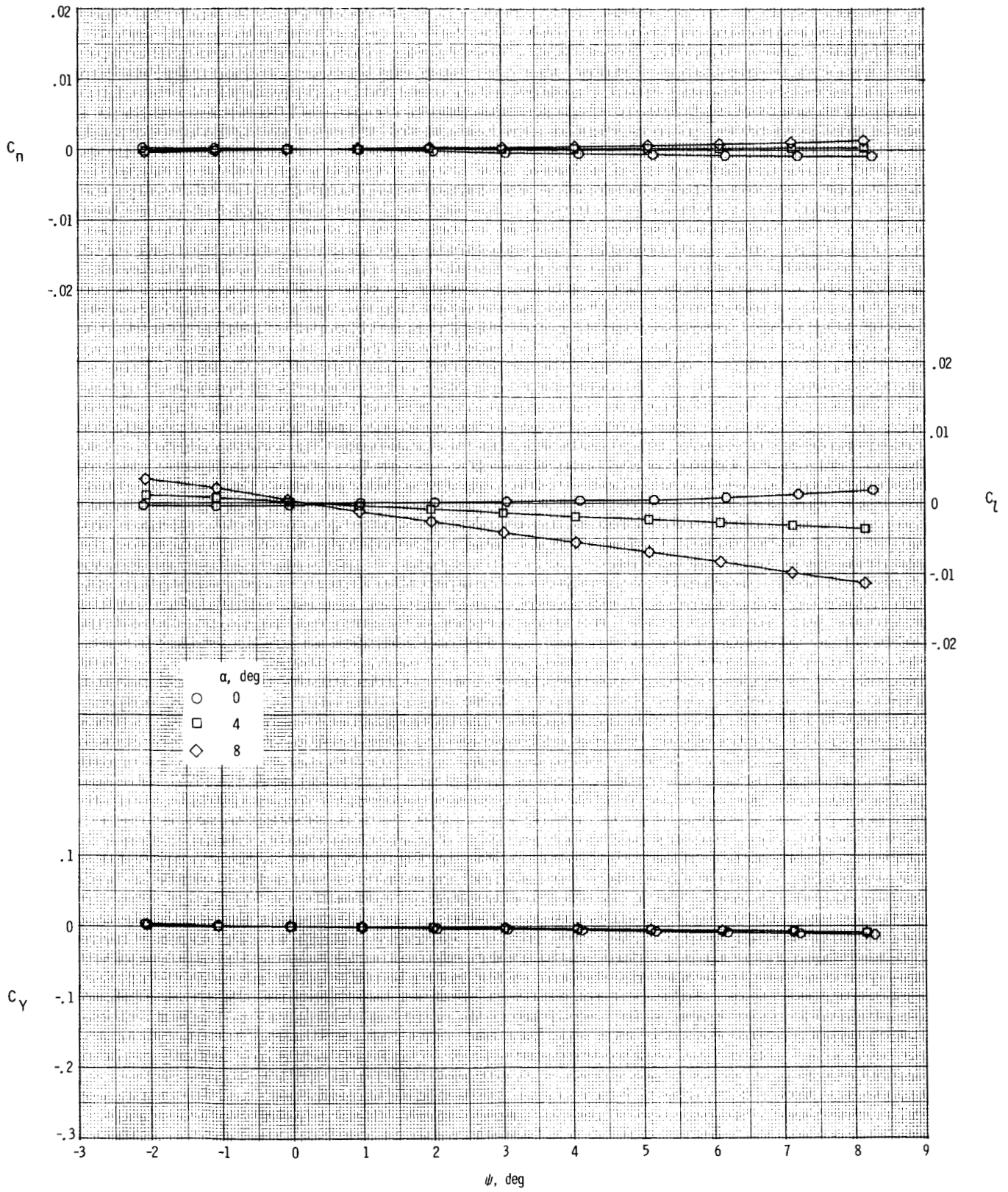

(a) $M = 1.8$.

Figure B4. Lateral coefficients plotted against ψ for severely constrained wing model. ($\Delta C_{p,\mathrm{LE}} = 0$).

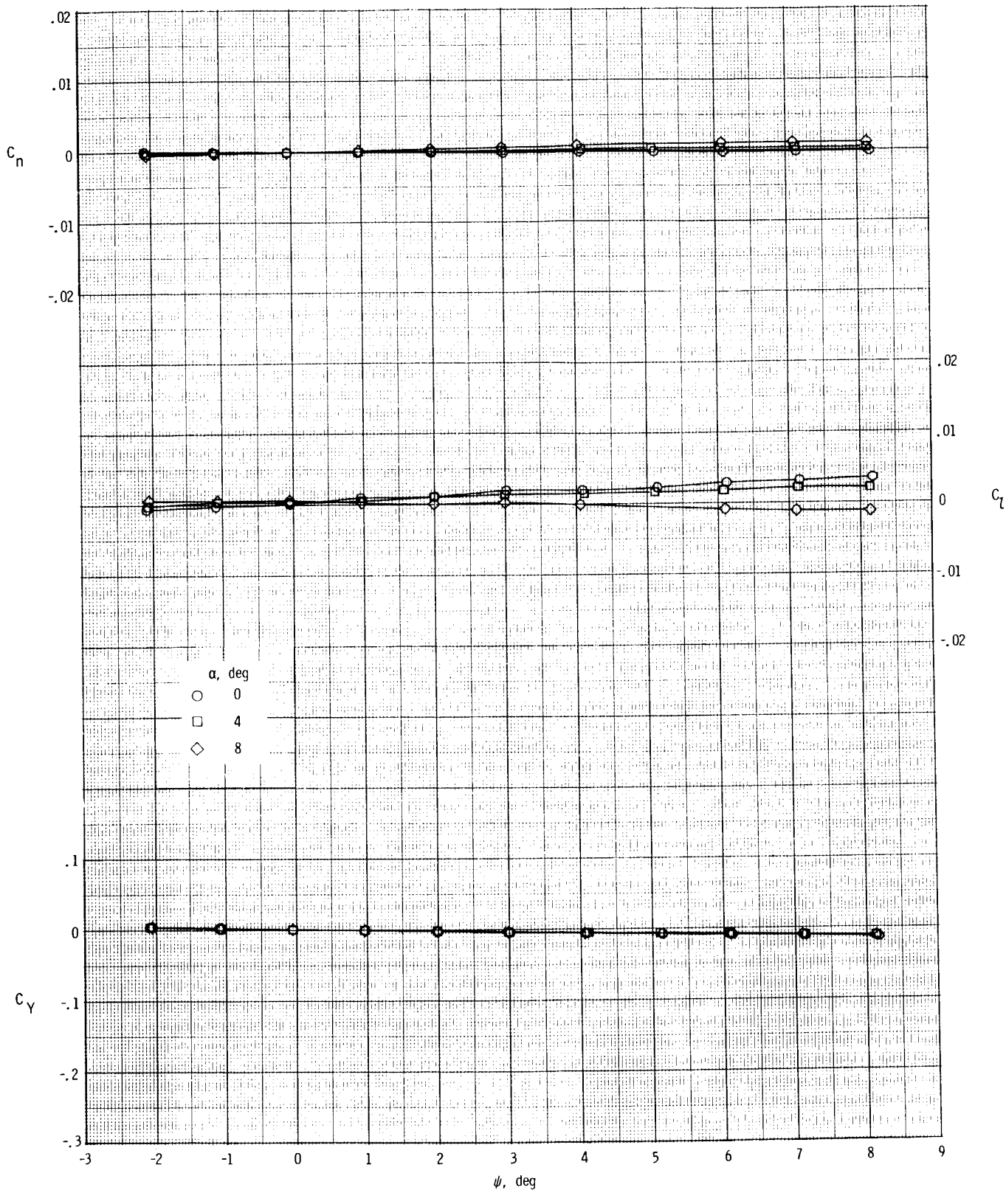

(b) $M = 2.8$.

Figure B4. Concluded.

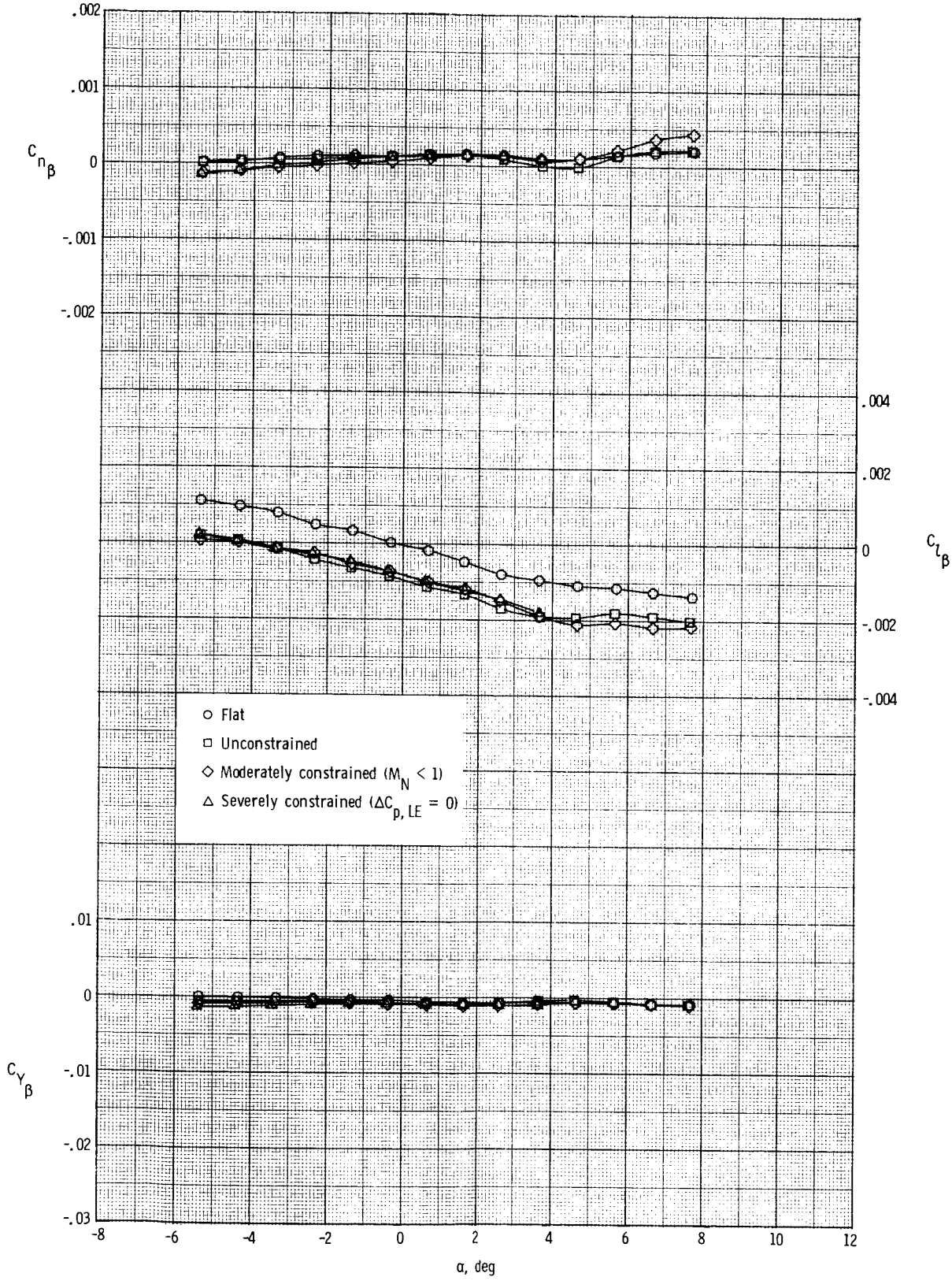

(a) $M = 1.8$.

Figure B5. Stability parameters as functions of angle of attack.

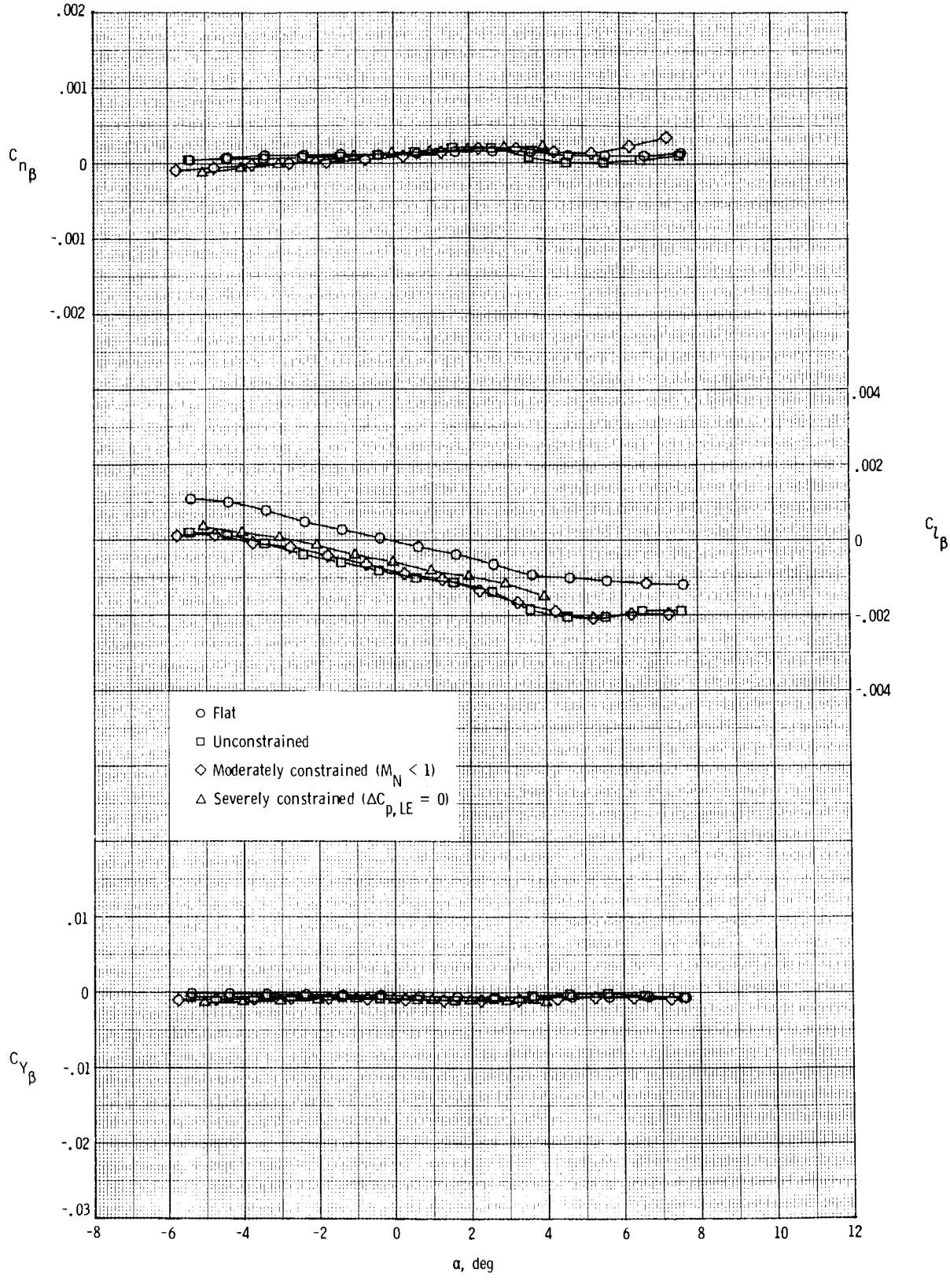

(b) $M = 2.0$.

Figure B5. Continued.

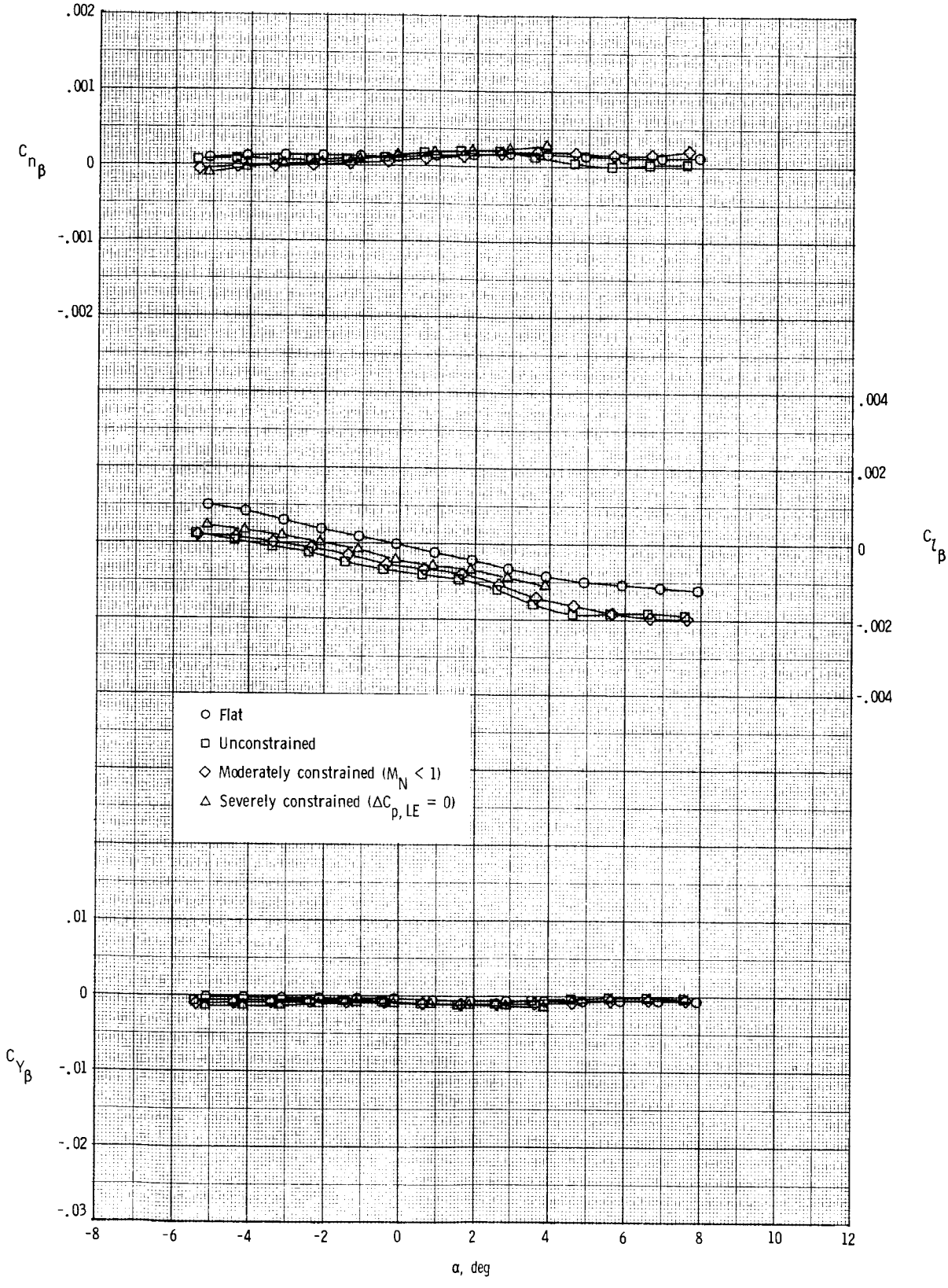

(c) $M = 2.16$.

Figure B5. Continued.

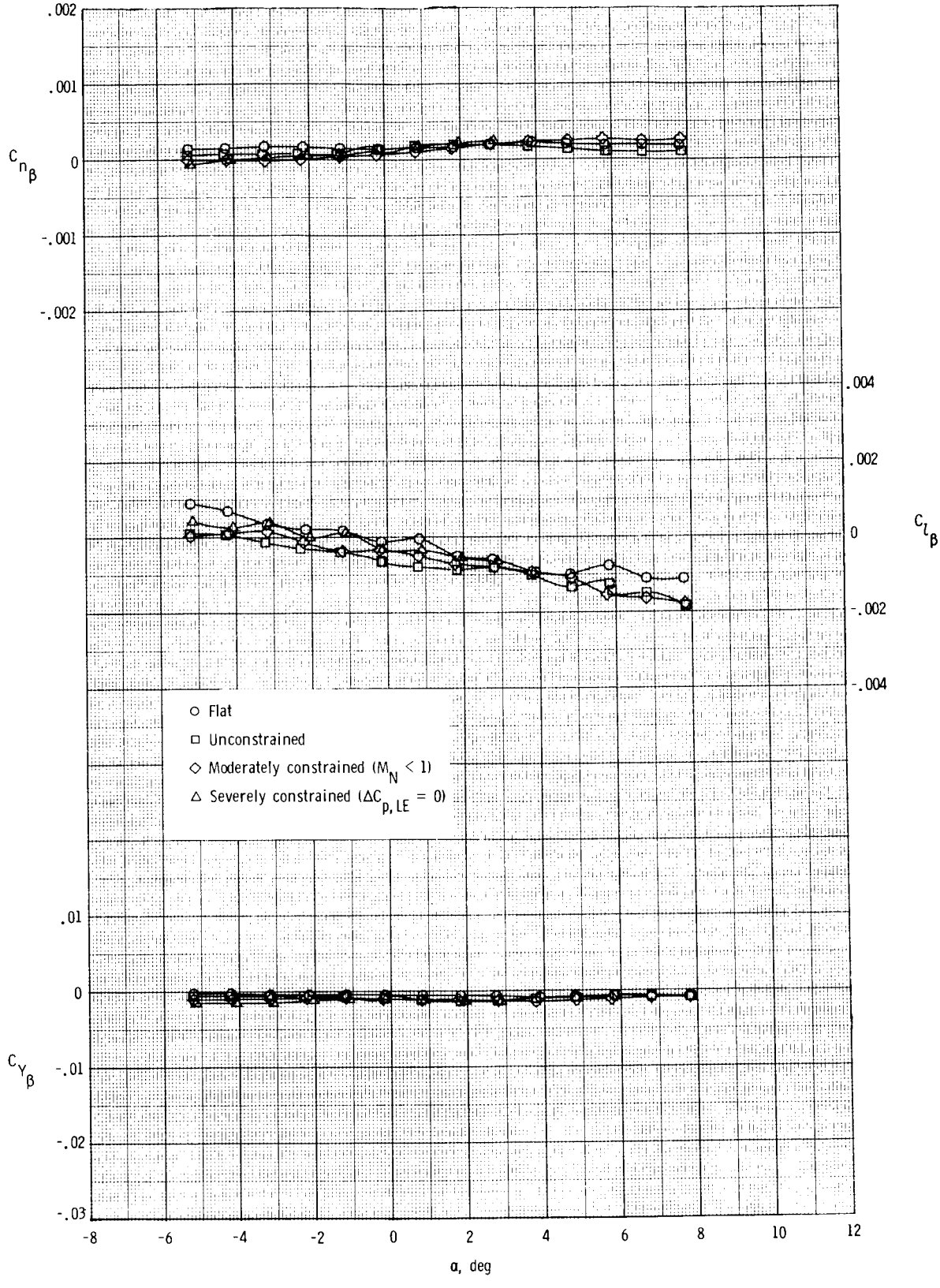

(d) $M = 2.4$.

Figure B5. Continued.

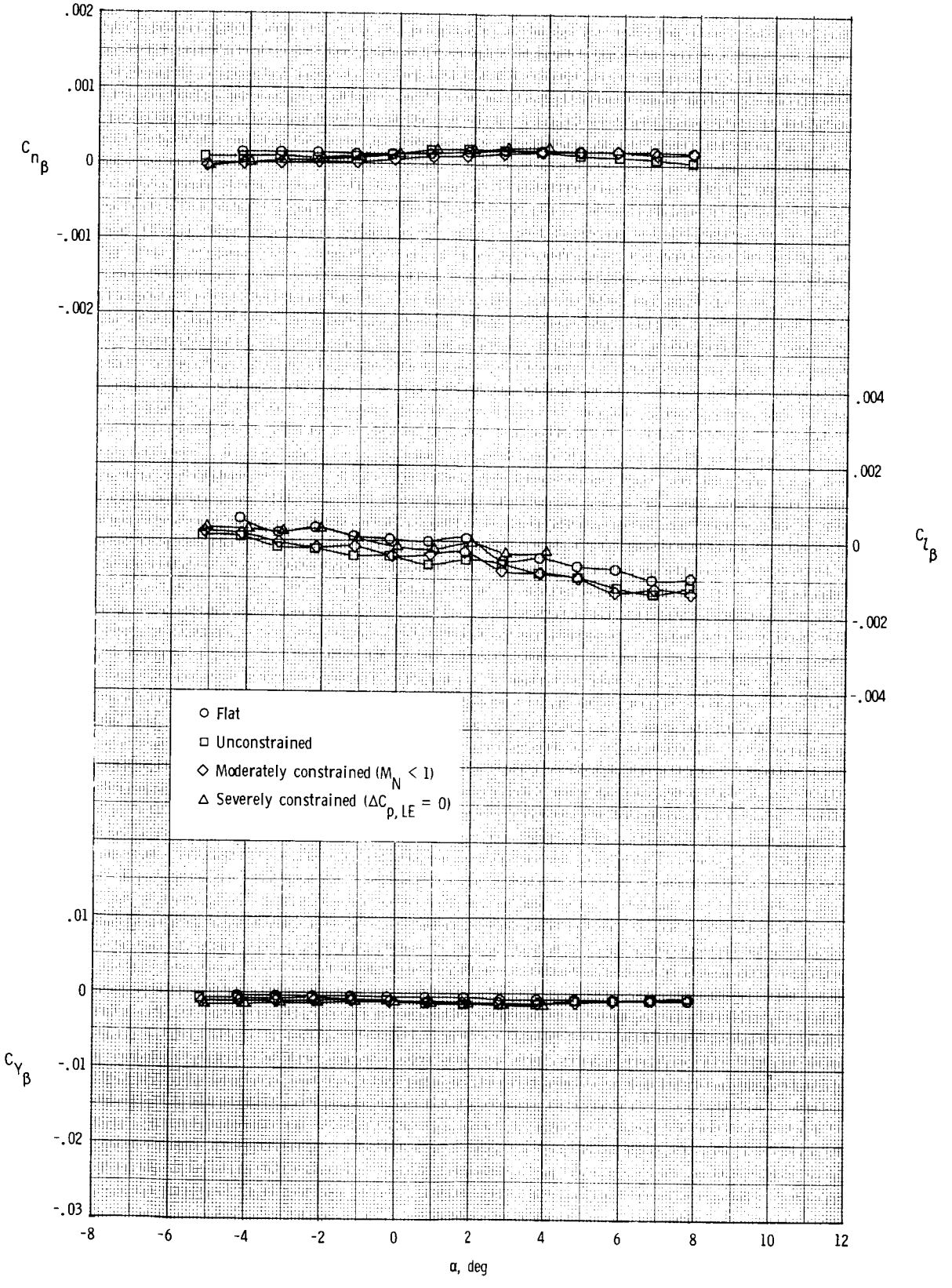

(e) $M = 2.6$.

Figure B5. Continued.

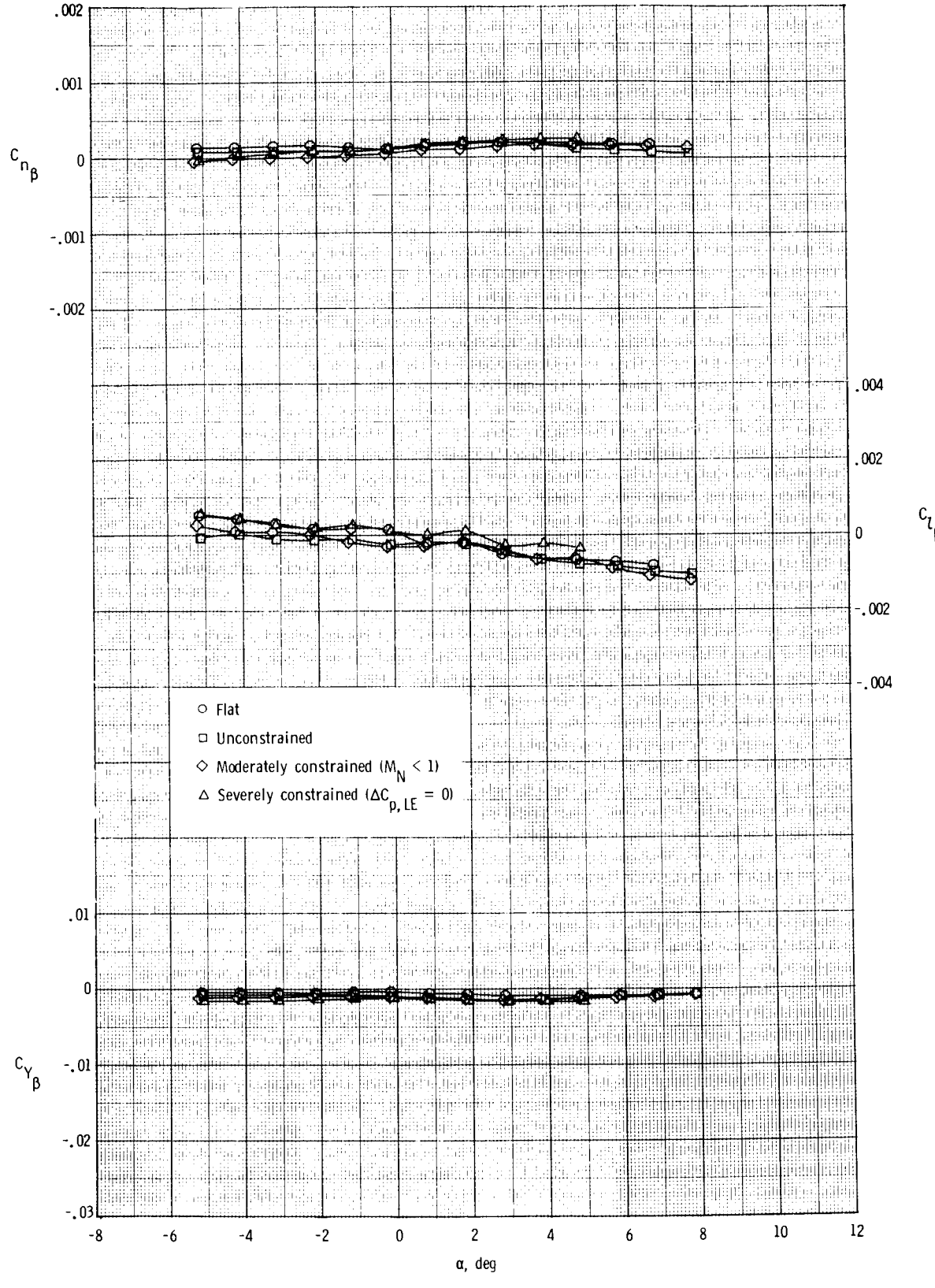

(f) $M = 2.8$.

Figure B5. Concluded.

1. Report No.	2. Government Accession No.	3. Recipient's Catalog No.
NASA TP-2446		

4. Title and Subtitle	5. Report Date
Effect of Leading-Edge Load Constraints on the Design and Performance of Supersonic Wings	July 1985
	6. Performing Organization Code: 505-43-23-10
7. Author(s): Christine M. Darden	8. Performing Organization Report No.: L-15841
9. Performing Organization Name and Address: NASA Langley Research Center, Hampton, VA 23665	10. Work Unit No.
	11. Contract or Grant No.
12. Sponsoring Agency Name and Address: National Aeronautics and Space Administration, Washington, DC 20546	13. Type of Report and Period Covered: Technical Paper
	14. Sponsoring Agency Code

15. Supplementary Notes

16. Abstract

A theoretical and experimental investigation was conducted to assess the effect of leading-edge load constraints on supersonic wing design and performance. In an effort to delay flow separation and the formation of leading-edge vortices, two constrained, linear-theory optimization approaches were used to limit the loadings on the leading edge of a variable-sweep planform design. Experimental force and moment tests were made on two constrained camber wings, a flat uncambered wing, and an optimum design with no constraints. Results indicate that vortex strength and separation regions were mildest on the severely and moderately constrained wings.

17. Key Words (Suggested by Authors(s))
Supersonic wing design
Wing performance
Vortex suppression
Limited leading-edge loadings

18. Distribution Statement
Unclassified—Unlimited

Subject Category 02

19. Security Classif.(of this report)	20. Security Classif.(of this page)	21. No. of Pages	22. Price
Unclassified	Unclassified	77	A05

For sale by the National Technical Information Service, Springfield, Virginia 22161

NASA-Langley, 1985

National Aeronautics and
Space Administration

Washington, D.C.
20546

Official Business
Penalty for Private Use, $300

BULK RATE
POSTAGE & FEES PAID
NASA Washington, DC
Permit No. G-27

NASA

POSTMASTER: If Undeliverable (Section 158 Postal Manual) Do Not Return